Authors response
We thank the editor for the opportunity to resubmit this paper. We have now made extensive changes and conducted further work and we look forward to the comments on this substantially revised and improved version of the paper. Our responses to the reviewers have now been extended to demonstrate the changes that have been made.

Reviewer 1
We thank the reviewer for their detailed review. We have broken down the comments into subheadings (*italic*) followed by our responses in plain text. Changes to the ms are in **bold**.

1. *The selection of candidate proxy records (Tables 1 and 2) seems to me to be incomplete and somewhat arbitrary. There are, for example, many more relatively long-term coral-based sea surface temperature (SST) reconstructions available in the NOAA Paleoclimate data base for the Pacific and Indian Oceans than those considered by the authors.*

[this is largely the same as our response to reviewer 2's comment 4.]
We endeavoured to include all precipitation and temperature proxies currently publicly available for the study region. As reviewer 1 notes, there are indeed several coral records available that were not included in this study. The reason for this is that it was stated explicitly in the associated publications that the recorded d18O signal was in fact a combination of SST and SSS (or SST and precipitation). Most authors also state that it is not possible to disentangle the two climate variables (McGregor & Gagan 2004, Hereid et al. 2013, Osborne et al. 2014) While this is not an issue when, for example, one is using the single proxy as a recorder of ENSO events in a location where SST and SSS have the same-sign impact on the d18O of the coral, it does present a problem for our method of reconstruction. As we are using temperature- and precipitation-specific EOF patterns, we need proxies that are as univariate as possible (i.e. only respond to one of these two climate variables). **In response to the comments, we have included more temperature and precipitation proxy records in the revised analysis, including a suite of coral records used in Tierney et al. (2015). The new proxy records are incorporated in Tables 1 and 2, and an updated discussion on the proxy selection is available in Appendix A. This has resulted in an additional 12 precipitation proxies and 55 temperature proxies.**

2. *There does not appear to be any screening of the various climate proxy records for their exhibiting a significant relationship with ENSO indices over the observational record period as, for example, undertaken by Li et al (2013) and Emile-Geay et al (2013). This would seem to be a crucial first step.*

[this is largely the same as our response to reviewer 2's comment 4.]
The answer to this second point raised by reviewer 1 leads on from the previous point. The point is that we use *any* precipitation or temperature proxy, and have their contribution to the reconstruction decided by the EOF weighting. The empirically informed add-one-in algorithm further informs the usefulness of the proxies in reconstructing the ENSO-like signal. If a certain proxy is also significantly influenced by other climatic oscillations, for example, it would be less likely to be included in the final proxy network (Section 4).

3. *The authors exclude several potential candidate proxy climate records on the basis of 'dating error' but there is no explanation, as far as I can see,*

how this was assessed. How, for example, was the 'dating error' determined for the Cole et al (1993) coral record (Table 1) when this is an annually-resolved and well-dated record?

As noted in the ms, the choice to exclude records with a dating error >=60 years is somewhat arbitrary but chosen as it is twice the averaging binwidth of 30 years. **The assessment of dating errors is described in Appendix A. After reviewing all proxy records, the Cole et al. (1993) coral record has been removed from the proxy list in the revised ms** as it is not clearly dominated by either temperature or precipitation (see Appendix A). This does not affect the reconstruction as it was previously rejected due to length (not dating error).

4. *The authors present their 'reconstructions' as 30-year averages (Figure 1). It is unclear to me how a 30-year average ENSO can be reconstructed when ENSO is a high-resolution climate signal operating on ~2-7 year timescales. Also, past and future ENSO variability is not just about changes in the mean state, it also should encompass a measure of variability and the frequency and intensity of the two phases (i.e. El Niño and La Niña).*

[this is largely the same as our response to reviewer 2's comment 1.]
Both reviewers raised the issue of reconciling 30-year averages and the interannual ENSO timescales. Our aim here was not to comment on ENSO interannual variability, frequency or amplitude as did Li et al. (2013) and Emile-Geay et al. (2013), but rather ENSO-*like* climate change similar to many long-term, lower resolution proxy studies (cf. Moy et al. 2002, Conroy et al. 2008, Yan et al. 2011). This was clearly not conveyed very well and we apologise for the confusion caused. We absolutely agree that it is not possible to translate this directly into ENSO variability, frequency and intensity and thank the reviewers for highlighting the need to clarify this. Our interest is in the extent to which climate change was El Nino-like or La Nina-like during the past 1000 years. Part of the motivation for this is the paper of Yan et al. (2011). which suggests that precipitation proxies indicate El Nino like change while temperature proxies indicate La Nina like change. Our understanding of current climate suggests that this is unlikely, but it would be very important if true. **We have adjusted the Introduction to emphasise that this aim. The Discussion is similarly rephrased and restructured to shift the focus to long-term ENSO-like changes.**

5. *Although the separate precipitation- and temperature-based reconstructions could be informative, why did the authors not develop a combined proxy reconstruction? Maybe the sum is greater than the parts?*

Reviewer 1 makes a good point about combining the precipitation and temperature reconstructions potentially being more informative as an overall reconstruction of El Nino-like climate change. However, as we mention in our response to comment 4, a major objective of this study was to investigate the apparent discrepancy between temperature and precipitation proxies as highlighted by Yan et al. (2011), and for this, separate reconstructions are necessary.

6. *Complete citations should be provided for all proxy data sets used (could be as Supplementary Material).*

All proxy records listed in Tables 1 and 2 are included in the References for the paper.

7. *Specific comments*

We thank reviewer 1 for their thorough comments. We address several individually below:

Page 5550, lines 10-11: IPCC (2013, Chapter 5) delineates the MCA as 950-1250AD and the LIA as 1450-1850AD. I suggest the authors modify their time periods accordingly to this standard.

We chose our definition of the MCA and LIA according to Yan et al. (2011)'s definition, as this paper was a main starting point for this work. **The sensitivity of our results to the choice of MCA and LIA (Masson-Delmotte et al., 2013; Mann et al., 2009) is tested and described in Section 4.1 in the revised ms.**

Page 5551, lines 21-22: There have, however, been recent modelling studies which do provide insights into how ENSO variability may change in a warming world (e.g. Power et al., 2013; Cai et al., 2015 a,b).

This observation and references are now incorporated in the Introduction.

Page 5552: I think this introduction should include a clear description and review of the various recent reconstructions of ENSO indices and the extent to which they agree or not (e.g. Braganza et al. 2009; McGregor et al., 2010; Li et al., 2013; Emile-Geay et al., 2013). This should appear before considering possible drivers of changes in ENSO variability.

See also comment 4. As the focus of this paper is on long-term ENSO-like climate states, a detailed discussion of high-frequency ENSO reconstructions is not relevant. In particular, Braganza et al. (2009) and McGregor et al. (2010) are too short to address the MCA-LIA difference which is a central question in this study. **Li et al. (2013) and Emile-Geay et al. (2013) are discussed in Section 5. There is, however, now a review of long-term ENSO-like behaviour evident in individual proxy records, and the apparent agreements and discrepancies, in the Introduction.**

Page 5554, lines 6-10: We still need some measure of the fidelity of these reconstructions to assess how well (or not) they are reproducing observed variations.//
Page 5555, lines 10-12: But the argument can also be made that longer but lower resolution proxy climate series are less likely to capture the inter-annual climate variability associated with ENSO.//
Page 5559, lines 3-6: Would some of these potential problems be filtered out by only using proxy climate records that have an ENSO signal in the observational record?//
Page 5560, lines 2-3 and lines 6-10: Surely you can still compare the time series of the reconstructions with observational records; it is not just about changes in the mean state of ENSO but also variability, intensity and frequency of extremes (El Niño and La Niña).//
Page 5566, lines 7-11: But comparisons could be made for the overlapping parts of the different ENSO reconstructions?//
Page 5572, lines 13-15: I think the authors need to convince the readers that 30-year averages are able to capture the inter-annual variability associated with

ENSO.

See comment 4 on long-term vs. interannual trends.

Page 5554, line 24: 'proxy precipitation'; Also see General Comment 1 above querying whether the authors have really assembled a comprehensive data base of available proxy climate records.//
Page 5561, lines 24-25: As indicated in General Comment 1, I think there were many more potential SST proxies that the authors could have used.//
Page 5564, lines 18-21: See earlier comments about several other SST proxies being available for the tropics.

See comment 1 re: proxy selection.

Page 5555, lines 3-4: What were the criteria used by Mann et al. (2008)?

The criteria are cited in Appendix A. **A brief description of the criteria is now also in Section 2.1 of the revised ms.**

Page 5555, lines 5-7: See General Comment 3 above requiring how 'dating errors' were determined. Also, what is the 30-year averaging period referred to here?

See comment 3 re: dating error. The 30-year averaging period simply refers to the fact that all proxy records are averaged (or interpolated) to 30-year resolution.

Page 5556, line 1: Why was SST not used rather than air temperature as ENSO is primarily a SST (and surface atmospheric circulation) phenomenon?

The data used in this study is the temperature at 1000hP, which can be considered equivalent to ocean skin temperature. Although ocean skin temperature is likely to be more variable at diurnal timescales, this will average out over the multi-annual scales used in this study. Moreover, comparisons between satellite-derived skin temperatures and bulk sea surface temperature (SST) from ships and buoys show a very strong correlation between the two over spatial scales (Schluessel et al., 1990) equivalent to the grid resolution of the data used here. Finally, although using a combination of air temperature and SST would still be ideal, it is also not desirable for practical reasons as the ocean grid used in models is different to the atmosphere grid.

Page 5556, line 12: What was the full period for the observational records?

The full period is AD 1851-2014 (Section 2.2). **Note we are now using the updated version 20CRv2c in the revised ms, which is longer by ~20 years.**

Page 5556, lines 12-14: What was the 'common period' used to standardize the proxy climate records?

The common period for the proxies is simply the period where all proxies have data. The actual dates shift depending on the network; however it is always at least 100 years long. This is described in Appendix B4.

Page 5556, lines 16-17: Did the time series of these EOF's show significant relationships with commonly used indices of ENSO (e.g. the SOI or Niño 3.4 SST index)?

Yes they do. The PCs associated with these EOFs indeed showed a significant relationship with ENSO indices, and **this is now addressed in Appendix B1**.

Page 5557, lines 21-22: How do these training and validation periods relate to known PDO-driven variations in ENSO strength and variability?

This comment is no longer relevant, as we have adapted the reconstruction method to use model data instead of 20CRv2c to perform the calibration and validation. **However, we have now also included a discussion of potential links with PDO in Section 5.**

Page 5563-5564: Given the inconclusive nature of the LOO results, why spend so much space discussing them?

As the method has changed substantially and calibration-validation is now done using model data, the LOO analysis is no longer relevant. **It has therefore been removed from the paper entirely.**

Page 5565, line 1: 'consistent positive correlation' – between what?

Between the GCM's temperature and precipitation PCs. **This is now stated more clearly in Section 5.**

Page 5571, lines 16-17: Do the authors mean temperature and precipitation reconstructions?

Yes, this refers to instances where the original authors have translated the proxy (e.g. d18O) into temperature or precipitation already. **This is now clarified in Appendix A.**

Page 5574, lines 2-21: How much variance was explained by EOF 1 for the temperature and precipitation data sets?

The 20CRv2c precipitation EOF captures 11.57% of the variance; the temperature EOF captures 9.75% (Appendix B1).

Page 5593, Table 1: Provide more details in the caption, e.g. what calendar year 'start' and 'end' refer to; also please provide full references (Supplementary material?) for cited papers and data sets.
Page 5594, Table 2: as for Table 1

Start and end years here are in Year BP; **this has been added to the captions**. Full references are already included in the References list. **Additional information on Signal-to-noise and weightings is now also included in the tables.**

Page 5564, lines 11-13: The statement 'The two ENSO reconstructions.........' contains two negatives which makes it hard to follow – does it mean they provide evidence of agreement?

The Discussion and Conclusion have been rephrased and restructured to improve clarity of these and other statements.

The remaining comments are generally aesthetic and have been incorporated in the revised ms where still relevant:
Page 5550, line 3: 'centred in the equatorial Pacific' rather than 'over'.
Page 5550, line 4: make it clear that there are two phases of ENSO which produce different surface climate anomalies throughout much of the tropics and, via teleconnections, to some higher latitude locations.
Page 5550, line 8: 'have produced different/dissimilar reconstructions' rather than 'varying'.
Page 5550, line 13: 'Empirical Orthogonal Function (EOF)'.
Page 5551, line 4: Indicate where these SST and surface pressure patterns occur.
Page 5551, line 10: Where did these deaths occur?
Page 5551, line 16: 'variability' rather than 'trends'.
Page 5551, line 24: 'proxy climate records' rather than just 'proxy records'.
Page 5552, lines 11-12: Provide references to support this statement
Page 5552, lines 20-21: Spell out AMOC and NAO.
Page 5553, line 1: Which 'discrepancies'? Also change 'trends' to 'variation or variability' as 'trend' tends to imply a uni-directional change.
Page 5553, line 5: Provide reference(s) for previous statements.
Page 5553, line 15: 'into past climate variability' – it is not just climate 'events'.
Page 5554, line 15: 'reconstructions' rather than 'proxies'.
Page 5557, lines 27-28: Reference for 'coefficient of efficiency'?
Page 5560, line 18: What is a 'coherent trend'?
Page 5561, line 15: Label and refer to figure components as Figure 3a and 3b rather than 'top' and 'bottom'.
Page 5562, line 3: Which 'maps'? refer to specific figure.
Page 5599, Figure 1: Is the 30-year a simple or weighted average?
Page 5601, Figure 3: Provide colour scale bar for EOF loadings; label a) and b).
Page 5604, Figure 6: Not very comprehensible figure.

Yours faithfully,

Lilo Henke

(References can be found after responses to Reviewer 2.)

Reviewer 2

We thank the reviewer for taking the time to provide a review. We have broken down the comments into subheadings (*italic*) followed by our responses in plain text. Changes to the ms are in **bold**.

1. *ENSO definition ENSO is an interannual phenomenon. Looking at 30-year averages and calling that ENSO is more than a stretch. That choice was not explained particularly well in the paper, though it has major consequences for the research, blurring interannual and decadal signals, and drastically reducing the number of degrees of freedom.*

[this is the largely same as our response to reviewer 1's comment 4.]
Both reviewers raised the issue of reconciling 30-year averages and the interannual ENSO timescales. Our aim here was not to comment on ENSO interannual variability, frequency or amplitude as did Li et al. (2013) and Emile-Geay et al. (2013), but rather ENSO-*like* climate change similar to many long-term, lower resolution proxy studies (cf. Moy et al. 2002, Conroy et al. 2008, Yan et al. 2011). This was clearly not conveyed very well and we apologise for the confusion caused. We absolutely agree that it is not possible to translate this directly into ENSO variability, frequency and intensity and thank the reviewers for highlighting the need to clarify this. Our interest is in the extent to which climate change was El Nino-like or La Nina-like during the past 1000 years. Part of the motivation for this is the paper of Yan et al. (2011). which suggests that precipitation proxies indicate El Nino like change while temperature proxies indicate La Nina like change. Our understanding of current climate suggests that this is unlikely, but it would be very important if true. **We have adjusted the Introduction to emphasise that this aim. The Discussion is similarly rephrased and restructured to shift the focus to long-term ENSO-like changes. We have also adjusted the methodology in response to the comment about degrees of freedom (see also response to comment 5c).**

In response to the comment about blurring interannual and decadal signals, we have also included a discussion on the PDO (Section 5).

2. *Climate target The whole point of pseudoproxy experiments is to have a known target to compare to. The authors choose instead an assimilated product (20CRv2), which is then "replicated in the time dimension to get a length of 1000 years" (B4, L12). This is madness. Why not use a CMIP5/PMIP3 simulation? Since the authors are not using their method to generate an actual reconstruction that they seem to believe in, they might as well stay in pseudoproxy land, where they would have perfect control over the experimental design. Instead, they have to make up some data from the 20C reanalysis through unspecified means, which is downright scary. At the very least, the generating mechanism for the data needs to be transparent.*

In the revised ms, we have used a modified scheme for calibrating and validating our proxy networks.

First, we run our calibration experiment, wherein we derive our optimal networks of proxy locations, using the PMIP last 1000 year simulation from a GCM (GCM_cal), as suggested by the reviewer. Because the PMIP simulations show a different ENSO pattern than 20CRv2, the quality of our reconstruction will be degraded. However, on balance, we agree that this is preferable to our previous reconstruction method that used 20CRv2 alone at the cost of satisfactorily representing degrees of freedom in the data.

Our validation experiment uses the PMIP last 1000 year simulation from a different GCM (GCM_val). This presents a difficult target for our networks, but one that makes some allowance for the fact that the real El Nino pattern that we run our reconstruction on is different from the El Nino pattern presented by the PMIP simulation used to calibrate our network. When calculating critical values, rather than using white noise to compare our pseudoproxy reconstruction against as in the original ms, we use a control (ie unforced) simulation from GCM_val processed via our networks in exactly the same way. In practice, the spectrum of the control reconstruction is very close to white due to the small variation in unforced ENSO dynamics on this timescale. However, it is not inconceivable that our reconstruction method introduces some unwanted autocorrelation, and so we agree with the reviewer that it makes sense to revise this.

GCM_cal and GCM_val are chosen based on the similarity of their ENSO-like EOF to that of 20CRv2c at the proxy locations (Appendix B2). This ensures that the process tests the sensitivity of the networks to variations in the representation of the ENSO pattern, while ensuring these different representations are still as realistic as possible.

3. *Pseudoproxy design The field has evolved a bit in recent years, now enabling the generation of more realistic pseudoproxies using proxy system models (Tolwinski-Ward et al, 2011; Dee et al 2015). Using an explicit process model of tree-ring growth, Evans and al (2015) found quite different results from the usual "climate + white noise" pseudoproxy design. They authors pay lip service to it in section 5.1 but don't actually use it. Given that their paper is entirely centered on pseudoproxies and that all these PSMs are publicly available, they have no excuse but to keep up with the times*

As indicated by the reviewer, one possible approach is to build pseudoproxies using a proxy system model. However, for many proxies this requires access to isotope enabled GCM data (Dee et al., 2015), which is not an option for the majority of available PMIP GCMs. We therefore concede this point as a caveat in our network selection and validation and one for further research. The VSlite tree ring model (Tolwinksi-Ward et al., 2011) only requires temperature and precipitation as inputs, however. **We have therefore produced all treering pseudoproxies using VSlite.**

In the new ms we also process our real proxy data using Inverse Transform Sampling so that they are more normally distributed (Emile-Geay et al. 2016). In the absence of detailed proxy models for each proxy, this is a sensible way of making the data more comparable to our simple pseudoproxies.

In addition, we have addressed another very important source of error in pseudoproxy reconstructions: the error in GCM representation of climate's spatiotemporal variability. These errors lead to suboptimal network selection due to inaccurate representation of the ENSO-like climate change pattern and other patterns of climate variability. By using two different GCMs for the calibration / validation exercise, we have tested the robustness of the proxy networks to this ENSO pattern (see also response to comment 2). It also gives us some limited insight into what extent our results are likely to be compromised by changes in the pattern of El Nino-like climate change (identified as an issue by Power et al., 2013 for future climate change).

As the reviewer notes, real proxies may show a response to a combination of these (and other) factors. Evans et al. (2014) explored this by testing a reconstruction based on pseudoproxies that respond to both temperature and precipitation. In our paper, we acknowledge this issue, and focus on proxies that are as much as possible just a function of either temperature or precipitation. This leads to the exclusion of some proxies that are well-known to be related to ENSO, but that respond to, for example, both temperature and salinity or temperature and precipitation (see response to reviewer's comment 4 below).

4. *Unjustified proxy selection Nowhere in the paper could I find a rational justification for the choice of proxies. It leaves out the best ENSO proxy developed for the past millennium (Cobb et al, 2003), and incorporates many dubious ones from regions that have only marginal teleconnections to ENSO.*

[this is largely the same as our response to reviewer 1's comment 1.]
We endeavoured to include all precipitation and temperature proxies currently publicly available for the study region. As reviewer 1 notes, there are indeed several coral records available that were not included in this study. The reason for this is that it was stated explicitly in the associated publications that the recorded d18O signal was in fact a combination of SST and SSS (or SST and precipitation). Most authors also state that it is not possible to disentangle the two climate variables (McGregor & Gagan 2004, Hereid et al. 2013, Osborne et al. 2014) While this is not an issue when, for example, one is using the single proxy as a recorder of ENSO events in a location where SST and SSS have the same-sign impact on the d18O of the coral, it does present a problem for our method of reconstruction. As we are using temperature- and precipitation-specific EOF patterns, we need proxies that are as univariate as possible (i.e. only respond to one of these two climate variables). **In response to the comments, we have included more temperature and precipitation proxy records in the revised analysis, including a suite of coral records used in Tierney et al. (2015). The new proxy records are incorporated in Tables 1 and 2, and an updated discussion on the proxy selection is available in Appendix A. This has resulted in an additional 12 precipitation proxies and 55 temperature proxies.**

After revising all proxy records, the Cobb et al. (2003) coral record is excluded in the new msdue to the fact that the signal is not clearly dominated by temperature but is a combination of temperature and salinity (Appendix A).

5. *fanciful statistics*

This comment consists of four parts, which we address here:

a) the statistical methodology used for reconstruction is an extreme version of principal component regression, truncated at 1 pattern. This in itself is not the worst thing, but PCR is known to yield extremely biased reconstructions in the presence of noise. Total least squares (orthogonal regression) can mitigate that a bit, but PCR isn't outlandish as a first pass. However, the effect of this truncation on ENSO reconstruction should be assessed. For instance, it is known that ENSO tends to be split among different modes (most commonly, EOFs 1 and 2 of monthly-mean SST), so only selecting one can leave out an important part of the signal.

We have experimented with using a more "optimal detection" style technique, where we regress data onto multiple EOFs in order to combat the bias the arises from mixing other signals not due to El Nino-like change into our reconstruction. However, we found that even at 2 EOFs data availability is too low to constrain estimates of changes in time. It is for this reason that we settled on an the empirical technique, whereby rather than use all available data (as in standard PCR) we successively add pseudoproxies that most improve (or least damage) the reconstruction in order to find the best possible network. We therefore attempt to avoid networks that mix in large non-El Nino-like signals, which may occur if we use all available proxies weighted by one EOF. The success or failure of the network is measured by the new validation procedure. (See response to comment 2 above.)

The reviewer states that multiple EOFs should be used to resolve the ENSO-like pattern. On annual and longer timescales this is not typical, both in studies of paleoclimate (e.g. Braganza, 2009) or GCM studies of future climate change where all output is known (e.g. Power et al. 2013). Unfortunately it is also not possible to investigate multiple EOFs given the data limitations we face. **Nevertheless, we have made clear in the revised ms that we are not addressing ENSO Modoki (which is often defined as EOF2 or a combination of EOF1 and 2; Section 5).**

b) But the worst part of the procedure is the generation the pseudoproxies and then double-dipping between the calibration and verification periods. The authors claim that it "somewhat compromises the independence of the validation"; actually, it completely compromises it. There is no validation unless it is entirely independent of calibration.

This is a very good point and we thank reviewer 2 for raising it. To mitigate this, **we have adjusted the method to use pairs of PMIP last-millennium model runs instead (see response to comment 2).** In each case, model A is used for calibration and model B for validation, ensuring complete separation. The new reconstruction has the weakness that it uses an ENSO-like pattern and temporal variability that is somewhat different to observations. However, because we are using pairs of models each with its own ENSO-like EOF pattern and temporal variability, we produce and investigate a measure of the impact of this problem in our pseudoproxy experiments.

c) The bottom line is that by focusing on 30-year averages, they leave themselves so few degrees of freedom that there is no room for validation any more. This would be mitigated by using long GCM integrations, (1000 years / 30 ~33 d.o.f., not very high, but better than 1 or 2). Even better would be too look at annual signals, since so many of the proxies are annually resolved and since ENSO is in the 2-7y band.

As explained in our response to comment 1 above, our interest is in long-term ENSO-like climate trends and not interannual variability. We therefore continue to investigate 30-year means. **However, we are now using PMIP simulations for both pseudoproxy target and critical benchmarks to improve the representation of degrees of freedom, as the reviewer suggests.**

d) Another major problem is that the CE statistic appears to be benchmarked against white noise predictors, whereas with 30 year averages one needs to account for very high levels of autocorrelation, which alone are enough to doom the results.

We now use R instead of CE as a benchmark, as testing showed that the nature of the reconstruction method renders CE unreliable (Appendix B5). In response to the reviewer's comments, however, we now benchmark against control runs (ie unforced simulations) taken from the PMIP archive and fed through our networks in the same way as the PMIP last 1000 year simulations. Contrary to the reviewer's statement, inspection of the autocorrelation of unforced ENSO variability in climate models is close to zero for thirty year means. Nevertheless, we agree that it is useful to establish this for our networks.

6. *spatial pattern the question of whether the MCA was El Niño or La Niña-like seems to have been largely motivated by the work of Mann et al (2009). Wang et al (2015) showed earlier last year that it was an artifact of the dataset and method they use, and that changing either would change the result. A paper focusing on this question should acknowledge this research*.

Unlike reviewer 2's assumption that this was motivated by Mann et al. (2009), the main point of departure for this work was Yan et al. (2011). **This is made clearer in the revised ms.** Our primary interest is in the possibility that temperature and precipitation patterns apparently show opposing ENSO-like patterns of change. However, **we have referenced and discussed Wang et al. (2015) in Section 5.**

7. *unclear methods a lot of the methodology is unusual enough that it needs to be very thoroughly presented here. I deplore the lack of equations to explain how certain things were done. Public code would be another way to enable an actual peer-review of the methodology.*

We apologise if reviewer 2 felt that the methodology was not clearly presented; we attempted to find the balance between conciseness and detail and have apparently not done this satisfactorily. **We have expanded the Methods sections (Section 3 and Appendix B), including more equations and a diagram of the network creation process (Figure 1).**

8. *Moy The record by Moy et al keeps being used as an "ENSO" proxy, though some of its authors have since retracted their interpretation of it. http://www.sciencedirect.com/science/article/pii/S0277379108001352 The community has got to stop clinging to an outdated interpretation*

We do not know any literature that explicitly questions the interpretation of this record as an ENSO proxy. The paper cited by reviewer 2 does not call this into question either. The only sentence in it referring to this record states “The middle–late Holocene increase in the flux of clastic sediment to alpine lakes in the tropical Andes is similar to the record of El Niño frequency (Rodbell et al., 1999; Moy et al., 2002), and thus may reflect a fundamental change in the nature of ENSO at this time.” (Rodbell et al. 2008). We are unable to act on the concerns of unnamed researchers outside the peer-review literature.

9. *quirky problematization Science progresses by "standing on the shoulders of giants". While none of the published ENSO reconstructions are perfect (they are most likely all wrong), they should serve as a starting point of the analysis. While the paper does cite recent ENSO reconstruction at one point or other, it seems to happen as an afterthought; instead, the divergence between published estimates should really be the point of departure of the analysis.*

We chose not to focus on these reconstructions in detail as our focus is really on comparing long-term trends paying particular attention to the difference between the MCA and the LIA. As stated in the discussion, those reconstructions focusing on interannual ENSO variability do not cover both these periods.

We hope that by having clarifiedour intention to look at ENSO-*like* climate trends rather than interannual ENSO variability the reviewer can agree that these high-resolution but shorter ENSO reconstructions are of less interest (except for methodological similarities and differences). Instead, we are taking the divergences among the multitude of long-term, lower-resolution ENSO proxies as our starting point, and particularly the conclusions of Yan et al. (2011). **We have emphasised this more clearly in the Introduction and Discussion of the new ms.**

Yours faithfully,

Lilo Henke

References

Braganza, K., Gergis, J. L., Power, S. B., Risbey, J. S., & Fowler, A. M. (2009). A multiproxy index of the El Niño-Southern Oscillation, A.D. 1525-1982. Journal of Geophysical Research: Atmospheres, 114, 1–17. doi:10.1029/2008JD010896

Cobb, K. M., Charles, C. D., Cheng, H., & Edwards, R. L. (2003). El Niño/Southern Oscillation and tropical Pacific climate during the last millennium. *Nature*, 424(July), 271–276. doi:10.1038/nature01779

Cole, J. E., Fairbanks, R. G., & Shen, G. T. (1993). Recent variability in the southern oscillation: isotopic results from a tarawa atoll coral. Science, 260(5115), 1790–1793. doi:10.1126/science.260.5115.1790

Conroy, J. L., Overpeck, J. T., Cole, J. E., Shanahan, T. M., & Steinitz-Kannan, M. (2008). Holocene changes in eastern tropical Pacific climate inferred from a Galápagos lake sediment record. *Quaternary Science Reviews*, 27, 1166–1180. doi:10.1016/j.quascirev.2008.02.015

Dee, S., Emile-Geay, J., Evans, M. N., Allam, A., Steig, E. J., & Thompson, D. M. (2015). PRYSM: An open-source framework for PRoxY System Modeling, with applications to oxygen-isotope systems. Journal of Advances in Modeling Earth Systems, 7, 1220–1247. doi:10.1002/ 2015MS000447

Emile-Geay, J., Cobb, K. M., Mann, M. E., & Wittenberg, A. T. (2013). Estimating central equatorial pacific SST variability over the past millennium. Part II: Reconstructions and Implications. *Journal of Climate*, 26, 2302–2328. doi:10.1175/JCLI-D-11-00511.1

Emile-Geay, J., & Tingley, M. (2016). Inferring climate variability from nonlinear proxies. Application to paleo-ENSO studies. *Climate of the Past*, 12, 31–50.

Evans, M. N., Smerdon, J. E., Kaplan, A., Tolwinski-Ward, S. E., & Gonzalez-Rouco, J. F. (2014). Climate field reconstruction uncertainty arising from multivariate and nonlinear properties of predictors. *Geophysical Research Letters*, 41(24), 9127–9134. doi:10.1002/2014GL062063

Hereid, K. a., Quinn, T. M., Taylor, F. W., Shen, C. C., Edwards, R. L., & Cheng, H. (2013). Coral record of reduced El Niño activity in the early 15th to middle 17th centuries. *Geology*, 41(October), 51–54. doi:10.1130/G33510.1

Li, J., Xie, S.-P., Cook, E. R., Morales, M. S., Christie, D. a., Johnson, N. C., … Fang, K. (2013). El Niño modulations over the past seven centuries. *Nature Climate Change*, 3(9), 822–826. doi:10.1038/nclimate1936

Mann, M. E., Zhang, Z., Hughes, M. K., Bradley, R. S., Miller, S. K., Rutherford, S., & Ni, F. (2008). Proxy-based reconstructions of hemispheric and global surface temperature variations over the past two millennia. Proceedings of the National Academy of Sciences of the United States of America, 105(36), 13252–13257. doi:10.1073/pnas.0805721105

Mann, M. E., Zhang, Z., Rutherford, S., Bradley, R. S., Hughes, M. K., Shindell, D., … Ni, F. (2009). Global Signatures and Dynamical Origins of the Little Ice Age and Medieval Climate Anomaly. Science, 326(5957), 1256–1260. doi:10.1126/science.1177303

Masson-Delmotte, V., Schulz, M., Abe-Ouchi, A., Beer, J., Ganopolski, A., González Rouco, J. F., … Rouco, J. F. G. (2013). Information from Paleoclimate Archives. In T. F. Stocker, D. Qin, G.-K. Plattner, M. Tignor, S. K. Allen, J. Boschung, … P. M. Midgley (Eds.), Climate Change 2013: The Physical Science Basis. Contribution of Working Group I to the Fifth Assessment Report of the Intergovernmental Panel on Climate Change (pp. 383–464). Cambridge, United Kingdom and New York, NY, USA: Cambridge University Press. doi:10.1017/CBO9781107415324

McGregor, H. V., & Gagan, M. K. (2004). Western Pacific coral δ18O records of anomalous Holocene variability in the El Nino-Southern Oscillation. *Geophysical Research Letters*, 31, 1–4. doi:10.1029/2004GL019972

Moy, A. D., Seltzer, G. O., Rodbell, D. T., & Andersons, D. M. (2002). Variability of El Niño/Southern Oscillation activity at millennial timescales during the Holocene epoch. *Nature*, 420, 162–165. doi:doi:10.1038/nature01194

Osborne, M. C., Dunbar, R. B., Mucciarone, D. a., Druffel, E., & Sanchez-Cabeza, J. A. (2014). A 215-yr coral δ18O time series from Palau records dynamics of the West Pacific Warm Pool following the end of the Little Ice Age. *Coral Reefs*, 33, 719–731. doi:10.1007/s00338-014-1146-1

Power, S., Delage, F., Chung, C., Kociuba, G., & Keay, K. (2013). Robust twenty-first-century projections of El Niño and related precipitation variability. *Nature*, 502(7472), 541–5. doi:10.1038/nature12580

Rodbell, D. T., Seltzer, G. O., Mark, B. G., Smith, J. A., & Abbott, M. B. (2008). Clastic sediment flux to tropical Andean lakes: records of glaciation and soil erosion. *Quaternary Science Reviews*, 27(15-16), 1612–1626. doi:10.1016/j.quascirev.2008.06.004

Schluessel, P., Emery, W. J., Grassl, H., & Mammen, T. (1990). On the bulk-skin temperature difference and its impact on satellite remote sensing of sea surface temperature. J. Geophys. Res., 95(C8), 13,341–13,356. doi:10.1029/JC095iC08p13341

Tolwinski-Ward, S. E., Evans, M. N., Hughes, M. K., & Anchukaitis, K. J. (2011). An efficient forward model of the climate controls on interannual variation in tree-ring width. *Climate Dynamics*, 36(11-12), 2419–2439. doi:10.1007/s00382-010-0945-5

Wang, J., Emile-Geay, J., Guillot, D., McKay, N. P., & Rajaratnam, B. (2015). Fragility of reconstructed temperature patterns over the Common Era: Implications for model evaluation. Geophysical Research Letters, 42(17), 7162–7170. doi:10.1002/2015GL065265

Yan, H., Sun, L., Wang, Y., Huang, W., Qiu, S., & Yang, C. (2011). A record of the Southern Oscillation Index for the past 2,000 years from precipitation proxies. *Nature Geoscience*, 4(9), 611–614. doi:10.1038/ngeo1231

Manuscript prepared for Clim. Past
with version 2014/09/16 7.15 Copernicus papers of the LaTeX class copernicus.cls.
Date: 14 July 2016

Was the Little Ice Age more or less El Niño-like than the ~~Mediaeval~~ Medieval Climate Anomaly? Evidence from hydrological and temperature proxy data

Lilo M.K. Henke[1], F. Hugo Lambert[2], and Dan J. Charman[1]

[1]Department of Geography, College of Life and Environmental Sciences, University of Exeter, Amory Building, Rennes Drive, Exeter, UK, EX4 4RJ
[2]Department of Mathematics, College of Engineering, Mathematics and Physical Sciences, Harrison Building, Streatham Campus, University of Exeter, North Park Road, Exeter, UK, EX4 4QF

Correspondence to: Lilo Henke (lmkh201@exeter.ac.uk)

Abstract. The El Niño-Southern Oscillation (ENSO) ~~, an ocean-atmosphere coupled oscillation over the equatorial Pacific,~~ is the most important source of global climate variability on ~~inter-annual time scales . It~~ interannual time scales and has substantial environmental and socio-economic consequences~~such as devastation of South American fish populations and increased forest fires in Indonesia~~. However, it is unclear how it interacts with large-scale climate states over longer (decadal to centennial) timescales. The instrumental ENSO record is too short for analysing long-term trends and variability ~~, hence proxy data is~~ and climate models are unable to simulate past ENSO states accurately. Proxy data are used to extend the record~~. However,~~ , but different proxy sources have produced ~~varying reconstructions of ENSO~~dissimilar reconstructions of long-term ENSO-like climate change, with some evidence for a temperature–precipitation divergence in ~~ENSO trends~~ ENSO-like climate over the past millennium, in particular during the ~~Mediaeval~~ Medieval Climate Anomaly (MCA; AD ~~-~~$\sim$800–1300) and the Little Ice Age (LIA; AD ~~-~~$\sim$1400–1850). This throws into question the stability of the modern ENSO system and its links to the global climate, which has implications for future projections. Here we use a new statistical approach using ~~EOF-based~~ Empirical Orthogonal Function (EOF) based weighting to create two new large-scale ~~ENSO reconstructions~~ reconstructions of ENSO-like climate change derived independently from precipitation proxies and temperature proxies respectively. The method is developed and validated using model-derived pseudoproxy experiments that address the effects of proxy dating error, resolution and noise to improve uncertainty estimations. ~~The precipitation ENSO reconstruction displays a significantly more El Niño-like state during the LIA than the MCA, while the temperature reconstruction shows no significant difference. The trends shown in the precipitation ENSO reconstruction are relatively robust to variations in the~~

~~precipitation EOF pattern~~We find no evidence that temperature and precipitation disagree over the ENSO-like state over the past millennium, but neither do they agree strongly. There is no statistically significant difference between the MCA and the LIA in either reconstruction. However, the temperature reconstruction suffers ~~significantly~~ from a lack of high-quality ~~, favourably located proxy records~~ proxy records located in ENSO-sensitve regions, which limits its ability to capture the large-scale ENSO signal. Further expansion of the palaeo-database and improvements to instrumental, satellite and model representations of ENSO are needed to fully resolve the discrepancies found among proxy records and establish the long term stability of this important mode of climatic variability.

1 Introduction

The El Niño-Southern Oscillation (ENSO) is the most influential source of ~~inter-annual~~ interannual variability in the modern climate. ~~Defined by anomalous sea surface temperatures (SSTs) and surface pressure patterns~~The 'warm' El Niño state is characterised by a weaker sea surface temperature (SST) gradient across the equatorial Pacific and a shift in precipitation from the western Pacific toward the central Pacific, while the 'cool' la Niña state is roughly the opposite. Although ENSO originates in the tropical Pacific, it has ~~substantial environmental and socio-economic consequences. For example, the 1997-1998 strong~~ far-reaching effects through teleconnections on some regions in higher latitudes, and El Niño ~~event caused intense forest and peat fires in Indonesia which led to additional carbon dioxide (CO$_2$) releases equivalent to 13-14of the contemporary global annual emissions (Page et al., 2002) . It also devastated fisheries along the Pacific coast of South America (cf Badjeck et al., 2010) , has been linked to disease outbreaks (cf Hjelle and Glass, 2000; Kovats et al., 2003) , and caused an estimated 22, 000 deaths and costs of over US36 billion (Buizer et al., 2000) .~~

~~It~~ years are generally anomalously warm on a global scale. However, it is unclear whether there is a link between anomalously warm or cool periods and the two ENSO states on decadal to centennial timescales. Given the severe socio-economic consequences of ENSO events (Hjelle and Glass, 2000; Page et al., 2002; Kovats et al., and a warmer future under continued anthropogenic warming, it is important to understand the ~~natural range of ENSO variability to determine whether events such as the 1997-98 El Niño are truly~~ '~~extreme'. Knowledge of inherent ENSO variability is vital for placing the relatively short observed record into a long-term context~~natural' long-term ENSO and its interaction with the climate. It allows for an evaluation of the effects of anthropogenic impacts on recent and future ENSO ~~trends, which is an area of active research (Collins, 2005; Guilyardi et al., 2009; Vecchi and Wittenberg, 2010; Bellenger et al., 2014) . Most current global climate~~ behaviour (Collins, 2005; Guilyardi et al., 2009; Vecchi and Wittenberg, 2010; Bellenger et al., 2014) .

Recent multi-model studies of projected changes in ENSO under anthropogenic warming suggest robust changes to ENSO-driven temperature and precipitation, including an increase in extreme

El Niño (Cai et al., 2015a) and La Niña (Cai et al., 2015b) events, and changes in the ENSO SST pattern and ENSO-driven precipitation variability (Power et al., 2013) . However, most current general circulation models (GCMs) ~~are deficient in their ability to~~ cannot simulate many aspects of the modern day ENSO accurately, often overestimating the western extent of the Pacific Cold Tongue and failing to correctly simulate central Pacific precipitation anomalies, ENSO feedbacks, and ENSO amplitude (Bellenger et al., 2014; Collins, 2005; van Oldenborgh et al., 2005).This translates into uncertainty over ~~their~~ simulations of past ~~(and future) changes in ENSO~~ENSO-like climate change, calling for alternative sources of climatic information to supplement, complement and corroborate the model and instrumental data. This is done using proxy climate records such as ~~tree rings~~treerings, tropical ice cores, sediment cores and corals (Jones and Mann, 2004) .

There are very few annually-resolved proxy records available longer than ∼500 years (Mann et al., 2008) . The issue with high-resolution proxies is that they tend to be short in length; trees and corals, for example, rarely live beyond a few centuries (Jones and Mann, 2004) . Some such highly resolved records are available for the more distant past, but these generally offer snapshots rather than continuous records (McCulloch et al., 1996; Corrège et al., 2000; Abram et al., 2009) . However, there are several long, lower-resolution proxy records of ENSO variability on decadal to millennial scales, often derived from lake sediments (cf Conroy et al., 2010) , marine sediments (cf Barron and Anderson, 2011) , or speleothems (cf Maupin et al., 2014) . While these are unable to capture the interannual frequency and amplitude of individual ENSO episodes, they provide an insight into longer-term ENSO-like climate states and average ENSO behaviour. Although there are some endeavours to combine some low-resolution proxies, often to capture spatial gradients (Conroy et al., 2010; Yan et al., 2011b; Anderson, 2012) , there has not, to our knowledge, been a comprehensive effort to systematically merge a large set of such low-resolution records to create a long-term reconstruction of ENSO-like climate variability. Doing this could shed light on the long-term stability of ENSO and its links with the wider climate, for example by examining ENSO behaviour under different dominant cool or warm climate states, which in turn can inform our understanding of potential future ENSO-like changes in a warmer world.

~~Proxy~~A number of proxy, instrumental and modelling studies ~~have shown~~ investigate links between ENSO and global ~~and remote regional~~ climate variability on ~~inter-annual~~interannual (Klein et al., 1999; Wang et al., 1999), decadal (Nelson et al., 2011), centennial (Mann et al., 2005; Trouet et al., 2012) and millennial (Cane, 2005; Ivanochko et al., 2005; Moy et al., 2002; Shin et al., 2006) time-scales. A wide range of proxy records and modelling studies point to substantial ~~changes in ENSO~~ shifts in the ENSO-like state of the climate linked to changes in solar variability on orbital time-scales (Clement et al., 2001; Barron and Anderson, 2011), movement of the Intertropical Convergence Zone (ITCZ; Partin et al., 2007; Gomez et al., 2004; Carré et al., 2005; Nelson et al., 2011) and changes in ocean circulation linked to sea level rise (Wanner et al., 2008; McGregor et al., 2008). In the more recent past, changes in solar irradiance and stratospheric aerosol loadings due to volcanic activity have played significant roles in modulating the hemispheric to global scale climate (Mann et al., 2009). The so-called ~~Mediaeval~~ Medieval Climate Anomaly (MCA; ca. AD 800–1200) and the Little Ice Age~~(LIA; ca. AD 1300–1850)~~ (LIA; ca. AD 1300–1850 Yan et al., 2011b) were periods of anomalously warm and cool conditions respectively, at least in the Northern Hemisphere if not globally~~. Proxy~~ (Jones and Mann, 2004; Mann et al., 2009) . Regarding ENSO-like behaviour however, proxy evidence for the past 2000 years appears to be more ambiguous~~regarding ENSO behaviour however~~. A range of proxies point to a more northerly ITCZ (Haug et al., 2001; Sachs et al., 2009; Tierney et al., 2010) during the MCA, which is characteristic of La Niña-like conditions and is in agreement with warming patterns found in multiproxy reconstructions of hemispheric and global scale temperature ~~(e.g. Mann et al., 2009)~~ (cf Mann et al., 2009) . Langton et al. (2008) similarly infer a reduction in ~~ENSO~~ El Niño-like activity during the MCA based on ocean basin ventilation changes in Indonesia. ~~Haug et al. (2001) propose a link with climatic processes in the northern mid-latitudes, such as a strengthened AMOC and a more positive NAO (see also Trouet et al., 2009, 2012) .~~ In contrast, a Southern Oscillation Index reconstruction based on two proxy records ~~(Yan et al., 2011a)~~ (Yan et al., 2011b) shows an El Niño-like state during the MCA and a La Niña-like LIA. This seems to be supported by a number of other precipitation proxies from the West Pacific ~~(Yan et al., 2011b)~~ (Yan et al., 2011a) and East Pacific (Moy et al., 2002). Other precipitation proxies indicate a highly variable ENSO during the LIA, including two multidecadal droughts in Java (Crausbay et al., 2006), high amplitude rainfall fluctuations in Madagascar (Brook et al., 1999), and three southerly ITCZ excursions (Haug et al., 2001).

These discrepancies in ~~ENSO trends between various~~ long-term ENSO-like variations between proxy records raise two important questions. The current dynamical understanding of ENSO is underpinned by the strong relationship between temperature and rainfall observed ~~in the modern day~~today, and the relationships between the ENSO 'source region~~,~~', the tropical Pacific, and teleconnected regions, which largely fall between 40°S and 40°N. ~~In light of apparently conflicting stories told by~~ As Yan et al. (2011b) highlight, however, temperature and precipitation ~~proxy records as highlighted by Yan et al. (2011a) , the first question is to what extent~~ proxies appear to disagree on the ENSO-like states of the MCA and the LIA. To what extent, therefore, does the modern-day precipitation–temperature relationship in the source and teleconnected regions ~~continues~~ continue to exist in the past~~.~~ ? The second question concerns the relation of ENSO to the wider climate; is there a link between global temperatures and long-term ENSO state on multidecadal to centennial time-scales? A comparison between the MCA and the LIA can give some insight into this, and may hold some clues to what we can expect under anthropogenic climate change.

~~Hence the~~ The use of proxy archives ~~such as corals, tree rings and sediment cores~~ can contribute valuable insights on past ~~climatic events and behaviours~~ climate variability by extending the instrumental records back in time, but substantial uncertainties remain. This is because all ~~proxies~~ reconstructions have inherent limitations and ambiguities that must be identified and dealt with appropriately. These include resolution, dating errors, noise, limited and/or skewed spatial coverage, and nonlinear responses to the climatic variable of interest (Jones et al., 2009). Various statistical techniques have been employed to create multiproxy reconstructions of climatological phenomena, broadly falling into the categories ‘composite plus scaling’ (CPS) or ‘climate field reconstruction’ (CFR) (Jones et al., 2009). CPS encompasses any method which involves combining standardised proxy records into a single reconstruction which is subsequently calibrated to a known timeseries of the target variable (e.g. instrumental temperature record) to provide a quantitative estimate of the variable. CFRs, on the other hand, aim to reconstruct large-scale spatial patterns of climatic change using covariance between proxies and instrumental data. Within both methods there is a wide variety of approaches; see Jones et al. (2009) for ~~more~~ detailed descriptions and examples of both CPS and a range of CFR methods. The focus of this study – comparing the climate signals in temperature and precipitation proxy records separately – calls for a slightly different approach.

Here we create two new ENSO reconstructions~~–~~, one derived from temperature proxies and one from precipitation proxies~~–~~, using a new method for assessing the stability of the modern-day ENSO patterns in the source region and the wider teleconnected regions. In a fashion similar to e.g. Braganza et al. (2009), proxy records are not tuned to instrumental data other than a simple location-dependent weighting. While this precludes direct quantitative comparisons, it removes the bias towards high-frequency trends that stems from calibrating to the relatively short (∼150 year) instrumental record (or indeed any short record; Cook et al., 1995; Jones and Mann, 2004). The method amplifies the ENSO component of proxy records and simultaneously attempts to quantify uncertainty related to noise and incomplete spatio-temporal data coverage, whilst maximising the use of a wide range of tropical proxies. With this, we aim to answer two questions:

1. Do temperature and precipitation proxies show consistent long-term ENSO behaviour over the last millennium?

2. Do the LIA and the MCA differ significantly in their mean ENSO state?

Section 2 provides a description of the proxy and instrumental/reanalysis data used in this study and a concise overview of the methodology is given in Sect. 3. The results and discussion of the findings are presented in Sects. ~~??~~ 4 and 5 respectively before revisiting the research questions and making concluding remarks in Sect. 6.

2 Data description

2.1 Proxy records

For this study, a comprehensive effort was made to collect all published proxy precipitation and temperature records between 40°S – 40°N that cover the last 2000 years. The large majority of records were accessed from the NOAA Paleoclimatology and Pangaea Databases (https://www.ncdc.noaa.gov/data-access/paleoclimatology-discussion/datasets). In addition, over 200 ~~tree ring~~ treering records were taken from the dataset used by Mann et al. (2008), and hence were subject to their criteria including length, intra-site signal coherence and sample density (see Appendix A for details). A set of coral records was taken from the dataset made available by Tierney et al. (2015) ; these were largely temperature proxies although some were assigned as precipitation proxies or excluded altogether based on information in the original publications (see Appendix A for details).

After collection, all records were screened for a maximum dating error of 60 years. Although somewhat arbitrary, this cut-off was decided by taking double the averaging ~~period~~ binwidth of 30 years that ~~is~~ was applied to the data prior to analysis (Appendix B3). This is a step towards addressing the issue of dating uncertainty while allowing a wider range of proxies to be utilised. Proxies with larger dating errors generally have lower (multi-annual to multi-decadal) resolution but are usually also much longer, and are arguably more useful for capturing long-term trends which may be less evident or reliable in annual-resolution proxies ~~(cf Cook et al., 1995; Esper et al., 2002; Mann et al., 2008, on low-frequency trends in t~~ Other quality judgements regarding temporal resolution, record length and proxy location are accounted for by the method ~~explained~~ set out in Sect. 3 and Appendix B.

2.2 Modern climate datasets

Instrumental climate data are the best available in terms of dating accuracy, calibration and physical basis (Jones and Mann, 2004). However, their spatial coverage is not complete and sharply decreases back in time. The nature of the method used in this study calls for full spatial coverage over a long period; therefore, reanalysis products are more suitable. These are combinations of instrumental and satellite data interpolated using models. The 20th Century Reanalysis Version ~~2 (20CRv2~~2c (20CRv2c) is the longest global dataset of atmospheric circulation available, spanning AD ~~1870-2010~~1851-2014. It is based on surface pressure, temperature and sea ice distribution data, filled in with a 'deterministic' Ensemble Kalman Filter (EKF). It has a spatial resolution of 2~~degree~~ °latitude × 2~~degree~~ °longitude × 24 vertical pressure levels, and a temporal resolution of up to 6 hours. It has been demonstrated that the ~~20CRv2~~ 20CRv2c is competent at representing the global tropospheric circulation as well as the mean state and variability of the hydroclimate – for a detailed description and evaluation of the product see Compo et al. (2011). The monthly mean surface air temperature and precipitation rate datasets were downloaded from the NOAA/OAR/ESRL PSD web site (~~http://www. esrl.noaa. gov/psd/)~~ http://www.esrl.noaa.gov/psd/). The 20CRv2c data were regridded to 2°×3° to be comparable to the model data described below (Sect. 2.3). The climatology (for the period 1851-2014) was removed to produce monthly anomalies, which were then averaged to annual resolution.

2.3 General circulation model simulations

There are several comprehensive modelling projects with the aim of improving comparability between general circulation models (GCMs) produced by different teams. GCMs taking part in these projects perform a set of simulations with standardised forcings and boundary conditions. For this study, the pre-industrial control (piControl; pre-1850 parameters, no external forcings) and historical (AD 1850– 2000) runs from the Coupled Model Intercomparison Project 5 (CMIP5; Taylor et al., 2012) were used, in addition to the last millennium (past1000; AD 850–1850) runs from the Paleoclimate Model Intercomparison Project 3 (PMIP3; Braconnot et al., 2011, 2012) . Of the six GCMs which have all three runs available, two were chosen for their similarity to 20CRv2c in terms of spatial ENSO representation (see Appendix B2) for precipitation (climate modelling groups in brackets):

- CCSM4 (National Center for Atmospheric Research)
- GISS-E2-R (NASA Goddard Institute for Space Studies)

And two for temperature:

- IPSL-CM5A-LR (Institut Pierre-Simon Laplace)
- BCC-CSM1-1 (Beijing Climate Center, China Meteorological Administration)

All model datasets were regridded to $2^\circ \times 3^\circ$, converted to anomalies and degraded to annual resolution to enable comparison between models and with 20CRv2c.

3 Methodology

The method used in this study ~~combines 20CRv2-derived temperature and precipitation ENSO patterns with a wide range of proxy records~~ consists of two stages: first, a temperature and a precipitation ensemble of proxy networks is created based on GCM-derived pseudoproxy experiments; then, these network ensembles are used to produce two ~~multiproxy ENSO reconstructions : one based on temperature proxies and one based on precipitation proxies. Through the use of so-called pseudoproxy experiments and an array of statistical approaches, it~~ independent reconstructions of ENSO-like climate change using the real proxy data weighted by temperature and precipitation ENSO patterns from 20CRv2c reanalysis data. This approach attempts to take into account the effects of proxy selection, the temporal limitations of individual proxies, and non-climatic noise. ~~Firstly, all data were normalised to a mean of zero and a standard deviation of one to account for the real proxy data not being calibrated to the instrumental record. The precipitation and temperature data were normalised over their full period, whereas the proxy data were normalised with respect to a common period for which all have data, which was always at least 100 years (see Sect. 3.3). Empirical Orthogonal Function (EOF) analysis was then performed on the 20CRv2 precipitation and temperature datasets, and the respective EOFs with the strongest ENSO-like patterns were retained (in both cases this was the first EOF). These form the basis for allocating weights to~~ A brief overview of the method is given here, with a more extensive description in Appendix B.

3.1 Pseudoproxy creation

Pseudoproxies are simulated proxies that attempt to mimic various sources of uncertainty inherent in the real proxy records.

~~Pseudoproxies were created using 20CRv2 data timeseries from the real proxy location, with added white noise to approximate the effects of~~ This ranges from adding white Gaussian noise with a prescribed signal-to-noise (SNR) ratio to approximate non-climatic ~~noise in the proxies~~random noise, to more sophisticated process-based additions that take into account effects such as dating error, nonlinear and multivariate responses of the proxy sensor to the climate variable, and sampling biases (Mann, 2002; Smerdon, 2012) . The utility of any pseudoproxy exercise lies in the fact that the answer to the question is known, as it can be derived directly from the original model dataset. By putting the 'signal plus noise' pseudoproxies through a method to make a reconstruction of the signal, it allows for inferences about the stability and limitations of the method, estimates of uncertainties due to noise and other proxy record characteristics and, as highlighted by ~~this method~~ the method used here, it provides a way of objectively and systematically selecting the most appropriate data ~~(see Smerdon, 2012, for a good introduction to pseudoproxy experiments) . The proxy records were combined into 1000 optimalproxy networks using such a pseudoproxy approach to automatically select the best combinations. In each of the 1000 runs the pseudoproxies were 'contaminated' by adding different random noise realisations. This approach also acted to filter out proxies whose resolution, length and timespan were unfavourable. Each network derived using pseudoproxies was then usedto create a real-world ENSO timeseries with associated errors using the real proxy data. The final ENSO reconstruction was taken as the mean of all network timeseries, with an uncertainty envelope determined by the ensemble range and the 5–95th percentile of individual members' error ranges. A brief overview follows here, with a detailed methodology~~ (see Smerdon, 2012, for an introduction to pseudoproxy experim

Ideally, all pseudoproxies in this study would be created from proxy system models (PSMs; e.g. Dee et al., 2015) . Unfortunately, many proxies (e.g. $\delta^{18}O$ from corals or speleothems) would require isotope-enabled GCMs which are not available for the model runs used in this study. treering widths (TRW), however, can be easily simulated using the VSLite Model, which is a freely available PSM desgined to estimate TRW based on minimal climatic input (Tolwinski-Ward et al., 2011; Breitenmoser et al., 2014; Evans et al., 2014) . It is a simplified version of the full Vaganov-Shashkin model (Vaganov et al., 2006; Anchukaitis et al., 2006; Vaganov et al., 2011) ar only requires temperature, precipitation and latitude information. All TRW records in the proxy dataset used in this study were thus represented using VSLite derived pseudo-TRW series. For the rest of the proxies, the GCM raw temperature or precipitation series were used.

White gaussian noise was added to all model temperature, precipitation and TRW series. Where the original publications (or in the case of the coral records, Tierney et al., 2015)) provided an indication of the strength of the proxy–climate relationship (e.g. R-value), the SNR was calculated. For all other records, a prescribed signal-to-noise ratio (SNR) of 0.4 (which corresponds to an R-value of ∼0.38) was used, as this has been shown to be a realistic average (Smerdon, 2012) . The median calculated SNR was 0.79 for precipitation and 0.57 for temperature, suggesting the prescribed SNR of 0.4 is a conservative estimate. The pseudoproxies were also degraded to reflect the length, timespan and resolution of the real proxies.

3.2 Network ensemble creation

The creation of a network ensemble was done using a calibration-validation scheme to assess the ability of various pseudoproxy combinations to reconstruct multi-decadal ENSO-like precipitation or temperature variations over the past millennium. As 20CRv2c only covers ∼160 years, it is not suitable for testing over these timespans and the past1000 runs from GCMs were used instead. To account for the fact that the ENSO patterns in GCMs are different from the pattern in 20CRv2c (and the real ENSO pattern is likely to be different again), two different GCMs are used for the calibration and validation stages. This means the sensitivity of the networks to the shape of the ENSO-like pattern is tested. GCM selection is described in Appendix ~~B. The entire process was done separately for precipitation and for temperature~~ B2. The precipitation and temperature calibration GCMs (GCM$_{cal}$) were CCSM4 and ISPL-CM5A-LR, respectively; the corresponding validation GCMs (GCM$_{val}$) were GISS-E2-R and BCC-CSM1-1.

3.3 ~~ENSO reconstruction~~

~~A~~ Using the GCM$_{cal}$ past1000 dataset, a thousand proxy networks were created via an ‘add-one-in’ pseudoproxy algorithm that automatically builds a network based on ~~which additional~~ how much each proxy improves the reconstructive power of the network ~~the most~~(Figure 1). Similar to a forward stepwise regression procedure, GCM$_{cal}$-derived pseudoproxies are gradually added to a ~~‘base’~~ ‘base’ network of zero ~~based on which creates the best *new* network~~ proxies, testing the quality of the network with each addition, until all proxies have been ~~included~~incorporated (Fig. 1 a&b). The final ~~‘optimal’~~ ‘optimal’ network is that which performed best over all steps (Fig. 1 c). By repeating the process 1000 times adding different random noise series ~~with a signal-to-noise ratio (SNR) of 0.4 each time (Smerdon, 2012) , it takes account of variations in ENSO’s influence at different locations and the presence of non-climatic proxy noise~~ to the pseudoproxies each iteration, it addresses the influence of stochastic processes on the ability of a proxy network to optimally reconstruct the large-scale ENSO pattern. ~~The 20CRv2 dataset from which the pseudoproxies were created was split into a training (1950–2010) and a validation (1871-1949) set~~

The reconstruction process itself is a weighted average approach, where the proxy weights are based on the ENSO-like EOF pattern of the GCM$_{cal}$ past1000 run (for the add-one-in network building) or 20CRv2c (for the final reconstruction). First, all (pseudo-)proxies in the network were normalised to a common period of at least 100 years (see Sect. 3.3) and transformed using an inverse transform sampling (ITS; Emile-Geay and Tingley, 2016) to approach a normal distribution. The

EOF ~~pattern (which dictates the proxy weights)was derived from only the training data. Pseudoproxies taken from the full (1871–2010) dataset were weighted ('trained') based on that EOF and networks created accordingly. The ability of these networks to estimate the trueENSO timeseries was then established by testing how well the reconstructions tracked the mean over the validation period using the~~ values W at the proxy locations i were scaled such that their absolute sum at each timestep t is 1 (Equation B3). This EOF scaling deals with the fact that the number of proxies available changes over time, preventing more proxy-dense periods from getting amplified. Each proxy series P was then weighted by its corresponding (scaled, time-variable) EOF value Wn_P. Finally, the n weighted proxy series Pw were summed to create a single reconstruction series $ENSO_r$ (Equation B4. This is essentially a '~~coefficient of efficiency~~sparse' ~~score (CE; Equation **??**). Since there is no standard significance test for CE~~reconstruction of the PC, which is the dot product of the full raw dataset and EOF. The quality of a network was assessed by comparing $ENSO_r$ with the PC using the Pearson rank correlation R (see Appendix B4).

Validation was performed in two steps. First,the 1000 networks produced with the GCM$_{cal}$ were used to make reconstructions using GCM$_{val}$ past1000 data and the GCM$_{cal}$ EOF. Using data from a different GCM ensures complete separation between the calibration and validation periods, and tests the sensitivity of the networks to the spatial stability of the EOF pattern, as the ENSO-like EOF from each model and from 20CRv2c is different. The switch from GCM$_{cal}$ to GCM$_{val}$ thus mirrors the switch between the GCMs and 20CRv2c. Each network was reconstructed 1000 times using GCM$_{val}$ pseudoproxies, again adding different noise realisations for each iteration. Validation test scores were calculated to check the quality of these validation reconstructions compared to the validation PC (calculated using EOF$_{cal}$ and GCM$_{val}$ past1000 data). Second, critical values ~~(CE$_{crit}$) were calculated for each network~~ for the validation test scores were calculated by repeating the ~~reconstructions using pure noise series in lieu of the pseudoproxies~~first validation step but using the GCM$_{val}$ piControl run. If the validation ~~CE~~ R-value of a network failed to exceed ~~CE~~R$_{crit}$, ~~the network's~~ its reconstruction was deemed to be no better than random noise and was consequently discarded.

3.3 Final reconstruction

The remaining networks were used to create an ensemble of ~~real ENSO reconstructions,~~ $ENSO_r$s using the real proxy data. The proxy records were first normalised to account for the different units (Equation B2~~; note this and other pre-processing steps were also applied to the pseudoproxies discussed above)~~) and subjected to an ITS transform, before undergoing the same reconstruction process used in the network creation. All ensemble members (~~ENSO timeseries derived from the networks~~$ENSO_r$) were then re-normalised to the reference period 0-650 yrBP to ensure comparability. The final ENSO reconstruction was taken as the ensemble mean, while the ensemble range ~~serves as~~ represents part of its uncertainty envelope.

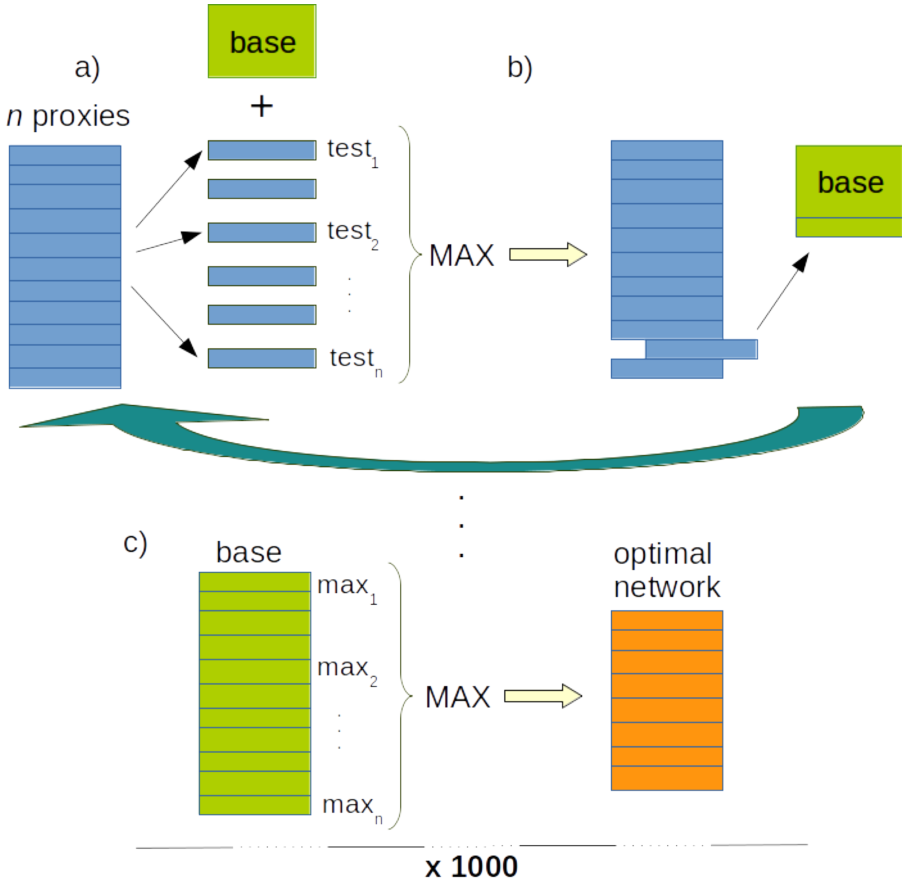

Figure 1. **Network creation process diagram.** Overview of the network creation process. a) A new network is created from the base network (*base*) plus each pseudoproxy individually, and tested for its reconstructive power. This results in n test scores; b) the highest score (max_n) is selected and the associated proxy is moved from the test-proxies to *base*. This is repeated until all test-proxies are incorporated into *base*. c) The 'optimal' network is selected by cutting *base* where max_n was highest. The entire process is repeated 1000 times, with new noise realisations being added to the pseudoproxies at the start of each run.

The last step in creating the ~~reconstructions~~ reconstruction was calculating the final error range. ~~As the proxy availability varies over time, root~~ Root mean square errors (RMSEs) were calculated for each ~~timestep separately. This was done by calculating the RMSE for a network that only contains the proxies available at that timestep: for reconstruction ensemble network n, the proxies available at time t were used as a frozen(unchanging) network to create 1000 pseudo-reconstructions from which RMSE values were calculated for time t. Repeated for each timestep, this resulted in 1000 absolute error value timeseries for each~~ network ~~n. This was translated into ensemble memberuncertainty limits by adding and subtracting the~~ during validation, providing 1000 ~~error series from the ENSO timeseries (to get~~ error estimates for each ensemble member. The 95th percentile for each member was calculated from this, and added and subtracted from the $ENSO_r$ series to find the maximum and minimum error limits~~respectively) and taking the 5-95~~th ~~percentile over their full range~~. The uncertainty envelope around the final ENSO reconstruction (i.e. the ensemble mean) is thus a combination of the reconstruction ensemble range and the error ranges for individual ensemble members.

~~While the pseudoproxy experiments described above give some information about the quality of the reconstructions in an ideal world (albeit with random noise), they cannot guarantee the quality of the real proxies. To test this, a leave-one-out(LOO) test was performed. It compares the correlation between a single proxy and the ENSO reconstruction made without that proxy in the real world and in an ideal world (again using pseudoproxies). If the expected (based on pseudoproxies) and observed (from the real proxies) correlations are very different (e.g. opposing signs), it calls for some caution in interpreting the reconstructions and/or using the proxy data. Issues with individual proxies could include systematic (non-random) non-ENSO signals linked to other climatic phenomena such as monsoons, biological processes (e.g. age-related changes in growth rates), or the non-climatic random noise may be higher than estimated (SNR>0.4) such that the ENSO signal is weaker than simulated by the pseudoproxy. The probability of a lower-than-predicted ENSO signal increases with sparser~~ $n-1$ ~~networks (the definition of 'too sparse' is very subjective, but see e.g. Mann et al., 2007, 2008; Tingley et al., 2012; W~~ ~~Alternatively, it could be speculated that the ENSO reconstruction made without the excluded proxy record is inaccurate. For example, at least one of the~~ ~~*included*~~ ~~proxies may not behave as expected. In this case, those proxies would presumably also show up with unexpected correlations. With so many possible causes for the different correlations, it is difficult to reject any one proxy outright. Instead, some degree of uncertainty must be accepted as proxy data will never be perfect. The impact of said proxies is checked by leaving them out of the network ensemble altogether and comparing this reduced reconstruction with the full version.~~

~~The combination of the validation methods and error estimates described here account for a range of uncertainty sources. The add-one-in approach and CE~~$_{crit}$ ~~threshold measure the expected (pseudo-world) ability of the proxy networks to reconstruct ENSO, while RMSE estimation explicitly takes into account the effect of the estimated proxy noise (which is also addressed by the add-one-in approach through network selection). The LOO test finally inspects the actual performance of the real proxies compared to their expected behaviour, providing a measure of confidence in how realistic the pseudoproxy experiments are, as well as serving as a check on the appropriateness of the real proxies.~~

3.4 LIA-MCA difference analysis

The absence of a known reference period to which the reconstructions can be calibrated precludes any absolute comparison of the result with recent trends. However, it is possible to ascertain whether the MCA and the LIA differ significantly in how 'El Niño-like' they are. Evaluating the LIA-MCA difference directly also removes the bias introduced by taking any reference period (Mann et al., 2009). To do this, the means over the two periods were taken and the MCA mean subtracted from the LIA mean. If the difference is significantly greater than zero, the LIA is more El Niño like than the MCA; if the difference is significantly less than zero, the MCA is more El Niño-like than the LIA.

4 Results: ENSO reconstructions

The final ENSO reconstructions for precipitation and temperature and their proxy network density are shown in ~~Fig. ??~~Figs. 2 and 3. The final number of networks included in the precipitation ensemble is ~~569~~1000, of which ~~274~~ 999 are unique (Fig. ~~??~~2a). The total number of proxies used is ~~23~~48, with a maximum of ~~22~~ 40 for a single network. Proxy availability increases steadily throughout time, save a slight drop off in the most recent period (Fig. ~~??~~2b). Although there is ~~some~~ spread in the ensemble, ~~particularly in the earliest period, there is a coherent trend~~ there are clear peaks and troughs visible. The within-ensemble coherence was tested by correlating 1000 randomly chosen pairs with each other. This confirmed that there is generally good agreement over the full period (~~0-1500~~ 100-1500 yrBP) as well as during the MCA and LIA individually ~~, with only a few negatively correlating ensemble members during the MCA~~ (Fig. 4). ~~There is a long-term trend towards more ENSO-like conditions evident in the precipitation reconstruction with a slowdown during the MCA.~~

The temperature reconstruction ensemble consists of ~~354~~ 617 optimal networks, all of which are unique (Fig. ~~??c~~3a). The within-ensemble correlations are ~~much~~ lower than for precipitation ~~though still mostly~~ in the LIA though still positive, and there is no distinct trend visible in the reconstruction. The total number of proxies used is 267, with a maximum of 116 for a single network. Despite the higher number of proxies available for temperature, the median proxy coverage (Fig. ~~??d~~ 3b black line) is ~~worse~~ lower compared to the precipitation reconstruction; while ~~over half the years in~~ roughly the most recent 1000 years of the precipitation reconstruction are based on a median of ~~11~~ 8 or more proxies, this ~~value is only 5.5 for temperature. This is despite the significantly higher number of available temperature proxies. However, most of these proxies are tree ring~~ is only true for the last ~450 years of the temperature reconstruction. The steep increase in Fig. 3b. reflects the high number of treering and coral series, all but a handful of which are less than 600 years long ~~(cf Mann et al., 2008) which is reflected in the steep increase in Fig. ??d, and the vast majority~~ (cf Mann et al., 2008; Tierney et al., 2015) and most of which are clustered in North America. ~~This limits the ability~~ The add-one-in method has mitigated some of the risk of co-varying, non-white noise in a subset of the proxies ~~to cancel out each other's noise and amplify their common ENSO signals, hence diminishing the quality of~~ skewing the resulting reconstruction; testing showed that when all North American treering records were added to the reconstruction, a regional non-ENSO trend obscured the ENSO signal (not shown). However, the ~~reconstruction. The uncertainty range on the temperature reconstruction accordingly increases back in time, much more~~

~~so than the precipitation reconstruction which shows a relatively consistent uncertainty band (note the different scales for the two reconstructions~~relatively poor spatial coverage elsewhere and the lack of long proxies leaves the reconstruction prone to spurious noise-driven trends in the earlier period. Unlike the precipitation ensemble, the temperature ensemble members vary quite widely among them, particularly in the early period (Fig. 4). Nevertheless, ~~in both cases~~ for both temperature and precipitation the error from proxy noise is overshadowed by the uncertainty associated with the choice of network – the ensemble spread makes up the bulk of the uncertainty envelope.

~~Figure ??~~ Figures 5 and 6 shows the proxy locations plotted onto the precipitation ~~(top) and temperature (bottom) EOF patterns. The size of the bubbles is an indication how many ensemble members contain the proxy, their colour is the relative EOF weighting with a darker shade being a higher weighting~~and temperature EOF patterns, respectively. The proxies included in the precipitation ensemble members are well-distributed over the western and eastern side of the Pacific, though missing good coverage of the central Pacific. The relatively uniform size of the bubbles suggests that there is no immediate preference of any one proxy over the others.

The spatial distribution of the temperature proxy locations, in contrast, is highly skewed towards North America (Fig. ~~??~~6), where most of the ~~tree ring~~ treering records are located~~. Although a wider range of proxies was considered initially including several in the western and central equatorial Pacific , these were rejected for various reasons including resolution, dating error, length, or low ability to capture the large-scale EOF pattern (see Appendix A and Tables 1 and 2)~~, and again the central Pacific lacks coverage. The combination of this poor spatial coverage, low temporal coverage (Fig. ~~??d~~2b) and wide ~~uncertainty envelope~~ ensemble range (about double that of precipitation) leads to the expectation that the temperature reconstruction is of ~~significantly~~ lower quality than the precipitation reconstruction. ~~This is indeed supported by the higher error range~~ There is no clear preference of any combination of proxies, with most proxies being selected equally often (i.e. equal bubble sizes). The fact that the similarity of the EOF patterns of GCM_{cal} and GCM_{val} to the 20CRv2c EOF pattern was lower for temperature than for precipitation (Appendix. B2) further reduces confidence in the temperature reconstruction.

~~These maps~~ Figures 5 and 6 illustrate the benefit of using the pseudoproxy approach in creating the 'optimal' networks. There is no direct correlation between proxy weighting (indicated by the bubble colour) and frequency of use, suggesting that other aspects such as resolution, length and the relationship to other proxy locations played a significant role in determining the usefulness of a proxy which would be difficult to judge from the outset. The fact that the choice of proxy network is the dominant source of error ~~(??a-c)~~ is further evidence of the utility of the pseudoproxy 'optimal' network method. The high clustering of temperature ~~tree ring~~ treering records in North America is an example of where the add-one-in method has worked to reduce the risk that some co-varying, non-white noise in a subset of the proxies skews the resulting reconstruction; testing showed that when all North American ~~tree ring~~ treering records were added to the reconstruction, a regional non-ENSO trend obscured the ENSO signal (not shown).

4.1 Comparing precipitation and temperature

Figure 7 shows the range of LIA-MCA differences for the individual members within the precipitation and temperature ensembles~~respectively. In the former case,~~ . The precipitation interquartile range indicates the LIA is ~~significantly~~ more El Niño-like than the MCA, though the difference is statistically insignificant ($p = 0.22$). For temperature, there is no evidence of any difference between the ENSO-like state of the MCA and the LIA, with a median value very close to 0 (~~$p < 0.01$). The temperaturecase is not clear, with the median difference falling on the zero line. The range is also much larger~~$p = 0.48$). There are also many more outliers (i.e. values outside the the 95% confidence interval) compared to precipitation, again reflecting the high uncertainty on the temperature reconstruction.

Figure. 8 shows the correlation between 1000 randomly chosen combinations of temperature and precipitation ensemble members as an indication of the agreement between the two climate variables. ~~The agreement is poor, with median correlations close to zero for all years as well as the MCA and the~~ There is no correlation – positive or negative – apparent between the temperature and the precipitation reconstructions, neither over the entire 1500 years nor over the MCA or LIA individually. ~~This is most likely~~ Whether this is a true physical phenomenon or simply a reflection of the high uncertainty on the ~~temperature reconstruction~~reconstructions is difficult to separate. Therefore, it is not possible to categorically determine a systematic difference between the ENSO signals in temperature and precipitation proxies.

4.2 ~~Leave-one-out results~~

~~The LOO test results are shown in Fig. **??**. Perfectly predicted proxies would fall on~~ The definitions of the MCA and the LIA used here are based on those given by Yan et al. (2011b) ; there are many alternative definitions, however (Jones and Mann, 2004) . To test the sensitivity of the results to the ~~1:1 line, with the most undesirable results in the top-left and bottom-right quadrants (where pseudoproxy and real proxy have opposing signs). As there is random noise in the pseudoproxies (and in addition the noise profiles in real proxies are likely to be more complex than assumed in the proxy experiments), it can be expected that their correlations with the ENSO reconstructions will differ fromthe pseudoproxy case to some degree. The LOO results are difficult to interpret, and there are no obvious trends. For both temperature and precipitation, real proxy correlations tend to be weaker than pseudoproxy correlations. There is no consistent relationship with proxy type (not shown) or EOF weighting (greyscale shading in Fig. **??**). However, there appears to be some link to proxy length particularly in temperature, with shorter proxy records more likely to perform poorly (dot size in Fig. **??**). The short proxies in this case tend to be tree rings located~~

~~in North America, so it is likely that this is a combination of length and location. It is possible that there is some covariability among these records that is not related to ENSO, obscuring the ENSO signal here. Moreover, it could be an expression of the 'segment length curse' where the ability of tree rings to capture low-frequency signals is limited by their length (Cook et al., 1995) . The two short temperature records with positive pseudoproxy correlations and negative real proxy correlations (bottom right quadrant), incidentally, are both coral records located in the southern West Pacific and are thus subject to different processes that can obfuscate the ENSO signal. Without more detailed analysis (and a larger sample size) it is impossible to make any statistically sound statements regarding these differences however.~~

~~As none of the temperature proxies in the anti-correlated quadrants (top-left and bottom-right) are identifiable for having a particularly high correlation in the real world, a blanket exclusionof all proxies in those two quadrants was performed to test their influence on the ENSO reconstruction (this is also possible to do in the temperature case as there is a sufficient number of remaining proxies). Despite removing 69 proxies, the reconstruction was not significantly affected with no statistically significant change in the MCA-LIA difference (not shown).~~

~~In the case of precipitation, two proxies have a strong positive correlations where a negative correlation is expected (top left quadrant) and one has a strong negative correlation where a positive correlation was expected (bottom right quadrant). Recreating the reconstruction ensemble excluding these proxies from all networks completely again did not significantly change the final ENSO ensemble, though it did slightly increase the~~ definition of these periods, we recalculated the LIA-MCA ~~difference (not shown)~~difference using two widely used alternative definitions: from Mann et al. (2009) (MCA = AD 950–1250, LIA = 1400–1700) and the Intergovernmental Panel on Climate Change (IPCC) Fifth Assessment Report (MCA = AD 950–1250, LIA = 1450–1850; Masson-Delmotte et al., 2013, , Fig. 9) . For precipitation, the difference between the two period is more pronounced for the alternative definitions, with a weakly significantly more El Niño-like LIA ($p < 0.1$). For temperature there is very little change; although the median is negative for the alternative definitions, the interquartile range still encompasses zero. The precipitation reconstruction thus suggests that the LIA was more El Niño-like than the MCA, but our conclusion that there is no evidence for any precipitation–temperature correlation stands.

5 Discussion

An important question addressed in this study is whether the modern-day links between ENSO-like temperature and precipitation ~~in ENSO~~ persist back in time. ~~The two ENSO reconstructions presented here provide no strong evidence of a disagreement over whether the LIA or the MCA was more El Niño-like. The precipitation reconstruction suggests the LIA is significantly more El Niño-like than the MCA. The difference between the two periods in the temperature reconstruction is consistent~~

~~with zero, but very uncertain. The disappointing quality of the temperature reconstruction, which limits the statistical robustness of the precipitation–temperature comparison, is likely due to the low number and unequal distribution of available datalocations. Most temperature proxies are located in teleconnected regions outside the ENSO source region, which have been shown to be subject to more temporal variability in precipitation–temperature relationships (Wilson et al., 2010; Coats et al., 2013; Gallant et al., 2013; Lewis an~~

~~Despite the shortcomings of GCMs in simulating the dynamics of ENSO, they are useful for assessing the coupling between equatorial Pacific SST change and impacts on global~~ There is no concrete evidence in this study of any correlation between the precipitation and temperature reconstructions, whether positive (as in the modern day) or negative (as suggested by Yan et al., 2011b) . This is contrary to expectations based on instrumental and modelling data, which both show a strong relationship between ENSO-like precipitation and temperature. To test the robustness of ~~this coupling in models~~the ENSO-like temperature–precipitation coupling in GCMs, we calculated the correlation between the temperature and precipitation ENSO-like EOF timeseries (PCs) in ~~five GCMs from the Coupled Model Intercomparison Project Phase 5 (~~the six CMIP5 ~~). All five show a consistently positive~~ GCMs listed in Appendix B2. Four of the six models show a significant ($p < 0.05$) positive precipitation–temperature correlation over the study region (40°S – 40°N) at annual and 30-year resolution for the historical ~~(AD 1850–2005)and last millennium (AD 850-1850) runs for both annual and 30-year resolution (~~$\cancel{R^2 \geq 0.76}$~~,~~ run ($0.74 \leq R^2 \leq 0.98$), and five out of six for the past1000 run ($0.30 \leq R^2 \leq 0.92$; not shown). This is similar to ~~the 20CRv2 data (~~$\cancel{R^2 = 0.87}$~~). Understanding and resolving this potential divergence in precipitation and temperature proxy data~~ coupling in the 20CRv2c data ($R^2 \geq 0.76$). The fact that the palaeodata apparently does not display this relationship over the past two millennia (cf Yan et al., 2011b, and this study) is thus interesting from a physical dynamical point of view as it contradicts ~~the~~ our conventional understanding of ~~ENSO~~long-term ENSO-like climate change.

There ~~are few other published ENSO-related multiproxy reconstructions based solely on precipitation proxies; these include Stahle et al. (1998) and Yan et al. (2011a) , which both focus on the Southern Oscillation Index (SOI, which is negatively correlated with ENSO). Stahle et al. (1998) use a network of tree rings to reconstruct winter SOI between AD 1706-1977. They note a slight tendency towards a stronger mean SOI (i.e. more La Niña-like state) in the latter part of the record, accompanied by increased variability. As this record only covers a fraction of the reconstruction presented in this paper and is focused on annual variability rather than (multi-)decadal trends we cannot draw conclusions about their similarity. A longer (2000 year) record is produced by Yan et al. (2011a) , who create a proxy SOI using~~ is also no evidence in the two reconstructions presented here that there was any significant difference in the mean ENSO-like climate state during the MCA and the LIA. This is also contrary to the findings of Yan et al. (2011b) . They create a SOI reconstruction (SOI_{pr}) from two precipitation proxies from the Galápagos (Conroy et al., 2008) and the Indo-Pacific

Warm Pool (Oppo et al., 2009), weighting them according to the relationship of local rainfall to the instrumental SOI. Interestingly, ~~the broad trends in their reconstruction are opposite to ours~~ SOI_{pr} shows broad trends opposite to the precipitation reconstruction presented here, with a more La Niña-like LIA compared to the MCA. While the two proxies used were considered for this study, they were both rejected due to high dating errors (average around 100 years). Several other precipitation (Tierney et al., 2010; Yan et al., 2011b) as well as temperature (Conroy et al., 2010) proxies supporting ~~the above study 's conclusions similarly have~~ conclusions of the Yan et al. (2011b) study were similarly rejected due to high dating errors~~. Additionally, a~~ , as were proxies supporting the opposite conclusion (Partin et al., 2007; Conroy et al., 2009) . Testing showed that applying the method described here using only the two proxies used by Yan et al. (2011b) produced highly similar results to their SOI reconstruction, suggesting it is not a methodological difference but rather related to proxy selection. A reconstruction based on only two ~~proxies is~~ (poorly dated) proxies is likely to be more vulnerable to spurious noise or other climatic influences distorting the ~~ENSO~~ signal, as is evidenced by the degradation back in time of the reconstructions presented in this study as the number of proxies declines. This highlights the need for more accurately dated proxy records, which remains an issue for low-resolution but long proxy archives such as marine sediments (Jones and Mann, 2004) .

A number of other (non-temperature or precipitation) ENSO-sensitive proxies that were not included in our reconstructions provide evidence for a more La Niña-like climate state in the MCA compared to the LIA, although the mean state of the LIA appears inconsistent. Sedimentary sterol concentrations in marine sediment off the Peru coast Makou et al. (2010) suggest the MCA coincides with a reduction in El Niño activity, with both El Niño and La Niña activity increasing from the late MCA onwards. Based on a range of North American proxies Graham et al. (2007) conclude that the MCA was characterised by arid conditions in western North America consistent with a La Niña-like state, followed by a wetter LIA. A basin ventilation record from the Western Pacific Warm Pool (WPWP) (Langton et al., 2008) agrees particularly well with the earlier part of our precipitation reconstruction. It shows a peak in El Niño activity at ∼1150 yrBP and a distinctive minimum during the MCA, followed by a more El Niño-like LIA characterised by a steady decline in activity. This decline is not apparent in our reconstruction, but is reflected in some other multi-millennial proxy records (Moy et al., 2002; Stott et al., 2004; Conr

Most ~~published temperature~~ multi-proxy reconstructions of ENSO ~~focus on one of the~~ variability are temperature-based, and focus on NINO regions. A NINO3 region (90°W–150°W and 5°S–5°N) temperature reconstruction by Mann et al. (2009) shows a slow millennial-scale warming trend (to a more El Niño-like state) from AD 1100 onwards, with relative cooling during the MCA compared to the LIA consistent with a La Niña-like state during the MCA. In contrast, Emile-Geay et al. (2013b) are unable to detect a systematic difference between the MCA and LIA in their Boreal winter NINO3.4 (120°W–170°W and 5°S– 5°N) SST reconstruction~~. This discrepancy~~ , which is consistent with the findings of this study. The discrepancy between the two ENSO reconstructions may be due to the difference in proxy networks, particularly the use of lower-resolution proxies here and by Mann et al. (2009) which contribute a substantial part of the signal, ~~or~~ due to the slightly different definition of the NINO regions~~. In addition to SOI and NINO-region reconstructions, there have been several attempts at reconstructing the coupled ocean-atmosphere ENSO trends and variability (Gergis and Fowler, 2006; Braganza et al., 2009; Gergis and Fowler, 2009; McGregor et al., 2010) . However, these are shorter (going back to AD 1500) thus precluding any comparison with the MCA.~~

~~A number of other (non-temperature or precipitation) ENSO-sensitive proxies that were not included in our reconstructions support the LIA-MCA difference evident inour reconstruction, although there is less agreement over the mean~~ , or the target season (Boreal winter versus annual). Other reasons may be related to the methodology or target instrumental dataset, particularly for low-frequency variability and amplitude. Work by Emile-Geay et al. (2013b) indicates that the results of many temperature reconstruction methods are sensitive to the target SST dataset used for calibration, and Wang et al. (2015) find that the La Niña-like pattern in the MCA evident in Mann et al. (2008) is not a robust feature across CFR methods. The fact that multi-proxy reconstructions are less likely to show strong differences between the ENSO-like state of the ~~LIA. Sedimentary sterol concentrations in marine sediment off the Peru coast Makou et al. (2010) , suggest the MCA coincides with a reduction in El Niño activity, with both El Niño and La Niña activity increasing from the late MCA onwards. Based on a range of North American proxies Graham et al. (2007) conclude that the MCA was characterised by arid conditions in western North America consistent with a La Niña-like state, followed by a wetter LIA. A basin ventilation record from the Western Pacific Warm Pool (WPWP)(Langton et al., 2008) agrees particularly well with the earlier part of our precipitation reconstruction. It shows a peak in El Niño activity at 1150 yrBP and a distinctive minimum during the MCA, followed by a more El Niño-like LIA characterised by a steady decline in activity. This decline is not apparent in our reconstruction, but is reflected in some other multi-millennial proxy records (Moy et al., 2002; Stott et al., 2004; Conroy et al., 2008) .~~ MCA and the LIA again highlights the potential sensitivity of individual records to non-physical trends, and suggests that conclusions drawn from single proxy records must be considered with caution.

An issue not addressed in this study is the role of different 'flavours' of ENSO patterns. A different type of ENSO pattern, first defined by Ashok et al. (2007) and dubbed ENSO Modoki, differs from the traditional ('canonical') ENSO pattern in the shift of postive SST anomalies from the western Pacific (mainly in NINO3 and NINO3.4) to the central Pacific (NINO4; 170°W–120°W and 5°S–5°N), and its mid-latitude teleconnections. It is sometimes defined as the EOF2 of detrended SST data (note that the data in this study was not detrended, hence here it would be EOF3 Ashok et al., 2007; Cai et al., 2015a, b) , or a combination of EOF1 and EOF2 (Takahashi et al., 2011; Karamperidou et al., 2015) . Some modelling studies suggest that ENSO Modoki will increase in frequency compared to canonical ENSO as a result of anthropogenic climate change (Yeh et al., 2009; Kim and Yu, 2012; Cai et al., 2015a, b) , and there is some model evidence that ENSO Modoki was also more common in the mid-Holocene (Karamperidou et al., 2015) . The difference in equatorial spatial pattern and teleconnections has implications for the interpretation of the proxy reconstructions in this study, as ENSO Modoki-like climate change may appear here as a reduction in ENSO-like activity.

The poor quality of the temperature reconstruction, which limits the statistical robustness of the precipitation–temperature comparison, is likely due to the low number and unequal distribution of available data locations. Most temperature proxies are located in teleconnected regions outside the ENSO source region, which have been shown to be subject to more temporal variability in precipitation–temperature relationships (Wilson et al., 2010; Coats et al., 2013; Gallant et al., 2013; Lewis and LeGrande, 2015) . A multi-region ~~tree ring~~ treering reconstruction of ENSO variability displays substantial variability in the strength of ENSO teleconnections over time and space (Li et al., 2013). The authors find that the Pacific Northwest and Texas-Mexican regions show highly unstable teleconnections (although there is no discussion on whether this is related to the different ENSO flavours). This may explain the lack of ~~ENSO~~ signal in the temperature reconstruction presented here, as many of the temperature proxies are located in these ~~regions~~teleconnected regions (Fig. 6). If the strength of the teleconnection has indeed changed over time, the weightings based on modern-day ENSO patterns would not reflect this~~and we would thus lose some ENSO signal~~; thus this reconstruction should be regarded as an indication of change of the modern-day ENSO-like climate pattern only. Without proxies located in the centre of action or more robustly teleconnected areas, ~~this~~ the loss of signal due to unstable teleconnections can be expected to be substantial as suggested by the results presented here.

An interesting observation of the EOF maps presented here (Fig. ~~??) is a distinct lack of~~ 5 and 6) is the low to no correlation between EOF weighting (bubble shading) and how often proxies are used ~~in a network. Two~~ (bubble size). Correlations of temperature proxy frequency of occurrence versus GCM-derived and 20CRv2c-derived EOF weighting are 0.23 and 0.20, respectively ($p < 0.05$); there is no significant correlation for temperature proxies ($p > 0.54$). Two possible explanations for this are i) the climatic noise in the high-occurrence but low-weighted areas is less spatially correlated with the noise elsewhere than in the low-occurrence but higher weighted areas; or ii) the length and resolution of the proxy records have a more important effect on a proxy's utility than its weighting. ~~The precipitation proxies ' frequency of use lends support to the former explanation, as they are all more or less selected a similar number of times regardless of proxy record length or resolution. The latter explanation finds support in the temperature proxy distribution, where several low-weighted but long tree rings (e.g. ca051; Table 2)in North America are strongly preferred by the networks. The reality is probably~~ For instance, the proxies off the Australian coast and in the west Pacific islands are mostly short ($<$ 500 years) coral records; while several of them have high weighting, their frequency of occurrence is very low. The proxy at the southern tip of Australia, in contrast, is a $\sim$ 3600 year long treering record, and is the most frequently used temperature proxy. Overall, however, temperature proxy length is only very weakly correlated to occurrence frequency ($R = 0.17, p < 0.05$). The SNR assigned to the temperature pseudoproxies is similarly only very weakly correlated to frequency ($R = 0.13, p < 0.05$). In the precipitation case, neither length nor SNR are significantly correlated to how often the proxies occur in the ensemble. The selection process is likely driven by a combination of ~~both these factors ,~~ these factors rather than any single factor, and is modulated by the number of proxies available. More detailed analysis will be needed to elucidate this.

There is some evidence that ENSO modulates the Pacific Decadal Oscillation (Yuan Zhang et al., 1997) on multidecadal timescales over the intrumental period (Newman et al., 2003) and further back in time (Verdon and Franks, 2006) . The PDO is an SST anomaly pattern resembling ENSO located in the extratropical North Pacific (20°N – 45°N). Comparison of the precipitation reconstruction in this study with a reconstruction of the PDO over AD 993–1996 (MacDonald and Case, 2005) shows a slight tendency for the precipitation and PDO series to have the same sign over the MCA and LIA separately, although the relationships are not statistically significant (not shown). There is no indication of any relationship between the PDO and the temperature reconstructions, despite the fact that many of the temperature proxies are located in potentially PDO-sensitive areas (most notably North America). MacDonald and Case (2005) find a strongly negative PDO during the MCA (roughly equivalent to a La Niña-like spatial pattern), which corresponds to the qualitatively La Niña-like tendency of the precipitation reconstruction presented here. While there may be some conflation of ENSO and PDO signals in the reconstructions due to the similarity of their spatial patterns, it is not possible to distinguish these signals here. Moreover, the lack of correlation with the PDO reconstruction suggests the reconstructions presented here are distinct from the PDO. D'Arrigo and Wilson (2006) find no significant correlation between the 9-year smoothed reconstruction of the Asian expression of the PDO (based on East Asian treerings as opposed to the often-used North American treerings) and Boreal winter NINO3 SST, suggesting the ENSO-PDO link may be spatially variable.

5.1 Reflections on the method

The method set out in this study is one of few which attempt to take into account the effect of real spatial *and* temporal patterns of proxy records, thus increasing our confidence in their ability to accurately evaluate the effectiveness of the networks. To our knowledge, this is the ~~first time that~~ only study in which realistic temporal proxy resolution has ~~also~~ been taken into account by the pseudoproxies, in addition to their length ~~(Emile-Geay et al., 2013a; Wang et al., 2014) .~~. This is an improvement of the pseudoproxy design used by, for example, (Wang et al., 2014) , who take into consideration the declining proxy availability back in time but not their resolution. The authors find that this already significantly impacts the quality of multi-proxy reconstructions, so the inclusion of proxy resolution as done here is likely to have further impacts. More extensive research is needed to quantify this however.

~~However, the~~ The 'optimal' network creation still has scope for improvement. Although we have screened for maximum dating errors, its effect on the included proxies is not explicitly ~~included. This~~

~~is an issue~~ assessed. This issue is often neglected in (multi) proxy reconstructions (but see Comboul et al., 2014, for a recent effort to address it systematically). Moreover, ~~our noise simulation~~ the noise simulation used here is relatively simplistic; the use of a wider noise spectrum (including red, and possibly even blue, noise) may alter the composition of the networks (Smerdon, 2012, and references therein). However, the issue remains that there is no easy way to determine the real noise spectrum of the proxies. ~~Further~~ With the advent of more isotope-enabled GCM simulations, further improvement could come from ~~more accurate estimations of the proxy-climate relationships via~~ the use of proxy system models ~~(e.g. Conroy et al., 2008; Evans et al., 2013; Russon et al., 2013; Stansell et al., 2013; Steinman et al., 2012; S~~ estimate more accurately the proxy-climate relationships (cf Conroy et al., 2008; Evans et al., 2013; Russon et al., 2013; Stansell et a

The choice of dataset from which to derive an EOF is also a source of uncertainty (cf Emile-Geay et al., 2013b), as differences in the EOF pattern will affect the weighting of the proxies. This is particularly pertinent for the precipitation reconstruction, as the modern-day ENSO precipitation signature is much less well-established than for temperature due to less and lower quality ~~data. To test the sensitivity of the results to the choice of dataset, we repeated the precipitation ENSO reconstruction using the Global Precipitation Climatology Project dataset (a combination of surface-based rain gauge data and satellite-derived estimates covering 1979-2012;). Note that since the dataset is much shorter (AD 1979–2010), it was not possible to divide it into a validation and a training set; instead, the entire dataset was used for both instances. This is the main reason this dataset was not used for the main analysis despite its arguably better representation of the precipitation ENSO pattern. Most importantly, the GPCP-based ENSO reconstruction also shows a significantly more El Niño-like LIA compared to the MCA. Although there were some differences in the EOF pattern of GPCP and 20CRv2, the final ENSO reconstructions showed very similar short-term trends (not shown). The long-term positive trend evident in the 20CRv2-based reconstruction was not present, however. This is most likely due to divergences in the prevalence of the proxies in the final ensemble.~~

~~In addition to the choice of modern dataset, another concern is temporal non-stationarity of EOF patterns within a single dataset. This~~ instrumental data. This is partially tested by using different GCMs to calibrate and validate the proxy networks. However, the true ENSO-like pattern has been non-stationary over time, as has been shown to ~~exist~~ be true in 20CRv2 for the NAO and Pacific North American (PNA), for example~~, by Raible et al. (2014)~~ (Raible et al., 2014) . We tested the stability of the ~~20CRv2~~ 20CRv2c temperature EOF used in this study by recalculating it for a running 30-year window and found substantial variability in the spatial pattern and amount of variance captured by the EOF. Further investigation is necessary to explore whether this result is an artefact of internal variability, is due to uncertainties in the reanalysis dataset, or reflects real changes in the nature of ENSO. Nevertheless, it highlights the vulnerability of the majority of ENSO reconstructions (including ours) to the assumption that the modern-day ENSO is a good analogue for the past.

6 Conclusions

~~We have presented two new ENSO reconstructions~~ Two reconstructions of ENSO-like climate change are presented, based on temperature- and precipitation-sensitive proxies respectively. The quality of the reconstructions degrades further back in time as there is less proxy data available, which is particularly detrimental to the temperature reconstruction. The main implications of these reconstructions are:

1. We find no evidence that ~~the ENSO-driven changes in precipitation and in temperature are in disagreement over the last millennium. The precipitation ENSO reconstruction suggests that the LIA was characterised by~~ temperature and precipitation proxies disagree over the ENSO-like state of the climate during the past two millennia. The two reconstructions in fact show little to no correlation, which is surprising as there is a strong relationship between temperature and precipitation ENSO behaviour at interannual timescales in instrumental/reanalysis data and GCMs.

2. The precipitation reconstruction shows a tendency for a more El Niño-like ~~state compared with~~ LIA compared to the MCA, ~~while there is no discernible difference visible~~ but the difference is not statistically significant and is not apparent in the temperature reconstruction~~(Fig. 7). The precipitation results hold when using 20CRv2 as well as GPCP for deriving the precipitation EOF, which is encouraging. The leave-one-out results hint at various possible sources of uncertainty and error, including proxy record length and type. However, excluding suspect proxies did not significantly change the results.~~

   . This result is insensitive to the choice of definition for the MCA and LIA.

3. A major limitation on our ability to accurately reconstruct ~~ENSO~~ ENSO-like climate change back in time is the lack of high-quality, long proxy records in the tropical and subtropical latitude bands, and we reiterate the need for continued efforts to collect such data. The discrepancies between the two series presented here and many other interannual and (multi-)decadal ENSO reconstructions are more likely to be reconciled with denser proxy networks in the ENSO source region, along with resampling of existing locations to increase the signal to noise ratio (Wang et al., 2014) . The pseudoproxy experiments described in this paper can quite easily be adapted to search for optimal locations from which additional proxy information would be the most beneficial, as previously done specifically for corals by Evans et al. (1998) (see also Comboul et al., 2015, for a recent endeavour).

4. A final caveat is the reliance on modern-day ENSO patterns and the implicit assumption of its stationarity through time. ~~Hopefully continued~~ Continued improvements in the ability of GCMs to accurately simulate and reproduce ENSO behaviour in conjunction with more high-quality proxy data will give both the palaeocommunity and the modelling community an in-

creasingly reliable foundation for creating, calibrating and evaluating palaeo-ENSO reconstructions.

Appendix A: Proxy data details

Tables 1 and 2 provide an overview of the proxy records collected for this study. Where a proxy was rejected, the reason is given. ‘AOI’ refers to a proxy not being selected for any networks by the ‘add-one-in’ algorithm. This could be due to poor ability to capture the EOF pattern related to location or time resolution. Records from the NOAA Paleoclimate Database are identified by original publications. Where there are multiple timeseries from one ~~record~~publication, an identifier suffix is added. The naming of this identifier is ~~always~~ based on the naming in the original database files or the proxy type (e.g. $\delta^{18}O$, Sr/Ca, etc.).

Most ~~tree ring~~ treering records were taken from the dataset used by Mann et al. (2008), which is a reduced set derived from the International ~~Tree Ring~~ treering Data Bank (ITRDB, version 5.03; www.ncdc.noaa.gov/paleo/treering.html). The naming for these series has not changed from the original (an abbreviated location followed by a core number). The ~~tree ring~~ treering series were subject to the following selection criteria (Mann et al., 2008):

> (i) series must cover at least the interval 1750 to 1970, (ii) correlation between individual cores for a given site must be 0.50 for this period, (iii) there must be at least eight samples during the screened period 1800–1960 and for every year used. Series that were redundant with other compilations [used in the Mann et al. (2008) study] were not included. Four other series were not included because of site- specific problems [...]. Of the remaining series, [some] had to be replaced because of format errors in the chronology file on the ITRDB [...], or because sample depth data were missing from the chronology file. [...] When sample depth data were absent, the raw ring-width data from ITRDB were used to recalculate the chronology using program ARSTAN (Version 6.05P), with the following settings: a) a single detrending fitting a cubic spline of 50% variance reduction function at 66.6% the length of each sample, no stabilization of variance or autoregressive modeling, indices computed as ratio, that is measurement divided by curve, and chronology calculated as biweight robust mean estimate.

~~Additional tree ring~~ The Tierney et al. (2015) coral dataset is a comprehensive compilation of coral data covering the last ~400 years. Most of the records in this database were used in this study as temperature proxies, with the following exceptions:

- DeLong et al. (2012, 2013, 2014) were replaced by the coral-derived SST series as presented in original publications

- Zinke et al. (2004); Kuhnert et al. (1999) were replaced by the coral-derived SST series as presented in Zinke et al. (2014)

- Goodkin et al. (2008) $\delta^{18}O$ and Sr/Ca were replaced by the coral-derived SST series as presented in the original publication

- Pfeiffer et al. (2004) was excluded as the original publication shows that advection-induced SSS changes dominates over temperature in the coral $\delta^{18}O$ on interannual timescales

- Swart et al. (1996b) was excluded as the original authors find no interannual $\delta^{18}O$-temperature relationship

- Swart et al. (1996a) was excluded as the original publication shows SSS dominates the interannual $\delta^{18}O$ signal and the $\delta^{18}O$-precipitation relationship is unstable

- For Abram et al. (2008); Cole et al. (1993); Nakamura et al. (2009) , the coral $\delta^{18}O$ signal is not clearly dominated by temperature but is a combination of T and P

- For Cobb et al. (2003); Felis et al. (2000, 2009); Gorman et al. (2012); Linsley et al. (2006); Urban et al. (2000); Zinke et al. (the coral $\delta^{18}O$ signal is not clearly dominated by temperature but is a combination of T and SSS

- Linsley et al. (1994) is interpreted as a precipitation record as the original study shows the $\delta^{18}O$ signal is 80% precipitation influence

- Felis et al. (2009) Sr/Ca and $\delta^{18}O$, Kuhnert et al. (2005) Sr/Ca, Quinn et al. (1996) , Quinn et al. (2006) Sr/Ca, Kilbourne et al. (2008) Sr/Ca and Druffel and Griffin (1999) $\delta^{18}O$ were excluded as their correlations with SST reported in Tierney et al. (2015) were of opposite sign to what is expected (i.e. positive when the physical processes should lead to a negetive correlation)

Additional treering and coral records were retrieved from the NOAA Paleoclimatology Database (http://www.ncdc.noaa.gov/data-access/paleoclimatology-data/datasets) and were used as presented there. Where available, temperature or precipitation ~~converted series were used~~ reconstructions were used (i.e. where the raw proxy series has already been converted). This was done to minimise biases due to nonlinearities in the raw proxy data which are accounted for in the conversion process. In some cases, two precipitation series were available for different seasons; these were summed (or averaged, depending on the type of data) to get a better approximate of an annual signal. While this may not be entirely accurate, annual signals are more desirable for the purpose of this study. Moreover, summing the records as opposed to treating them as individual records makes very little difference due to the nature of the method (weighting and summing the series). For ~~coral records~~corals, spliced records were used where ~~possible to maximise the~~ available to maximise their length.

Proxy records with dating errors > 60 years were excluded from the analysis. The dating error was taken from the original publications where it was reported; otherwise it was derived from the age model results in the raw data files. In the latter case, the maximum error reported for the past 2000 years was used; larger errors further back in time were thus not taken into account as they are irrelevant for this study.

Appendix B: Detailed methods

The method developed in this study was used to create separate temperature and precipitation-based ~~ENSO reconstructions~~ reconstructions of ENSO-like climate change made from weighted temperature and precipitation proxy records respectively. The weights were based on Empirical Orthogonal Function (EOF) patterns derived from general circulation models (GCMs) and the Twentieth Century Reanalysis Project Version ~~2 (20CRv2). The EOFs were selected on the basis of their ability to represent the precipitation and temperature signatures of ENSO. The available proxy records were combined into 1000~~ 2c (20CRv2c). First, an ensemble of 'optimal' proxy networks ~~using a pseudoproxy approachto automatically select the best combinations in the presence of white noise. This also acted to filter out proxies whose resolution, length or timespan were unfavourable. Each network was then used to create an ENSO timeseries with an associated error range. The final ENSO reconstruction was taken as the mean of all network timeseries, with an uncertainty envelope determined by the ensemble range and the 5–95^{t}h percentile of individual members' error ranges~~is created using a GCM-based cross-validated 'add-one-in' approach. These networks are then applied to real proxy data to create a separate precipitation and temperature reconstruction of ENSO-like climate change over the past two millennia. Each step is described in more detail below.

B0.1 ~~Pre-processing the data~~

~~All proxy timeseries were first averaged or interpolated to 30-year values. Since the proxy data have different units and cannot be compared directly, they were all normalised to a common period ($a:b$) where all proxies contain data within the network via the equation:~~

$$Pnorm_t = \frac{P_t - \mu_{a:b}}{\sigma_{a:b}}$$

~~where $Pnorm_t$ is the normalised proxy value at time t, P_t is the original value at time t, $\mu_{a:b}$ is the mean value of proxy P between common period $a:b$, and $\sigma_{a:b}$ is the corresponding standard deviation. The length of $a:b$ was ensured to be at least 100 years to reduce the probability of μ and σ being dominated by noise. In some cases this led to rejection of some proxies due to their length or their starting or ending too late or too early compared to the other records. This process of normalisation is similar to the method used in Wilson et al. (2010) . To reduce overrepresentation of more densely sampled locations, proxies that fell in the same grid box were averaged after normalisation.~~

B1 ~~Method calibration and validation~~

~~When performing pseudoproxy experiments, it is important to implement some form of verification of the results. Cross-validation is frequently used for testing the quality of statistical reconstruction and prediction methods (Mann et al., 2007; Emile-Geay et al., 2013a; Stahle et al., 1998) . It involves testing the method using independent data; that is, data that is not used to develop the method. Here, this is done by separating the 20CRv2 data into a training(1950-2010) and a validation(1871-1949) set. This division is based on the fact that a higher percentage of the more recent reanalysis data is computed from observational data rather than model infilling. It is thus of higher quality and more likely to give a realistic EOF pattern to use for calibrating the proxy networks. It could also be argued that the validation testing is more stringent, as the validation data is more likely to contain noise or inaccuracies and thus lower the validation scores.~~

~~There are several measures of quality for validation statistics, the most common of which are the coefficient of determination R^2, the reduction of error (RE) and the coefficient of efficiency (CE). Comprehensive discussions on the relative merits and pitfalls of these measures can be found in the literature (cf Cook et al., 1995; Emile-Geay et al., 2013a) . We chose to use CE as it is more stringent than RE and is more suitable for low-frequency reconstruction skill than R^2 (Bürger, 2007; Emile-Geay et al., 2013a) . CE is calculated as follows:~~

$$\cancel{CE = 1 - \frac{\sum_{i=1}^{n}(z-\hat{z})^2}{\sum_{i=1}^{n}(z-\mu_v)^2}}$$

~~Where z is the observed value, $\hat{z}$ is the estimated value, and μ_v is the mean of z over the validation period. CE scores range from -∞ to +1, with 1 being a perfect score. The remaining methods sections further elaborate on where the training and validation partitioning comes into effect.~~

B1 ~~EOF calculation~~ Empirical Orthogonal Function analysis

Empirical Orthogonal Function (EOF) analysis decomposes a spatiotemporal dataset into stationary time-varying coefficients. For a dataset of spatial resolution $x \times y$ and n time steps, it produces n maps (EOFs) of $x \times y$. The first map (EOF1) captures the largest fraction of variance of the original data. Each subsequent map maximises the amount of remaining variance captured, ~~while~~ whilst being completely uncorrelated (orthogonal) to all preceding maps. Every EOF map is accompanied by a principal component (PC) timeseries of length n, which describes how the magnitude and sign of the EOF pattern varies ~~throughout the dataset~~over n. The first few EOFs can usually be attributed to physical dynamical phenomena such as seasonality or ENSO. By only retaining the leading EOFs, a dataset can be 'cleaned' of the (assumedly) random noise captured by the lower-order EOFs.

EOF analysis was applied to the ~~training set of the normalised 20CRv2~~ 20CRv2c annual mean surface temperature and precipitation rate datasets to extract ENSO-like temperature and precipitation patterns respectively. The ~~data were not detrended prior to EOF calculation as this may~~

~~remove some information about long-term trends in ENSO variability. The time series correlation of the normalised versus non-normalised ENSOEOFs was very high ($R^2 > 0.74$ for 20CRv2 and GPCP, not shown~~EOF patterns were derived from annual data because while this study does not attempt to reconstruct interannual variability, it is concerned with climate changes that exhibit the classic ENSO-like spatial pattern. The EOFs were selected on the basis of their ability to capture the temporal evolution ENSO, measured by comparing the PC timeseries to three ENSO indices: MEI.ext (Wolter and Timlin, 2011) , NINO3.4 and SOI (both available from http://www.cpc.ncep.noaa.gov/data/indices/). In both temperature and precipitation, ~~the first EOF~~ EOF2 displayed the signature ENSO pattern and had the highest correlation with the ENSO indices (precipitation $R^2 > 0.62$, temperature $R^2 > 0.66$), and was thus selected as a basis for weighting the proxies. ~~PCs were calculated for the full (PC_{t+v}), training (PC_t~~The precipitation and temperature EOF2 explain 11.57% and 9.75% of variance, respectively. These EOFs were used for the final reconstructions of ENSO-like climate change.

B2 GCM data

For the creation of the network ensemble, GCM data was employed. The objective of the 'add-one-in' method is to create networks which accurately reconstruct the long-term (30-year averaged) ENSO signal. 20CRv2c covers less than 200 years, which is too short for meaningful evaluation of low-frequency change, particularly if the dataset is to be partitioned into calibration and validation sets. GCMs, meanwhile, offer much longer datasets. Although they cannot simulate the real temporal climate change and variability of the past 1000 years, they are still useful for the building of proxy network ensembles, which asks only that they simulate realistic modes of spatiotemporal variability (i.e. EOF patterns). For the pseudoproxy experiment, the past1000 runs from two different GCMs were used for calibration (GCM$_{cal}$) and validation (~~PC_v) datasets~~GCM$_{val}$).

The following six GCMs (followed by their climate modelling groups in brackets) were considered as they have past1000 runs available:

- CCSM4 (National Center for Atmospheric Research)
- GISS-E2-R (NASA Goddard Institute for Space Studies)
- MPI-ESM-P (Max-Planck-Institut für Meteorologie (Max Planck Institute for Meteorology))
- IPSL-CM5A-LR (Institutenstitut Pierre-Simon Laplace)
- BCC-CSM1-1 (Beijing Climate Center, China Meteorological Administration)
- MIROC-ESM (Atmosphere and Ocean Research Institute (The University of Tokyo), National Institute for Environmental Studies, and Japan Agency for Marine-Earth Science and Technology)

All model datasets were regridded to 2°×3°.

B3 ~~Optimal proxy network creation~~

~~After screening proxy records as described in Sect. 2.1, a pseudoproxy experiment was conducted to create an~~ Each GCM produces a different ENSO-like EOF pattern, with varying biases (Bellenger et al., 2014; Collins, 2005) ; there is further variation among the different model runs. For this study, the most '~~optimal network~~accurate' ~~ensemble.~~ GCM past1000 runs were selected, in the sense that their EOF values at proxy locations were most similar to the corresponding 20CRv2c values, which is the most realistic EOF pattern of modern-day ENSO available here. The real modern ENSO pattern will be different again, as will the real ENSO pattern of the past 1–2 millennia. By calibrating and validating the networks on datasets with slightly varying realisations of this ENSO pattern, the sensitivity of the networks to these variations is tested. EOF analysis was performed on the piControl and past1000 runs of the six GCMs, for precipitation and temperature separately. For each analysis, the first three EOFs were retained for comparison to the 20CRv2c ENSO-like EOF. The GCM EOF values of grid boxes with proxies were compared to the corresponding 20CRv2c grid boxes via Pearson rank correlation. The two GCMs with the highest correlations with 20CRv2c across the two runs were chosen as GCM$_{cal}$ and GCM$_{val}$ for precipitation and temperature separately. As a result, CCSM4 ($R \geq 0.79$ in piControl and past1000) and GISS-E2-R ($R \geq 0.75$) were chosen as GCM$_{cal}$ and GCM$_{val}$ for precipitation; ISPL-CM5A-LR ($R \geq 0.46$) and BCC-CSM1-1 ($R \geq 0.44$) were chosen as GCM$_{cal}$ and GCM$_{val}$ for temperature.

B3 Pseudoproxies

Since there is no straightforward way of assessing the quality or relevance of a proxy beyond the selection criteria already discussed, a pseudoproxy approach can aid in making a more objective and refined decision on how to optimise the use of available proxy data (Smerdon, 2012). Since for pseudoproxies the '~~ideal~~ real world' is known (in this case the ~~20CRv2~~ GCM derived EOFs and PCs), it is possible to quantify the skill of the reconstruction. While a 'blanket' approach (in which every available record is used) may sound attractive, it increases the risk that some covarying, non-white noise in a subset of the proxies skews the resulting reconstruction. This is, for example, pertinent in North America where there is high clustering of ~~tree ring~~ treering records. Testing showed that when all records were added to the reconstruction, a regional ~~non-ENSO~~ trend obscured the ~~ENSO~~ ENSO-like signal (not shown). The only case in which it is certain that using all available proxies is preferred, is when each gridbox contains a (non-climatic) noise-free proxy such that the network gives complete spatial and temporal coverage.

~~For the pseudoproxy experiment, the 20CRv2 datasetswere first replicated in the time dimension to get a length of 1000 years. Pseudoproxies were created by taking timeseries from the reanalysis datasets at~~ Pseudoproxies are model or instrumental data series that are degraded by applying transformations and/or adding noise to simulate the behaviour of a real proxy (Mann, 2002) . Proxy system models (Evans et al., 2013; Dee et al., 201 to characterise the mechanistic and forward processes connecting the response of a proxy archive to an environmental signal and the subsequent observation of this response; this includes accounting for nonlinearities, multivariate responses, and measurement limitations. Many PSMs require an isotope-enabled GCM or other data not available in the original sources of the proxy data collected for this study, but the VSLite model is an easily implemented PSM for simulating treering widths (TRW) which needs minimal input (Tolwinski-Ward et al., 2011; Breitenmoser et al., 2014; Evans et al., 2014) . Using the R package *VSLiteR* available from GitHub (https://github.com/suztolwinskiward/VSLiteR), GCM precipitation and temperature data were combined to create pseudo-TRW datasets, with which TRW proxies were represented in the pseudoproxy experiment here. The rest of the proxies were represented by the GCM raw temperature or precipitation series.

These precipitation, temperature and TRW series (taken from the real proxy locations~~and applying~~) were firstly degraded by adding white Gaussian noise. Information on true signal-to-noise ratios (SNR) of the various proxies is sparse in the literature. However, where data was available on the relationship between the proxy and the target climate variable in the form of R-values, SNR can be calculated via the following equation (Smerdon, 2012) :

$$SNR = \frac{R}{\sqrt{1-R^2}} \tag{B1}$$

Several original publications on individual publications provide such information(see Tables 1 and 2), and Tierney et al. (2015) have conducted a systematic comparison of most coral records included here against the Hadley Centre Global Sea Ice and Sea Surface Temperature (HadISST) 1900-1990 dataset. Where no concrete information was available, a value of SNR=0.4 was prescribed. While this has been shown to be a realistic average (Smerdon, 2012) , comparison with the calculated SNRs in this study suggests it is in fact a relatively conservative value.

After the addition of noise, the pseudoproxies were degraded further to reflect the length, timespan and resolution of the real proxies. Real proxies' temporal resolution between ~~100-1100 yrBP~~ 0-1000 yrBP was applied; this period was chosen as it is the focus of this ~~study~~stuδy. The resolution was recreated by assuming that each data point represents an average of the previous unsampled years; for example in a proxy with a 10-year resolution, data point n was recreated by taking the average over points $(n-9):n$. ~~White Gaussian noise was added with a signal-to-noise ratio (SNR) of 0.4, which is considered a realistic average ratio for climate proxies (Mann et al., 2007; Smerdon, 2012) . Data on real SNRs is sparse in the original literature~~

B4 Calibration: network creation

After screening proxy records, selecting GCMs and creating pseudoproxies, a pseudoproxy experiment was conducted to create an 'optimal network' ensemble. The calibration stage builds proxy networks in a stepwise manner by incrementally adding the proxy that maximally improves the quality of the network reconstruction. All proxies were first subjected to inverse transform sampling (ITS) using the MATLAB script (translated to R) available at https://github.com/CommonClimate/common-climate/blob/master/gaussianize.m. ITS converts the distribution of a timeseries to a standard normal distribution, thus reducing the bias introduced by nonlinearities inherent to many proxy records (Emile-Geay and Tingley, 2016) . Lastly, the pseudoproxies were averaged to 30 years ~~,~~ (using a simple average) to prevent high-resolution records from dominating the signal. This averaging period was chosen as our focus is on long-term ENSO state rather than inter-annual variability~~.~~, and reflects the resolution of many individual low-frequency proxy reconstructions (cf Yan et al., 2011a, b; Anderson, 2012; Rodysill et al., 2012

Then at each stage (for each interim network), the pseudoproxies in the network (derived from GCM$_{cal}$ past1000) were first normalised to a common period $(a:b)$ where all proxies data via the equation:

$$Pn_t = \frac{P_t - \mu_{a:b}}{\sigma_{a:b}} \tag{B2}$$

where Pn_t is the normalised proxy value at time t, P_t is the original value at time t, $\mu_{a:b}$ is the mean value of proxy P between common period $a:b$, and $\sigma_{a:b}$ is the corresponding standard deviation. The length of $a:b$ was ensured to be at least 100 years to reduce the influence of noise on μ and σ. In some cases, this requirement led to the rejection of one or more proxies as their length or position in time were not compatible with the other records. This process of normalisation is similar to the method used in Wilson et al. (2010) . Proxies that fall in the same grid box were averaged after normalisation. This prevents overrepresentation of those locations, and improves their SNR by cancelling out some of the stochastic noise and amplifying their signal (Wang et al., 2014) .

Each normalised pseudoproxy Pn at location $[x,y]$ was multiplied by a scaled version of the EOF value at location $[x,y]$. The scaling was such that at each timestep the absolute sum of the weights was 1, which accounts for the fact that the number of locations with proxy data varies over the reconstructed period (especially the beginning and end). The weight of a given proxy location i can thus be considered an indication of the relative sensitivity of a location to ENSO which changes depending on the number of proxies n available at each timestep t and their associated EOF values W:

$$Wn_{it} = \frac{W_{it}}{\sum_{i=1}^{n} |W_{it}|} \tag{B3}$$

Finally, the n weighted proxy series Pw were summed to create a single reconstruction series $ENSO_r$:

$$Pw_t = P_t \times Wn_{Pt} \tag{B4}$$

$$ENSO_r = \sum_{i=1}^{n} Pw_i \tag{B5}$$

This is essentially a '~~optimalnetworkalgorithm is an add-one-in~~sparse' ~~methodology whereby pseudoproxies derived from the (t+v) 20CRv2 dataset were added one by one to find the combination that produced~~

~~the highest correlation with the expected outcome (i.e. the PC_{t+v} timeseries). The use of the full t+v was necessary to enable the calculation of 30-year means. While this somewhat compromises the independence of the validation, using only the calibration dataset of 50 years would likely have been more detrimental. The important separation here is between the EOF pattern (derived from the training data) and the calculation of the validation statistic CE (using μ_v).~~ reconstruction of the PC, which is the dot product of the full raw dataset and EOF. The quality of a network was assessed by comparing $ENSO_r$ with the PC using the Pearson rank correlation R.

The ~~ENSO reconstruction procedure described below in 3.3 was run repeatedly, starting with a basenetwork of zero proxies and adding each proxy separately. Once all networks had been tested individually, the proxy whose reconstruction ($ENSO$) gave the best CE value (using $z = PC_{t+v}$, $\hat{z} = ENSO$ and $\mu_v = PC_v$) was added to the base network. This process was repeated with the remaining proxies until all proxies were incorporated in the base network. The proxy combination which gave the overall highest CE was then saved as the optimalnetwork. Finally, the entire process from creating pseudoproxies to selecting the optimal network~~ entire calibration process was repeated 1000 times~~using different noise in each run~~, each time using pseudoproxies with newly generated noise iterations, resulting in 1000 proxy networks.

B5 Validation: network evaluation

The validation stage tests the robustness of the networks using independent data. A 1000 pseudoproxy versions were created of each calibration network using GCM$_{val}$ pseudoproxies, and tested for their ability to reconstruct the target (the PC created using the GCM$_{cal}$ EOF and the GCM$_{val}$ past1000 dataset) by calculating R. There are several measures of quality for validation statistics, the most common of which are the coefficient of determination R^2, the reduction of error (RE) and the coefficient of efficiency (CE; Cook et al., 1994) . Discussions on the relative merits and pitfalls of these measures can be found in the literature (cf Cook et al., 1995; Emile-Geay et al., 2013a) . Although CE is generally regarded as the appropriate indicator for low-frequency reconstructions (Bürger, 2007; Emile-Geay et al., 2 the nature of the method described here reduces its effectiveness as a measure of quality. The past1000 and piControl runs have little (or no) external forcing driving the simulation, hence they have very little low-frequency variability or trends. Moreover, the data is z-normalised at various stages, removing any differences in means. As the CE effectively tracks changes in the mean, this removal of the mean renders CE sensitive to spurious results. The diagnostic R was instead chosen as tests showed that it was more effective at picking high-quality reconstructions than CE and $RMSE$, though generally a high R value did correspond to high CE and low $RMSE$ (not shown). R is essentially equivalent to using R^2, but retains the ability to distinguish between positive and negative correlations.

The ~~add-one-in method picks proxy combinations based on an improvement in CE, but it does not necessarily guarantee that the final network actually produces a good ENSO reconstruction. This~~

~~was tested by comparing the pseudoproxy CE to a threshold value CE$_{crit}$. This critical value was~~ R-values from the 1000×1000 validation reconstructions (R_{val}) were then compared to critical values R_{crit} calculated for each network~~by running~~. Again, 1000 ~~ENSO reconstructions replacing the (signal+noise) pseudoproxy series in the networkwith pure noise, and calculating~~ reconstructions were made for each network, but using GCM$_{val}$ piControl data instead of past1000. The piControl run contains no external forcing and so is essentially noise, but retains the inherent climatological spatial correlations. From these reconstructions, R_{crit} for each network was determined by taking the 95th percentile of ~~their CE values. To compare,~~ the R-values of the corresponding 1000 ~~pseudoproxy ENSOs were also made; if 95of the pseudoproxy CE values were higher than CE$_{crit}$~~reconstructions. Where $R_{val} \geq R_{crit}$, the network was retained; where $R_{val} < R_{crit}$, the network was deemed ~~to be useful and was retained for the final reconstruction~~unfit and was discarded. Networks sensitive to the choice of dataset are thus weeded out.

The combination of using pseudoproxies, the add-one-in approach and ~~CE$_{crit}$~~ R_{crit} simultaneously accounts for proxy temporal resolution, spatial distribution and temporal coverage (i.e. proxy start and end dates), and gives an estimate of the uncertainty due to proxy noise. However, an important assumption is that the *signal* in all proxies is solely temperature or precipitation, and it is thus still a 'best case' estimate.

B6 ~~EOF-weighted~~ Proxy ENSO ~~reconstruction~~ ensemble

The 'optimal' networks that passed the ~~CE~~ R_{crit} test were used to create an ensemble of real proxy ~~ENSO reconstructions~~ reconstructions of ENSO-like climate change. The remaining ~~ones~~ networks may not all be unique, further reducing the effective number of networks. ~~Multiply occurring networks are assumedly~~ Presumably, networks that occur multiple times are more effective proxy combinations; retaining the duplicates accordingly upweights these networks in the final reconstruction. ~~The ENSO reconstruction for each ensemble member (network) was conducted in a series of steps: calculating proxy weights, combining the proxy records into ENSO reconstructions, calculating mean squared errors, and creating a proxy reconstruction ensemble. Each step is explained in more detail below.~~

B6.1 ~~Proxy weighting and ENSO reconstruction~~

~~The proxy weights were determined by the EOF pattern derived from 20CRv2. The value of this EOF indicates to what extent the precipitation or temperature is expected to be influenced by ENSO at a given location, with highly negative and highly positive regions displaying strong ENSO linkages. Each normalised proxy P at location $[x,y]$ was multiplied by a scaled version of the EOF value at location $[x,y]$. The scaling was such that at each timestep the absolute sum of the weights was 1, which accounts for the fact that the number of locations with proxy data varies over the reconstructed period (especially the beginning and end). The weight of a given proxy location i can thus be~~

~~considered an indication of the location's relative sensitivity to ENSO which changes depending on the number of proxies n available at each timestep and their associated EOF values:~~

$$EOFnorm_i = \frac{EOF_i}{\sum_{i=1}^{n} |EOF_i|}$$

~~Once weighted, the proxy records were summed to obtain a single timeseries to make an ENSO reconstruction.~~

B6.1 ~~Error estimation~~

Error estimates for the ~~ENSO reconstructions were derived again using a pseudoproxy method similar to the optimal networks creation. As the proxy availability varies over time, root mean square errors (RMSEs) were calculated for each timestep separately. This was done by calculating the RMSE for a network that only contains the proxies available at that timestep: for reconstruction ensemble network n, the proxies available at time t were used as a frozen(unchanging) network to create 1000 pseudo-reconstructions from which RMSE values were calculated for time t. Repeated for each timestep, this resulted in 1000 absolute error value timeseries for each network n~~reconstructions were made using the 1000×1000 $RMSE$ values calculated at the validation stage. This was translated into ensemble member uncertainty limits by adding and subtracting the 1000 error series from the ~~ENSO~~ reconstruction timeseries (to get the maximum and minimum error limits respectively) and taking the 5-95th percentile over their full range. This error estimation explicitly takes into account the impact of network choice as well as random error affecting the proxies.

B6.1 ~~Proxy ENSO ensemble~~

~~Once ENSO~~ Once proxy reconstructions and associated uncertainty estimates were calculated for all ~~networks (ensemble members)~~ensemble members, they were renormalised to 100-650 yrBP to make the trends and amplitudes comparable, within and between temperature and precipitation. The period 100-650 yrBP was chosen because it was common to all ~~ENSO~~ reconstruction timeseries and only covers one of the two periods of interest (the LIA). Although calibration to the instrumental period would potentially allow us to quantify the ~~ENSO amplitudes~~absolute amplitude, this was not done for two reasons. Firstly, the proxy data coverage during the instrumental period and the preceding century was relatively low, reducing the confidence in the reconstruction during that period; calibrating to this period would thus increase the uncertainty on the rest of the reconstruction. Secondly, any calibration to the instrumental data is necessarily biased towards high-frequency trends (Mann et al., 2008). Within a 30-year averaged series, the number of comparison points with the instrumental period is extremely low. The final proxy ~~ENSO~~ reconstruction was calculated as the ensemble mean. The corresponding error estimate is a combination of the reconstruction ensemble range and the error ranges for individual ensemble members.

Acknowledgements. Many thanks to the Databases of the NOAA World Data Center for Paleoclimatology and Pangaea and all contributing authors for making available the proxy data used in this study.

The GPCP and 20th Century Reanalysis V2 data were provided by the NOAA/OAR/ESRL PSD, Boulder, Colorado, USA, from their Web site at http://www.esrl.noaa.gov/psd/.

Support for the Twentieth Century Reanalysis Project dataset is provided by the U.S. Department of Energy, Office of Science Innovative and Novel Computational Impact on Theory and Experiment (DOE INCITE) program, and Office of Biological and Environmental Research (BER), and by the National Oceanic and Atmospheric Administration Climate Program Office.

The GPCP combined precipitation data were developed and computed by the NASA/Goddard Space Flight Center's Laboratory for Atmospheres as a contribution to the GEWEX Global Precipitation Climatology Project.

We acknowledge the World Climate Research Programme's Working Group on Coupled Modelling, which is responsible for CMIP, and we thank the climate modeling groups listed in B2 for producing and making available their model output. For CMIP the U.S. Department of Energy's Program for Climate Model Diagnosis and Intercomparison provides coordinating support and led development of software infrastructure in partnership with the Global Organization for Earth System Science Portals.

L. Henke was supported by a University of Exeter Climate Change and Sustainable Futures studentship.

References

Abram, N. J., Gagan, M. K., Cole, J. E., Hantoro, W. S., and Mudelsee, M.: Recent intensification of tropical climate variability in the Indian Ocean, Nat. Geosci., 1, 849–853, doi:10.1038/ngeo357, 2008.

Abram, N. J., McGregor, H. V., Gagan, M. K., Hantoro, W. S., and Suwargadi, B. W.: Oscillations in the southern extent of the Indo-Pacific Warm Pool during the mid-Holocene, Quat. Sci. Rev., 28, 2794–2803, doi:10.1016/j.quascirev.2009.07.006, 2009.

Alibert, C. and Kinsley, L.: A 170-year Sr/Ca and Ba/Ca coral record from the western Pacific warm pool: 2. A window into variability of the New Ireland Coastal Undercurrent, J. Geophys. Res. Ocean., 113, 1–10, doi:10.1029/2007JC004263, 2008.

Anchukaitis, K. J. and Evans, M. N.: Tropical cloud forest climate variability and the demise of the Monteverde golden toad., Proc. Natl. Acad. Sci. U. S. A., 107, 5036–5040, doi:10.1073/pnas.0908572107, 2010.

Anchukaitis, K. J., Evans, M. N., Kaplan, A., Vaganov, E. A., Hughes, M. K., Grissino-Mayer, H. D., and Cane, M. A.: Forward modeling of regional scale tree-ring patterns in the southeastern United States and the recent influence of summer drought, Geophys. Res. Lett., 33, 2–5, doi:10.1029/2005GL025050, 2006.

Anderson, L.: Holocene record of precipitation seasonality from lake calcite δ^{18}O in the central Rocky Mountains, United States, Geology, 39, 211–214, doi:10.1130/G31575.1, 2011.

Anderson, L.: Rocky Mountain hydroclimate: Holocene variability and the role of insolation, ENSO, and the North American Monsoon, Glob. Planet. Change, 92-93, 198–208, doi:10.1016/j.gloplacha.2012.05.012, 2012.

Apastaégui, J., Cruz, F. W., Sifeddine, A., Vuille, M., Espinoza, J. C., Guyot, J. L., Khodri, M., Strikis, N., Santos, R. V., Cheng, H., Edwards, L., Carvalho, E., and Santini, W.: Hydroclimate variability of the northwestern Amazon Basin near the Andean foothills of Peru related to the South American Monsoon System during the last 1600 years, Clim. Past, 10, 1967–1981, doi:10.5194/cp-10-1967-2014, 2014.

Asami, R.: Interannual and decadal variability of the western Pacific sea surface condition for the years 1787–2000: Reconstruction based on stable isotope record from a Guam coral, J. Geophys. Res., 110, C05 018, doi:10.1029/2004JC002555, 2005.

Ashok, K., Behera, S. K., Rao, S. A., Weng, H., and Yamagata, T.: El Niño Modoki and its possible teleconnection, J. Geophys. Res. Ocean., 112, 1–27, doi:10.1029/2006JC003798, 2007.

Asmerom, Y., Polyak, V., Burns, S. J., and Rassmussen, J.: Solar forcing of Holocene climate: New insights from a speleothem record, southwestern United States, Geology, 35, 1–4, doi:10.1130/G22865A.1, 2007.

Badjeck, M.-C., Allison, E. H., Halls, A. S., and Dulvy, N. K.: Impacts of climate variability and change on fishery-based livelihoods, Mar. Policy, 34, 375–383, doi:10.1016/j.marpol.2009.08.007, 2010.

Bagnato, S., Linsley, B. K., Howe, S. S., Wellington, G. M., and Salinger, J.: Coral oxygen isotope records of interdecadal climate variations in the South Pacific Convergence Zone region, Geochemistry, Geophys. Geosystems, 6, 1–8, doi:10.1029/2004GC000879, 2005.

Baker, P. A., Fritz, S. C., Burns, S. J., Ekdahl, E., and Rigsby, C. A.: The Nature and Origin of Decadal to Millennial Scale Climate Variability in the Southern Tropics of South America: The Holocene Record of Lago Umayo, Peru, in: Past Clim. Var. South Am. Surround. Reg. From Last Glacial Maximum to Holocene, edited by Vimeux, F., Sylvestre, F., and Khodri, M., chap. 13, pp. 301–322, Springer Netherlands, Dordrecht, 14 edn., doi:10.1007/978-90-481-2672-9_13, 2009.

Bale, R. J., Robertson, I., Salzer, M. W., Loader, N. J., Leavitt, S. W., Gagen, M., Harlan, T. P., and McCarroll, D.: An annually resolved bristlecone pine carbon isotope chronology for the last millennium, Quat. Res., 76, 22–29, doi:10.1016/j.yqres.2011.05.004, 2011.

Barron, J. A.: High-resolution climatic evolution of coastal northern California during the past 16,000 years, Paleoceanography, 18, doi:10.1029/2002PA000768, 1020, 2003.

Barron, J. A. and Anderson, L.: Enhanced Late Holocene ENSO/PDO expression along the margins of the eastern North Pacific, Quat. Int., 235, 3–12, doi:10.1016/j.quaint.2010.02.026, 2011.

Bellenger, H., Guilyardi, E., Leloup, J., Lengaigne, M., and Vialard, J.: ENSO representation in climate models: From CMIP3 to CMIP5, Clim. Dyn., 42, 1999–2018, doi:10.1007/s00382-013-1783-z, 2014.

Berke, M. A., Johnson, T. C., Werne, J. P., Schouten, S., and Sinninghe Damsté, J. S.: A mid-Holocene thermal maximum at the end of the African Humid Period, Earth Planet. Sci. Lett., 351-352, 95–104, doi:10.1016/j.epsl.2012.07.008, 2012.

Bird, B. W., Abbott, M. B., Rodbell, D. T., and Vuille, M.: Holocene tropical South American hydroclimate revealed from a decadally resolved lake sediment $\delta^{18}O$ record, Earth Planet. Sci. Lett., 310, 192–202, doi:10.1016/j.epsl.2011.08.040, 2011.

Black, D. E., Abahazi, M. A., Thunell, R. C., Kaplan, A., Tappa, E. J., and Peterson, L. C.: An 8-century tropical Atlantic SST record from the Cariaco Basin: Baseline variability, twentieth-century warming, and Atlantic hurricane frequency, Paleoceanography, 22, 1–10, doi:10.1029/2007PA001427, 2007.

Boiseau, M., Ghil, M., and Juillet-Leclerc, A.: Climatic trends and interdecadal variability from South-Central Pacific coral records, Geophys. Res. Lett., 26, 2881–2884, 1999.

Bonnefille, R. and Chalié, F.: Pollen-inferred precipitation time-series from equatorial mountains, Africa, the last 40 kyr BP, Glob. Planet. Change, 26, 25–50, doi:10.1016/S0921-8181(00)00032-1, 2000.

Braconnot, P., Harrison, S. P., Otto-Bliesner, B. L., Abe-Ouchi, A., Jungclaus, J. H., and Peterschmitt, J.-Y.: The Paleoclimate Modeling Intercomparison Project contribution to CMIP5, CLIVAR Exch. Newsl., 16, 15–19, 2011.

Braconnot, P., Harrison, S. P., Kageyama, M., Bartlein, P. J., Masson-Delmotte, V., Abe-Ouchi, A., Otto-Bliesner, B., and Zhao, Y.: Evaluation of climate models using palaeoclimatic data, Nat. Clim. Chang., 2, 417–424, doi:10.1038/nclimate1456, 2012.

Braganza, K., Gergis, J. L., Power, S. B., Risbey, J. S., and Fowler, A. M.: A multiproxy index of the El Niño-Southern Oscillation, A.D. 1525-1982, J. Geophys. Res. Atmos., 114, 1–17, doi:10.1029/2008JD010896, 2009.

Breitenmoser, P., Brönnimann, S., and Frank, D.: Forward modelling of tree-ring width and comparison with a global network of tree-ring chronologies, Clim. Past, 10, 437–449, doi:10.5194/cp-10-437-2014, 2014.

Brook, G., Sheen, S.-W., Rafter, M., Railsback, L. B., and Lundberg, J.: A high-resolution proxy record of rainfall and ENSO since AD 1550 from layering in stalagmites from Anjohibe Cave, Madagascar, The Holocene, 9, 695–705, doi:10.1191/095968399677907790, 1999.

Buckley, B. M., Anchukaitis, K. J., Penny, D., Fletcher, R., Cook, E. R., Sano, M., Nam, L. C., Wichienkeeo, A., Minh, T. T., and Hong, T. M.: Climate as a contributing factor in the demise of Angkor, Cambodia., Proc. Natl. Acad. Sci. U. S. A., 107, 6748–6752, doi:10.1073/pnas.0910827107, 2010.

Buizer, J. L., Foster, J., and Lund, D.: Global impacts and regional actions: Preparing for the 1997-98 El Niño, Bull. Am. Meteorol. Soc., 81, 2121–2139, doi:10.1175/1520-0477(2000)081<2121:GIARAP>2.3.CO;2, 2000.

Bürger, G.: On the verification of climate reconstructions, Clim. Past, 3, 397–409, doi:10.5194/cpd-3-249-2007, 2007.

Cai, W., Santoso, A., Wang, G., Yeh, S.-w., An, S.-i., Cobb, K. M., Collins, M., Guilyardi, E., Jin, F.-f., Kug, J.-s., Lengaigne, M., and McPhaden, M. J.: ENSO and greenhouse warming, Nat. Publ. Gr., 5, 849–859, doi:10.1038/nclimate2743, 2015a.

Cai, W., Wang, G., Santoso, A., McPhaden, M. J., Wu, L., Jin, F.-F., Timmermann, A., Collins, M., Vecchi, G., Lengaigne, M., England, M. H., Dommenget, D., Takahashi, K., and Guilyardi, E.: Increased frequency of extreme La Niña events under greenhouse warming, Nat. Clim. Chang., 5, 132–137, doi:10.1038/nclimate2492, 2015b.

Cane, M. A.: The evolution of El Niño, past and future, Earth Planet. Sci. Lett., 230, 227–240, doi:10.1016/j.epsl.2004.12.003, 2005.

Carré, M., Bentaleb, I., Fontugne, M., and Lavallée, D.: Strong El Niño events during the early Holocene: stable isotope evidence from Peruvian sea shells, The Holocene, 15, 42–47, doi:10.1191/0959683605h1782rp, 2005.

Charles, C. D.: Interaction Between the ENSO and the Asian Monsoon in a Coral Record of Tropical Climate, Science, 227, 925–928, doi:10.1126/science.277.5328.925, 1997.

Charles, C. D., Cobb, K. M., Moore, M. D., and Fairbanks, R. G.: Monsoon-tropical ocean interaction in a network of coral records spanning the 20th century, Mar. Geol., 201, 207–222, doi:10.1016/S0025-3227(03)00217-2, 2003.

Chen, J., Chen, F., Zhang, E., Brooks, S. J., Zhou, A., and Zhang, J.: A 1000-year chironomid-based salinity reconstruction from varved sediments of Sugan Lake, Qaidam Basin, arid Northwest China, and its palaeoclimatic significance, Chinese Sci. Bull., 54, 3749–3759, doi:10.1007/s11434-009-0201-8, 2009.

Christie, D. A., Boninsegna, J. A., Cleaveland, M. K., Lara, A., Le Quesne, C., Morales, M. S., Mudelsee, M., Stahle, D. W., and Villalba, R.: Aridity changes in the Temperate-Mediterranean transition of the Andes since AD 1346 reconstructed from tree-rings, Clim. Dyn., 36, 1505–1521, doi:10.1007/s00382-009-0723-4, 2011.

Cleaveland, M. K., Stahle, D. W., Therrell, M. D., Villanueva-Diaz, J., and Burns, B. T.: Tree-ring reconstructed winter precipitation and tropical teleconnections in Durango, Mexico, Clim. Change, 59, 369–388, doi:10.1023/A:1024835630188, 2003.

Clement, A. C., Cane, M. A., and Seager, R.: An orbitally driven tropical source for abrupt climate change, J. Clim., 14, 2369–2375, doi:10.1175/1520-0442(2001)014<2369:AODTSF>2.0.CO;2, 2001.

Coats, S., Smerdon, J. E., Cook, B. I., and Seager, R.: Stationarity of the tropical pacific teleconnection to North America in CMIP5/PMIP3 model simulations, Geophys. Res. Lett., 40, 4927–4932, doi:10.1002/grl.50938, 2013.

Cobb, K. M., Charles, C. D., Cheng, H., and Edwards, R. L.: El Niño/Southern Oscillation and tropical Pacific climate during the last millennium., Nature, 424, 271–276, doi:10.1038/nature01779, 2003.

Cole, J. E.: Tropical Pacific forcing of decadal SST variability in the western Indian Ocean over the past two centuries, Science, 287, 617–619, doi:10.1126/science.287.5453.617, 2000.

Cole, J. E., Fairbanks, R. G., and Shen, G. T.: Recent variability in the Southern Oscillation: isotopic results from a tarawa atoll coral., Science, 260, 1790–1793, doi:10.1126/science.260.5115.1790, 1993.

Collins, M.: El Niño- or La Niña-like climate change?, Clim. Dyn., 24, 89–104, doi:10.1007/s00382-004-0478-x, 2005.

Comboul, M., Emile-Geay, J., Evans, M. N., Mirnateghi, N., Cobb, K. M., and Thompson, D. M.: A probabilistic model of chronological errors in layer-counted climate proxies: Applications to annually banded coral archives, Clim. Past, 10, 825–841, doi:10.5194/cp-10-825-2014, 2014.

Comboul, M., Emile-Geay, J., Hakim, G. J., and Evans, M. N.: Paleoclimate Sampling as a Sensor Placement Problem, J. Clim., 28, 7717–7740, 2015.

Compo, G. P., Whitaker, J. S., Sardeshmukh, P. D., Matsui, N., Allan, R. J., Yin, X., Gleason, B. E., Vose, R. S., Rutledge, G., Bessemoulin, P., Bronnimann, S., Brunet, M., Crouthamel, R. I., Grant, A. N., Groisman, P. Y., Jones, P. D., Kruk, M. C., Kruger, A. C., Marshall, G. J., Maugeri, M., Mok, H. Y., Nordli, O., Ross, T. F., Trigo, R. M., Wang, X. L., Woodruff, S. D., and Worley, S. J.: The Twentieth Century Reanalysis Project, Q. J. R. Meteorol. Soc., 137, 1–28, doi:10.1002/qj.776, 2011.

Conroy, J., Overpeck, J. T., and Cole, J. E.: El Niño-Southern Oscillation and changes in the zonal gradient of tropical Pacific sea surface temperature over the last 1.2 ka, PAGES News, 18, 1–5, 2010.

Conroy, J. L., Overpeck, J. T., Cole, J. E., Shanahan, T. M., and Steinitz-Kannan, M.: Holocene changes in eastern tropical Pacific climate inferred from a Galápagos lake sediment record, Quat. Sci. Rev., 27, 1166–1180, doi:10.1016/j.quascirev.2008.02.015, 2008.

Conroy, J. L., Restrepo, A., Overpeck, J. T., Steinitz-Kannan, M., Cole, J. E., Bush, M. B., and Colinvaux, P. A.: Unprecedented recent warming of surface temperatures in the eastern tropical Pacific Ocean, Nat. Geosci., 2, 46–50, doi:10.1038/ngeo390, 2009.

Cook, E. R., Briffa, K. R., and Jones, P. D.: Spatial regression methods in dendroclimatology: A review and comparison of two techniques, Int. J. Climatol., 14, 379–402, doi:10.1002/joc.3370140404, 1994.

Cook, E. R., Briffa, K. R., Meko, D. M., Graybill, D. A., and Funkhouser, G.: The 'segment length curse' in long tree-ring chronology development for palaeoclimatic studies, The Holocene, 5, 229–237, 1995.

Cook, E. R., Buckley, B. M., D'Arrigo, R. D., and Peterson, M. J.: Warm-season temperatures since 1600 BC reconstructed from Tasmanian tree rings and their relationship to large-scale sea surface temperature anomalies, Clim. Dyn., 16, 79–91, doi:10.1007/s003820050006, 2000.

Corrège, T., Delcroix, T., Récy, J., Beck, W., Cabioch, G., and Le Cornec, F.: Evidence for stronger El Niño-Southern Oscillation (ENSO) events in a mid-Holocene massive coral, Paleoceanography, 15, 465–470, 2000.

Crausbay, S. D., Russell, J. M., and Schnurrenberger, D. W.: A ca. 800-year lithologic record of drought from sub-annually laminated lake sediment, East Java, J. Paleolimnol., 35, 641–659, doi:10.1007/s10933-005-4440-7, 2006.

Cronin, T. M., Dwyer, G. S., Kamiya, T., Schwede, S., and Willard, D. A.: Medieval Warm Period, Little Ice Age and 20th century temperature variability from Chesapeake Bay, Glob. Planet. Change, 36, 17–29, doi:10.1016/S0921-8181(02)00161-3, 2003.

Cronin, T. M., Thunell, R., Dwyer, G. S., Saenger, C., Mann, M. E., Vann, C., and Seal, I. R.: Multiproxy evidence of Holocene climate variability from estuarine sediments, eastern North America, Paleoceanography, 20, doi:10.1029/2005PA001145, 2005.

Curtis, J. H., Hodelle, D. A., and Brenner, M.: Climate variability on the Yucatán Peninsula (Mexico) during the past 3500 years, and implications for Maya cultural evolution, Quat. Res., 46, 37–47, doi:10.1006/qres.1996.0042, 1996.

Damassa, T. D., Cole, J. E., Barnett, H. R., Ault, T. R., and McClanahan, T. R.: Enhanced multidecadal climate variability in the seventeenth century from coral isotope records in the western Indian Ocean, Paleoceanography, 21, PA2016, doi:10.1029/2005PA001217, 2006.

D'Arrigo, R. and Wilson, R.: On the Asian expression of the PDO, Int. J. Climatol., 26, 1607–1617, doi:10.1002/joc.1326, 2006.

Dee, S., Emile-Geay, J., Evans, M. N., Allam, A., Steig, E. J., and Thompson, D. M.: PRYSM: An open-source framework for PRoxY System Modeling, with applications to oxygen-isotope systems, J. Adv. Model. Earth Syst., 7, 1220–1247, doi:10.1002/ 2015MS000447, 2015.

DeLong, K. L., Quinn, T. M., Taylor, F. W., Lin, K., and Shen, C.-C.: Sea surface temperature variability in the southwest tropical Pacific since AD 1649, Nat. Clim. Chang., 2, 799–804, doi:10.1038/nclimate1583, 2012.

DeLong, K. L., Quinn, T. M., Taylor, F. W., Shen, C. C., and Lin, K.: Improving coral-base paleoclimate reconstructions by replicating 350years of coral Sr/Ca variations, Palaeogeogr. Palaeoclimatol. Palaeoecol., 373, 6–24, doi:10.1016/j.palaeo.2012.08.019, 2013.

DeLong, K. L., Flannery, J. A., Poore, R. Z., Quinn, T. M., Maupin, C. R., Lin, K., and Shen, C. C.: A reconstruction of sea surface temperature variability in the southeastern Gulf of Mexico from 1734 to 2008 C.E. using cross-dated Sr/Ca records from the coral Siderastrea siderea, Paleoceanography, 29, 403–422, doi:10.1002/2013PA002524, 2014.

Denniston, R. F., Villarini, G., Gonzales, A. N., Wyrwoll, K.-H., Polyak, V. J., Ummenhofer, C. C., Lachniet, M. S., Wanamaker, A. D., Humphreys, W. F., Woods, D., and Cugley, J.: Extreme rainfall activity in the Australian tropics reflects changes in the El Niño/Southern Oscillation over the last two millennia., Proc. Natl. Acad. Sci. U. S. A., 112, 4576–4581, doi:10.1073/pnas.1422270112, 2015.

Díaz, S. C., Therrell, M. D., Stahle, D. W., and Cleaveland, M. K.: Chihuahua (Mexico) winter-spring precipitation reconstructed from tree-rings, 1647-1992, Clim. Res., 22, 237–244, doi:10.3354/cr022237, 2002.

Druffel, E. R. M. and Griffin, S.: Variability of surface ocean radiocarbon and stable isotopes in the southwestern Pacific, J. Geophys. Res. Ocean., 104, 23 607–23 613, doi:10.1029/1999jc900212, 1999.

Dunbar, R. B., Wellington, G. M., Colgan, M. W., and Glynn, P. W.: Eastern Pacific sea surface temperature since 1600 A.D.: The $\delta^{18}O$ record of climate variability in Galápagos Corals, Paleoceanography, 9, 291–315, doi:10.1029/93PA03501, 1994.

Emile-Geay, J. and Tingley, M.: Inferring climate variability from nonlinear proxies. Application to paleo-ENSO studies., Clim. Past, 12, 31–50, doi:10.5194/cp-12-31-2016, 2016.

Emile-Geay, J., Cobb, K. M., Mann, M. E., and Wittenberg, A. T.: Estimating central equatorial pacific SST variability over the past millennium. Part I: Methodology and validation, J. Clim., 26, 2302–2328, doi:10.1175/JCLI-D-11-00510.1, 2013a.

Emile-Geay, J., Cobb, K. M., Mann, M. E., and Wittenberg, A. T.: Estimating central equatorial pacific SST variability over the past millennium. Part II: Reconstructions and Implications, J. Clim., 26, 2329–2352, doi:10.1175/JCLI-D-11-00511.1, 2013b.

Esper, J., Cook, E. R., and Schweingruber, F. H.: Low-frequency signals in long tree-ring chronologies for reconstructing past temperature variability., Science, 295, 2250–2253, doi:10.1126/science.1066208, 2002.

Evans, M. N., Kaplan, A., and Cane, M. A.: Optimal sites for coral-based reconstruction of global sea surface temperature, Paleoceanography, 13, 502–516, doi:10.1029/98PA02132, 1998.

Evans, M. N., Tolwinski-Ward, S. E., Thompson, D. M., and Anchukaitis, K. J.: Applications of proxy system modeling in high resolution paleoclimatology, Quat. Sci. Rev., 76, 16–28, 2013.

Evans, M. N., Smerdon, J. E., Kaplan, A., Tolwinski-Ward, S. E., and González-Rouco, J. F.: Climate field reconstruction uncertainty arising from multivariate and nonlinear properties of predictors, Geophys. Res. Lett., 41, 9127–9134, doi:10.1002/2014GL062063, 2014.

Faulstich, H. L., Woodhouse, C. A., and Griffin, D.: Reconstructed cool- and warm-season precipitation over the tribal lands of northeastern Arizona, Clim. Change, 118, 457–468, doi:10.1007/s10584-012-0626-y, 2013.

Felis, T., Pätzold, J., Loya, Y., Fine, M., Nawar, A. H., and Wefer, G.: A coral oxygen isotope record from the northern Red Sea documenting NAO, ENSO, and North Pacific teleconnections on Middle East climate variability since the year 1750, Paleoceanography, 15, 679–694, doi:10.1029/1999PA000477, 2000.

Felis, T., Suzuki, A., Kuhnert, H., Dima, M., Lohmann, G., and Kawahata, H.: Subtropical coral reveals abrupt early-twentieth-century freshening in the western North Pacific Ocean, Geology, 37, 527–530, doi:10.1130/G25581A.1, 2009.

Felis, T., Suzuki, A., Kuhnert, H., Rimbu, N., and Kawahata, H.: Pacific decadal oscillation documented in a coral record of North Pacific winter temperature since 1873, Geophys. Res. Lett., 37, 2000–2005, doi:10.1029/2010GL043572, 2010.

Gallant, A. J. E., Phipps, S. J., Karoly, D. J., Mullan, A. B., and Lorrey, A. M.: Nonstationary Australasian teleconnections and implications for paleoclimate reconstructions, J. Clim., 26, 8827–8849, doi:10.1175/JCLI-D-12-00338.1, 2013.

Gergis, J. L. and Fowler, A. M.: How unusual was late 20th century El Niño-Southern Oscillation (ENSO)? Assessing evidence from tree-ring, coral, ice-core and documentary palaeoarchives, A.D. 1525-2002, Adv. Geosci., 6, 173–179, doi:10.5194/adgeo-6-173-2006, 2006.

Gergis, J. L. and Fowler, A. M.: A history of ENSO events since A.D. 1525: Implications for future climate change, Clim. Change, 92, 343–387, doi:10.1007/s10584-008-9476-z, 2009.

Gomez, B., Carter, L., Trustrum, N. A., Palmer, A. S., and Roberts, A. P.: El Niño-Southern Oscillation signal associated with middle Holocene climate change in intercorrelated terrestrial and marine sediment cores, North Island, New Zealand, Geology, 32, 653–656, doi:10.1130/G20720.1, 2004.

Goni, M. A., Thunell, R. C., Woodwort, M. P., and Müller-Karger, F. E.: Changes in wind-driven upwelling during the last three centuries: Interocean teleconnections, Geophys. Res. Lett., 33, 3–6, doi:10.1029/2006GL026415, 2006.

Goodkin, N. F., Hughen, K. A., Curry, W. B., Doney, S. C., and Ostermann, D. R.: Sea surface temperature and salinity variability at Bermuda during the end of the Little Ice Age, Paleoceanography, 23, 1–13, doi:10.1029/2007PA001532, 2008.

Gorman, M. K., Quinn, T. M., Taylor, F. W., Partin, J. W., Cabioch, G., Austin, J. A., Pelletier, B., Ballu, V., Maes, C., and Saustrup, S.: A coral-based reconstruction of sea surface salinity at Sabine Bank, Vanuatu from 1842 to 2007 CE, Paleoceanography, 27, 1–13, doi:10.1029/2012PA002302, 2012.

Graham, N. E., Hughes, M. K., Ammann, C. M., Cobb, K. M., Hoerling, M. P., Kennett, D. J., Kennett, J. P., Rein, B., Stott, L., Wigand, P. E., and Xu, T.: Tropical Pacific - Mid-latitude teleconnections in medieval times, Clim. Change, 83, 241–285, doi:10.1007/s10584-007-9239-2, 2007.

Griffin, D., Woodhouse, C. A., Meko, D. M., Stahle, D. W., Faulstich, H. L., Carrillo, C., Touchan, R., Castro, C. L., and Leavitt, S. W.: North American monsoon precipitation reconstructed from tree-ring latewood, Geophys. Res. Lett., 40, 954–958, doi:10.1002/grl.50184, 2013.

Guilderson, T. P. and Schrag, D. P.: Reliability of coral isotope records from the Western Pacific Warm Pool: A comparison using age-optimized records, Paleoceanography, 14, 457, doi:10.1029/1999PA900024, 1999.

Guilyardi, E., Wittenberg, A., Fedorov, A., Collins, M., Wang, C., Capotondi, A., van Oldenborgh, G. J., and Stockdale, T.: Understanding El Niño in ocean-atmosphere general circulation models: Progress and challenges, Bull. Am. Meteorol. Soc., 90, 325–340, doi:10.1175/2008BAMS2387.1, 2009.

Haug, G. H., Hughen, K. A., Sigman, D. M., Peterson, L. C., and Röhl, U.: Southward migration of the intertropical convergence zone through the Holocene., Science, 293, 1304–1308, doi:10.1126/science.1059725, 2001.

Heiss, G. A.: Coral reefs in the Red Sea: Growth, production and stable isotopes., GEOMAR Rep., 32, 1–141, 1994.

Hendy, E. J., Gagan, M. K., and Lough, J. M.: Chronological control of coral records using luminescent lines and evidence for non-stationary ENSO teleconnections in northeast Australia, The Holocene, 13, 187–199, doi:10.1191/0959683603hl606rp, 2003.

Hetzinger, S., Pfeiffer, M., Dullo, W. C., Garbe-Schönberg, D., and Halfar, J.: Rapid 20th century warming in the Caribbean and impact of remote forcing on climate in the northern tropical Atlantic as recorded in a Guadeloupe coral, Palaeogeogr. Palaeoclimatol. Palaeoecol., 296, 111–124, doi:10.1016/j.palaeo.2010.06.019, 2010.

Hjelle, B. and Glass, G. E.: Outbreak of hantavirus infection in the Four Corners region of the United States in the wake of the 1997-1998 El Niño-Southern Oscillation., J. Infect. Dis., 181, 1569–1573, doi:10.1086/315467, 2000.

Hodell, D. A., Curtis, J. H., and Brenner, M.: Possible role of climate in the collapse of Classic Maya civilization, Nature, 375, 391–394, doi:10.1038/375391a0, 1995.

Ivanochko, T. S., Ganeshram, R. S., Brummer, G. J. a., Ganssen, G., Jung, S. J. a., Moreton, S. G., and Kroon, D.: Variations in tropical convection as an amplifier of global climate change at the millennial scale, Earth Planet. Sci. Lett., 235, 302–314, doi:10.1016/j.epsl.2005.04.002, 2005.

Jones, P., Briffa, K., Osborn, T., Lough, J., van Ommen, T., Vinther, B., Luterbacher, J., Wahl, E., Zwiers, F., Mann, M., Schmidt, G., Ammann, C., Buckley, B., Cobb, K., Esper, J., Goosse, H., Graham, N., Jansen, E., Kiefer, T., Kull, C., Küttel, M., Mosley-Thompson, E., Overpeck, J., Riedwyl, N., Schulz, M., Tudhope, A., Villalba, R., Wanner, H., Wolff, E. W., Xoplaki, E., Kuttel, M., Mosley-Thompson, E., Overpeck, J., Riedwyl, N., Schulz, M., Tudhope, A., Villalba, R., Wanner, H., Wolff, E. W., and Xoplaki, E.: High-resolution palaeoclimatology of the last millennium: a review of current status and future prospects, The Holocene, 19, 3–49, doi:10.1177/0959683608098952, 2009.

Jones, P. D. and Mann, M. E.: Climate over past millennia, Rev. Geophys., 42, 1–42, doi:10.1029/2003RG000143, 2004.

Karamperidou, C., Di Nezio, P. N., Timmermann, A., Jin, F. F., and Cobb, K. M.: The response of ENSO flavors to mid-Holocene climate: Implications for proxy interpretation, Paleoceanography, pp. 527–547, doi:10.1002/2014PA002742, 2015.

Keigwin, L. D.: The Little Ice Age and Medieval Warm Period in the Sargasso Sea, Science, 274, 1504–1508, doi:10.1126/science.274.5292.1504, 1996.

Kellerhals, T., Brütsch, S., Sigl, M., Knüsel, S., Gäggeler, H. W., and Schwikowski, M.: Ammonium concentration in ice cores: A new proxy for regional temperature reconstruction?, J. Geophys. Res. Atmos., 115, 1–8, doi:10.1029/2009JD012603, 2010.

Kennett, D., Breitenbach, S., Aquino, V., Asmerom, Y., Awe, J., Baldini, J., Bartlein, P., Culleton, B., Ebert, C., Jazwa, C., Macri, M., Marwan, N., Polyak, V., Prufer, K., Ridley, H., Sodemann, H., Winterhalder, B., and Haug, G.: Development and disintegration of Maya political systems in response to climate change., Science, 788, 788–791, doi:10.1126/science.1226299, 2012.

Khider, D., Jackson, C. S., and Stott, L. D.: Assessing millennial-scale variability during the Holocene: A perspective from the western tropical Pacific, Paleoceanography, 29, 143–159, doi:10.1002/2013PA002534, 2014.

Kilbourne, K. H., Quinn, T. M., Webb, R., Guilderson, T., Nyberg, J., and Winter, A.: Paleoclimate proxy perspective on Caribbean climate since the year 1751: Evidence of cooler temperatures and multidecadal variability, Paleoceanography, 23, 1–14, doi:10.1029/2008PA001598, 2008.

Kim, S. T. and Yu, J. Y.: The two types of ENSO in CMIP5 models, Geophys. Res. Lett., 39, 1–6, doi:10.1029/2012GL052006, 2012.

Klein, S. a., Soden, B. J., and Lau, N. C.: Remote sea surface temperature variations during ENSO: Evidence for a tropical atmospheric bridge, J. Clim., 12, 917–932, doi:10.1175/1520-0442(1999)012<0917:RSSTVD>2.0.CO;2, 1999.

Kovats, R. S., Bouma, M. J., Hajat, S., Worrall, E., and Haines, A.: El Niño and health, Lancet, 362, 1481–1489, 2003.

Krusic, P. J., Cook, E. R., Dukpa, D., Putnam, A. E., Rupper, S., and Schaefer, J.: Six hundred thirty-eight years of summer temperature variability over the Bhutanese Himalaya, Geophys. Res. Lett., 42, 2988–2994, doi:10.1002/2015GL063566.Received, 2015.

Kuhnert, H., Pätzold, J., Hatcher, B., Wyrwoll, K. H., Eisenhauer, A., Collins, L. B., Zhu, Z. R., and Wefer, G.: A 200-year coral stable oxygen isotope record from a high-latitude reef off Western Australia, Coral Reefs, 18, 1–12, doi:10.1007/s003380050147, 1999.

Kuhnert, H., Pätzold, J., Wyrwoll, K. H., and Wefer, G.: Monitoring climate variability over the past 116 years in coral oxygen isotopes from Ningaloo Reef, Western Australia, Int. J. Earth Sci., 88, 725–732, doi:10.1007/s005310050300, 2000.

Kuhnert, H., Crüger, T., and Pätzold, J.: NAO signature in a Bermuda coral Sr/Ca record, Geochemistry, Geophys. Geosystems, 6, doi:10.1029/2004GC000786, 2005.

Langton, S. J., Linsley, B. K., Robinson, R. S., Rosenthal, Y., Oppo, D. W., Eglinton, T. I., Howe, S. S., Djajadihardja, Y. S., and Syamsudin, F.: 3500 yr record of centennial-scale climate variability from the Western Pacific Warm Pool, Geology, 36, 795–798, doi:10.1130/G24926A.1, 2008.

Lewis, S. C. and LeGrande, A. N.: Stability of ENSO and its tropical Pacific teleconnections over the Last Millennium, Clim. Past, 11, 1347–1360, doi:10.5194/cp-11-1347-2015, 2015.

Li, J., Xie, S.-P., Cook, E. R., Morales, M. S., Christie, D. A., Johnson, N. C., Chen, F., D'Arrigo, R., Fowler, A. M., Gou, X., and Fang, K.: El Niño modulations over the past seven centuries, Nat. Clim. Chang., 3, 822–826, doi:10.1038/nclimate1936, 2013.

Linsley, B. K., Dunbar, R. B., Wellington, G. M., and Mucciarone, D. A.: A coral-based reconstruction of Intertropical Convergence Zone variability over Central America since 1707, J. Geophys. Res., 99, 9977–9994, doi:10.1029/94JC00360, 1994.

Linsley, B. K., Ren, L., Dunbar, R. B., and Howe, S. S.: El Niño Southern Oscillation (ENSO) and decadal-scale climate variability at 10°N in the eastern Pacific from 1893 to 1994: A coral-based reconstruction from Clipperton Atoll, Paleoceanography, 15, 322–335, doi:10.1029/1999PA000428, 2000.

Linsley, B. K., Kaplan, A., Gouriou, Y., Salinger, J., DeMenocal, P. B., Wellington, G. M., and Howe, S. S.: Tracking the extent of the South Pacific Convergence Zone since the early 1600s, Geochemistry, Geophys. Geosystems, 7, 1–15, doi:10.1029/2005GC001115, 2006.

MacDonald, G. M. and Case, R. A.: Variations in the Pacific Decadal Oscillation over the past millennium, Geophys. Res. Lett., 32, 1–4, doi:10.1029/2005GL022478, 2005.

Makou, M. C., Eglinton, T. I., Oppo, D. W., and Hughen, K. A.: Postglacial changes in El Niño and La Niña behavior, Geology, 38, 43–46, doi:10.1130/G30366.1, 2010.

Mann, M. E.: Climate reconstruction using 'Pseudoproxies', Geophys. Res. Lett., 29, 10–13, doi:10.1029/2001GL014554, 2002.

Mann, M. E., Cane, M. A., Zebiak, S. E., and Clement, A. C.: Volcanic and solar forcing of the tropical Pacific over the past 1000 years, J. Clim., 18, 447–456, doi:10.1175/JCLI-3276.1, 2005.

Mann, M. E., Rutherford, S., Wahl, E., and Ammann, C.: Robustness of proxy-based climate field reconstruction methods, J. Geophys. Res. Atmos., 112, 1–18, doi:10.1029/2006JD008272, 2007.

Mann, M. E., Zhang, Z., Hughes, M. K., Bradley, R. S., Miller, S. K., Rutherford, S., and Ni, F.: Proxy-based reconstructions of hemispheric and global surface temperature variations over the past two millennia., Proc. Natl. Acad. Sci. U. S. A., 105, 13 252–13 257, doi:10.1073/pnas.0805721105, 2008.

Mann, M. E., Zhang, Z., Rutherford, S., Bradley, R. S., Hughes, M. K., Shindell, D., Ammann, C., Faluvegi, G., and Ni, F.: Global signatures and dynamical origins of the Little Ice Age and Medieval Climate Anomaly., Science, 326, 1256–1260, doi:10.1126/science.1177303, 2009.

Marchitto, T. M., Muscheler, R., Ortiz, J. D., Carriquiry, J. D., and van Geen, A.: Dynamical response of the tropical Pacific Ocean to solar forcing during the early Holocene., Science, 330, 1378–1381, doi:10.1126/science.1194887, 2010.

Masson-Delmotte, V., Schulz, M., Abe-Ouchi, A., Beer, J., Ganopolski, A., González Rouco, J. F., Jansen, E., Lambeck, K., Luterbacher, J., Naish, T., Osborn, T., Otto-Bliesner, B., Quinn, T., Ramesh, R., Rojas, M., Shao, X., Timmermann, A., and Rouco, J. F. G.: Information from Paleoclimate Archives, in: Clim. Chang. 2013 Phys. Sci. Basis. Contrib. Work. Gr. I to Fifth Assess. Rep. Intergov. Panel Clim. Chang., edited by

Stocker, T., Qin, D., Plattner, G.-K., Tignor, M., Allen, S. K., Boschung, J., Nauels, A., Xia, Y., Bex, V., and Midgley, P., pp. 383–464, Cambridge University Press, Cambridge, United Kingdom and New York, NY, USA, doi:10.1017/CBO9781107415324, 2013.

Maupin, C. R., Partin, J. W., Shen, C.-C., Quinn, T. M., Lin, K., Taylor, F. W., Banner, J. L., Thirumalai, K., and Sinclair, D. J.: Persistent decadal-scale rainfall variability in the tropical South Pacific Convergence Zone through the past six centuries, Clim. Past, 10, 1319–1332, doi:10.5194/cp-10-1319-2014, 2014.

McCulloch, M., Mortimer, G., Esat, T., Xianhua, L., Pillans, B., and Chappell, J.: High resolution windows into early Holocene climate: Sr/Ca coral records from the Huon Peninsula, Earth Planet. Sci. Lett., 138, 169–178, doi:10.1016/0012-821X(95)00230-A, 1996.

McGregor, H. V., Gagan, M. K., McCulloch, M. T., Hodge, E., and Mortimer, G.: Mid-Holocene variability in the marine ^{14}C reservoir age for northern coastal Papua New Guinea, Quat. Geochronol., 3, 213–225, doi:10.1016/j.quageo.2007.11.002, 2008.

McGregor, S., Timmermann, A., and Timm, O.: A unified proxy for ENSO and PDO variability since 1650, Clim. Past, 6, 1–17, doi:10.5194/cpd-5-2177-2009, 2010.

Medina-Elizalde, M., Burns, S. J., Lea, D. W., Asmerom, Y., von Gunten, L., Polyak, V., Vuille, M., and Karmalkar, A.: High resolution stalagmite climate record from the Yucatán Peninsula spanning the Maya terminal classic period, Earth Planet. Sci. Lett., 298, 255–262, doi:10.1016/j.epsl.2010.08.016, 2010.

Metcalfe, S., Jones, M., Davies, S., Noren, A., and MacKenzie, A.: Climate variability over the last two millenia in the North American Monsoon region, recorded in laminated lake sediments from Labuna de Juanacatlán, Mexico, The Holocene, 20, 1195–1206, doi:10.1177/0959683610371994, 2010.

Moustafa, Y. A.: Paleoclimatic reconstructions of the northern Red Sea during the Holocene inferred from stable isotope records of modern and fossil corals and molluscs, Berichte aus dem Fachbereich Geowissenschaften, Univ. Bremen, pp. 1–102, 2000.

Moy, A. D., Seltzer, G. O., Rodbell, D. T., and Andersons, D. M.: Variability of El Niño/Southern Oscillation activity at millennial timescales during the Holocene epoch, Nature, 420, 162–165, doi:doi:10.1038/nature01194, 2002.

Nakamura, N., Kayanne, H., Iijima, H., McClanahan, T. R., Behera, S. K., and Yamagata, T.: Mode shift in the Indian Ocean climate under global warming stress, Geophys. Res. Lett., 36, 3–7, doi:10.1029/2009GL040590, 2009.

Nelson, D. B., Abbott, M. B., Steinman, B., Polissar, P. J., Stansell, N. D., Ortiz, J. D., Rosenmeier, M. F., Finney, B. P., and Riedel, J.: Drought variability in the Pacific Northwest from a 6,000-yr lake sediment record., Proc. Natl. Acad. Sci. U. S. A., 108, 3870–3875, doi:10.1073/pnas.1009194108, 2011.

Newman, M., Compo, G. P., and Alexander, M. A.: ENSO-forced variability of the Pacific Decadal Oscillation, J. Clim., 16, 3853–3857, doi:10.1175/1520-0442(2003)016<3853:EVOTPD>2.0.CO;2, 2003.

Nurhati, I. S., Cobb, K. M., Charles, C. D., and Dunbar, R. B.: Late 20th century warming and freshening in the central tropical Pacific, Geophys. Res. Lett., 36, 1–4, doi:10.1029/2009GL040270, 2009.

Oppo, D. W., Rosenthal, Y., and Linsley, B. K.: 2,000-year-long temperature and hydrology reconstructions from the Indo-Pacific warm pool., Nature, 460, 1113–1116, doi:10.1038/nature08233, 2009.

Page, S. E., Siegert, F., Rieley, J. O., Boehm, H.-D. V., Jaya, A., and Limin, S.: The amount of carbon released from peat and forest fires in Indonesia during 1997., Nature, 420, 61–65, doi:10.1038/nature01131, 2002.

Partin, J. W., Cobb, K. M., Adkins, J. F., Clark, B., and Fernandez, D. P.: Millennial-scale trends in west Pacific warm pool hydrology since the Last Glacial Maximum., Nature, 449, 452–455, doi:10.1038/nature08125, 2007.

Partin, J. W., Quinn, T. M., Shen, C. C., Emile-Geay, J., Taylor, F. W., Maupin, C. R., Lin, K., Jackson, C. S., Banner, J. L., Sinclair, D. J., and Huh, C. A.: Multidecadal rainfall variability in south pacific convergence zone as revealed by stalagmite geochemistry, Geology, 41, 1143–1146, doi:10.1130/G34718.1, 2013.

Pfeiffer, M., Timm, O., Dullo, W. C., and Podlech, S.: Oceanic forcing of interannual and multidecadal climate variability in the southwestern Indian Ocean: Evidence from a 160 year coral isotopic record (La Réunion, 55°E, 21°S), Paleoceanography, 19, 1–14, doi:10.1029/2003PA000964, 2004.

Pohl, K., Therrell, M. D., Blay, G. S., Ayotte, N., Hernandez, J. J. C., Castro, S. D., Oviedo, E. C., Elvir, J. A., Elizondo, M. G., Opland, D., Park, J., Pederson, G., Salazar, S. B., Selem, L. V., Villanueva-Diaz, J., and Stahle, D. W.: A cool season precipitation reconstruction for Satillo, Mexico, Tree-ring Res., 95, 11–19, 2003.

Power, S., Delage, F., Chung, C., Kociuba, G., and Keay, K.: Robust twenty-first-century projections of El Niño and related precipitation variability., Nature, 502, 541–5, doi:10.1038/nature12580, 2013.

Powers, L. A., Johnson, T. C., Werne, J. P., Castañeda, I. S., Hopmans, E. C., Sinninghe Damsté, J. S., and Schouten, S.: Organic geochemical records of environmental variability in Lake Malawi during the last 700 years, Part I: The TEX86 temperature record, Palaeogeogr. Palaeoclimatol. Palaeoecol., 303, 133–139, doi:10.1016/j.palaeo.2010.09.006, 2011.

Quinn, T. M., Crowley, T. J., and Taylor, F. W.: New stable isotope results from a 173-year coral from Espiritu Santo, Vanuatu, Geophys. Res. Lett., 23, 3413–3416, doi:10.1029/96GL03169, 1996.

Quinn, T. M., Crowley, T. J., Taylor, F. W., Henin, C., Joannot, P., and Join, Y.: A multicentury stable isotope record from a New Caledonia coral: Interannual and decadal sea surface temperature variability in the southwest Pacific since 1657 A.D, Paleoceanography, 13, 412–426, doi:doi:10.1029/98PA00401, 1998.

Quinn, T. M., Taylor, F. W., and Crowley, T. J.: Coral-based climate variability in the Western Pacific Warm Pool since 1867, J. Geophys. Res., 111, 1–11, doi:10.1029/2005JC003243, 2006.

Raible, C. C., Lehner, F., González-Rouco, J. F., and Fernández-Donado, L.: Changing correlation structures of the Northern Hemisphere atmospheric circulation from 1000 to 2100 AD, Clim. Past, 10, 537–550, doi:10.5194/cp-10-537-2014, 2014.

Rasbury, M. and Aharon, P.: ENSO-controlled rainfall variability records archived in tropical stalagmites from the mid-ocean island of Niue, South Pacific, Geochemistry, Geophys. Geosystems, 7, doi:10.1029/2005GC001232, 2006.

Reuter, J., Stott, L., Khider, D., Sinha, A., Cheng, H., and Edwards, R. L.: A new perspective on the hydroclimate variability in northern South America during the Little Ice Age, Geophys. Res. Lett., 36, 1–5, doi:10.1029/2009GL041051, 2009.

Richey, J. N., Poore, R. Z., Flower, B. P., Quinn, T. M., and Hollander, D. J.: Regionally coherent Little Ice Age cooling in the Atlantic Warm Pool, Geophys. Res. Lett., 36, 3–7, doi:10.1029/2009GL040445, 2009.

Rodbell, D. T.: An 15,000-Year Record of El Niño-Driven Alluviation in Southwestern Ecuador, Science, 283, 516–520, doi:10.1126/science.283.5401.516, 1999.

Rodysill, J. R., Russell, J. M., Bijaksana, S., Brown, E. T., Safiuddin, L. O., and Eggermont, H.: A paleolimnological record of rainfall and drought from East Java, Indonesia during the last 1,400 years, J. Paleolimnol., 47, 125–139, doi:10.1007/s10933-011-9564-3, 2012.

Russell, J. M. and Johnson, T. C.: Little Ice Age drought in equatorial Africa: Intertropical convergence zone migrations and El Niño-Southern Oscillation variability, Geology, 35, 21–24, doi:10.1130/G23125A.1, 2007.

Russell, J. M., Vogel, H., Konecky, B. L., Bijaksana, S., Huang, Y., Melles, M., Wattrus, N., Costa, K., and King, J. W.: Glacial forcing of central Indonesian hydroclimate since 60,000 y B.P., Proc. Natl. Acad. Sci. U. S. A., 111, 5100–5105, doi:10.1073/pnas.1402373111, 2014.

Russon, T., Tudhope, A. W., Hegerl, G. C., Collins, M., and Tindall, J.: Inter-annual tropical Pacific climate variability in an isotope-enabled CGCM: Implications for interpreting coral stable oxygen isotope records of ENSO, Clim. Past, 9, 1543–1557, doi:10.5194/cp-9-1543-2013, 2013.

Sachs, J. P., Sachse, D., Smittenberg, R. H., Zhang, Z., Battisti, D. S., and Golubic, S.: Southward movement of the Pacific intertropical convergence zone AD 1400–1850, Nat. Geosci., 2, 519–525, doi:10.1038/ngeo554, 2009.

Saenger, C., Cohen, A. L., Oppo, D. W., Halley, R. B., and Carilli, J. E.: Surface-temperature trends and variability in the low-latitude North Atlantic since 1552, Nat. Geosci., 2, 492–495, doi:10.1038/ngeo552, 2009.

Saenger, C., Came, R. E., Oppo, D. W., Keigwin, L. D., and Cohen, A. L.: Regional climate variability in the western subtropical North Atlantic during the past two millennia, Paleoceanography, 26, 1–12, doi:10.1029/2010PA002038, 2011.

Shin, S. I., Sardeshmukh, P. D., Webb, R. S., Oglesby, R. J., and Barsugli, J. J.: Understanding the mid-Holocene climate, J. Clim., 19, 2801–2817, doi:10.1175/JCLI3733.1, 2006.

Smerdon, J. E.: Climate models as a test bed for climate reconstruction methods: Pseudoproxy experiments, Wiley Interdiscip. Rev. Clim. Chang., 3, 63–77, doi:10.1002/wcc.149, 2012.

Stahle, D. S., D'Arrigo, R. D., Krusic, P. J., Cleaveland, M. K., Cook, E. R., Allan, R. J., Cole, J. E., Dunbar, R. B., Therrell, M. D., Gay, D. A., Moore, M. D., Stokes, M. A., Burns, B. T., Villanueva-Diaz, J., and Thompson, L. G.: Experimental Dendroclimatic Reconstruction of the Southern Oscillation, Bull. Am. Meteorol. Soc., 79, 2137–2152, doi:10.1175/1520-0477(1998)079<2137:EDROTS>2.0.CO;2, 1998.

Stahle, D. W., Diaz, J. V., Burnette, D. J., Paredes, J. C., Heim, R. R., Fye, F. K., Soto, R. A., Therrell, M. D., and Cleaveland, M. K.: Major Mesoamerican droughts of the past millennium, Geophys. Res. Lett., 38, 2–5, doi:10.1029/2010GL046472, 2011.

Stansell, N. D., Steinman, B. A., Abbott, M. B., Rubinov, M., and Roman-Lacayo, M.: Lacustrine stable isotope record of precipitation changes in Nicaragua during the Little Ice Age and Medieval Climate Anomaly, Geology, 41, 151–154, doi:10.1130/G33736.1, 2013.

Steinman, B. A., Abbott, M. B., Mann, M. E., Stansell, N. D., and Finney, B. P.: 1,500 year quantitative reconstruction of winter precipitation in the Pacific Northwest, Proc. Natl. Acad. Sci., 109, 11 619–11 623, doi:10.1073/pnas.1201083109, 2012.

Stott, L., Poulsen, C., Lund, S., and Thunell, R.: Super ENSO and global climate oscillations at millennial time scales., Science, 297, 222–226, doi:10.1126/science.1071627, 2002.

Stott, L., Cannariato, K., Thunell, R., Haug, G. H., Koutavas, A., and Lund, S.: Decline of surface temperature and salinity in the western tropical Pacific Ocean in the Holocene epoch, Nature, 431, 56–59, doi:10.1038/nature02903, 2004.

Sturm, C., Zhang, Q., and Noone, D.: An introduction to stable water isotopes in climate models: benefits of forward proxy modelling for paleoclimatology, Clim. Past, 6, 115–129, doi:10.5194/cpd-5-1697-2009, 2010.

Sundqvist, H. S., Holmgren, K., Fohlmeister, J., Zhang, Q., Matthews, M. B., Spötl, C., and Körnich, H.: Evidence of a large cooling between 1690 and 1740 AD in southern Africa., Sci. Rep., 3, 1–6, doi:10.1038/srep01767, 2013.

Swart, P. K., Dodge, R. E., and Hudson, H. J.: A 240-year stable oxygen and carbon isotopic record in a coral from South Florida: implications for the prediction of precipitation in Southern Florida, Palaios, 11, 362–375, doi:10.2307/3515246, 1996a.

Swart, P. K., Healy, G., Dodge, R. E., Kramer, P., Hudson, J. H., Halley, R. B., and Robblee, M. B.: The stable oxygen and carbon isotopic record of climatic and anthropogenic influence., Palaeogeogr., Palaeoclim., Palaeoecol., 123, 219–237 [4–5], 1996b.

Takahashi, K., Montecinos, A., Goubanova, K., and Dewitte, B.: ENSO regimes: Reinterpreting the canonical and Modoki El Niño, Geophys. Res. Lett., 38, 1–5, doi:10.1029/2011GL047364, 2011.

Tan, L., Cai, Y., Cheng, H., An, Z., and Edwards, R. L.: Summer monsoon precipitation variations in central China over the past 750 years derived from a high-resolution absolute-dated stalagmite, Palaeogeogr. Palaeoclimatol. Palaeoecol., 280, 432–439, doi:10.1016/j.palaeo.2009.06.030, 2009.

Taylor, K. E., Stouffer, R. J., and Meehl, G. A.: An overview of CMIP5 and the experiment design, Bull. Am. Meteorol. Soc., 93, 485–498, doi:10.1175/BAMS-D-11-00094.1, 2012.

Thompson, D. M., Ault, T. R., Evans, M. N., Cole, J. E., and Emile-Geay, J.: Comparison of observed and simulated tropical climate trends using a forward model of coral δ^{18}O, Geophys. Res. Lett., 38, 1–6, doi:10.1029/2011GL048224, 2011.

Thompson, L. G. and et Al.: Tropical climate instability: the last glacial cycle from a Qinghai - Tibetan ice core, Science, 276, 1821–1825, doi:10.1126/science.276.5320.1821, 1997.

Thompson, L. G., Mosley-Thompson, E., Davis, M. E., Lin, P.-N. P.-N., Henderson, K. A., Cole-Dai, J., Bolzan, J. F., and Liu, K.-b.: Late Glacial Stage and Holocene Tropical Ice Core Records from Huascaran, Peru, Science, 269, 46–50, doi:10.1017/CBO9781107415324.004, 1995.

Thompson, L. G., Mosley-Thompson, E., Davis, M. E., Henderson, K. A., Brecher, H. H., Zagorodnov, V. S., Mashiotta, T. A., Lin, P.-n., Mikhalenko, V. N., Hardy, D. R., and Beer, J.: Kilimanjaro ice core records: evidence of holocene climate change in tropical Africa., Science, 298, 589–593, doi:10.1126/science.1073198, 2002.

Thompson, L. G., Mosley-Thompson, E., Davis, M. E., Lin, P., Henderson, K., and Mashiotta, T. A.: Tropical glacier and ice core evidence of climate change on annual to millenial time scales, Clim. Change, 59, 137–155, 2003.

Thompson, L. G., Yao, T., Davis, M. E., Mosley-Thompson, E., Mashiotta, T. A., Lin, P. N., Mikhalenko, V. N., and Zagorodnov, V. S.: Holocene climate variability archived in the Puruogangri ice cap on the central Tibetan Plateau, Ann. Glaciol., 43, 61–69, doi:10.3189/172756406781812357, 2006.

Thompson, L. G., Mosley-Thompson, E., Davis, M. E., Zagorodnov, V. S., Howat, I. M., Mikhalenko, V. N., and Lin, P.-N.: Annually resolved ice core records of tropical climate variability over the past ∼1800 years., Science, 340, 945–950, doi:10.1126/science.1234210, 2013.

Tierney, J. E., Oppo, D. W., Rosenthal, Y., Russell, J. M., and Linsley, B. K.: Coordinated hydrological regimes in the Indo-Pacific region during the past two millennia, Paleoceanography, 25, 1–7, doi:10.1029/2009PA001871, 2010.

Tierney, J. E., Lewis, S. C., Cook, B. I., LeGrande, A. N., and Schmidt, G. A.: Model, proxy and isotopic perspectives on the East African Humid Period, Earth Planet. Sci. Lett., 307, 103–112, doi:10.1016/j.epsl.2011.04.038, 2011.

Tierney, J. E., Abram, N. J., Anchukaitis, K. J., Evans, M. N., Giry, C., Kilbourne, K. H., Saenger, C. P., Wu, H. C., and Zinke, J.: Tropical sea surface temperatures for the past four centuries reconstructed from coral archives, Paleoceanography, 30, 226–252, doi:10.1002/2014PA002717, 2015.

Tingley, M. P., Craigmile, P. F., Haran, M., Li, B., Mannshardt, E., and Rajaratnam, B.: Piecing together the past: Statistical insights into paleoclimatic reconstructions, Quat. Sci. Rev., 35, 1–22, doi:10.1016/j.quascirev.2012.01.012, 2012.

Tiwari, M., Nagoji, S. S., and Ganeshram, R. S.: Multi-centennial scale SST and Indian summer monsoon precipitation variability since mid-Holocene and its nonlinear response to solar activity, The Holocene, 25, 1415–1424, doi:10.1177/0959683615585840, 2015.

Tolwinski-Ward, S. E., Evans, M. N., Hughes, M. K., and Anchukaitis, K. J.: An efficient forward model of the climate controls on interannual variation in tree-ring width, Clim. Dyn., 36, 2419–2439, doi:10.1007/s00382-010-0945-5, 2011.

Treydte, K. S., Schleser, G. H., Helle, G., Frank, D. C., Winiger, M., Haug, G. H., and Esper, J.: The twentieth century was the wettest period in northern Pakistan over the past millennium., Nature, 440, 1179–1182, doi:10.1038/nature04743, 2006.

Trouet, V., Esper, J., Graham, N. E., Baker, A., Scourse, J. D., and Frank, D. C.: Persistent positive North Atlantic oscillation mode dominated the Medieval Climate Anomaly., Science, 324, 78–80, doi:10.1126/science.1166349, 2009.

Trouet, V., Scourse, J. D., and Raible, C. C.: North Atlantic storminess and Atlantic Meridional Overturning Circulation during the last Millennium: Reconciling contradictory proxy records of NAO variability, Glob. Planet. Change, 84-85, 48–55, doi:10.1016/j.gloplacha.2011.10.003, 2012.

Tudhope, A., Chilcott, C. P., McCulloch, M. T., Cook, E. R., Chappell, J., Ellam, R. M., Lea, D. W., Lough, J. M., and Shimmield, G. B.: Variability in the El Niño-Southern Oscillation through a glacial-interglacial cycle., Science, 291, 1511–1517, doi:10.1126/science.1057969, 2001.

Urban, F. E., Cole, J. E., and Overpeck, J. T.: Influence of mean climate change on climate variability from a 155-year tropical Pacific coral record, Nature, 407, 989–993, doi:10.1038/35039597, 2000.

Vaganov, E. A., Hughes, M. K., and Shashkin, A. V.: Growth Dynamics of Conifer Tree Rings: Images of Past and Future Environments, Springer-Verlag Berlin Heidelberg, New York, 1 edn., doi:10.1007/3-540-31298-6, 2006.

Vaganov, E. A., Anchukaitis, K. J., and Evans, M. N.: How well understood are the processes that create dendroclimatic records? A mechanistic model of the climatic control on conifer tree-ring growth dynamics, in:

Dendroclimatology Prog. Prospect., edited by Hughes, M. K., Swetnam, T. W., and Diaz, H. F., vol. 11, pp. 37–75, Springer Netherlands, doi:10.1007/978-1-4020-5725-0, 2011.

van Hengstum, P. J., Donnelly, J. P., Kingston, A. W., Williams, B. E., Scott, D. B., Reinhardt, E. G., Little, S. N., and Patterson, W. P.: Low-frequency storminess signal at Bermuda linked to cooling events in the North Atlantic region, Paleoceanography, 30, 52–76, doi:doi:10.1002/2014PA002662, 2015.

van Oldenborgh, G. J., Philip, S. Y., and Collins, M.: El Niño in a changing climate : a multi-model study, Ocean Sci., 1, 81–95, doi:10.5194/os-1-81-2005, 2005.

Vasquez-Bedoya, L. F., Cohen, A. L., Oppo, D. W., and Blanchon, P.: Corals record persistent multidecadal SST variability in the Atlantic Warm Pool since 1775 AD, Paleoceanography, 27, 1–9, doi:10.1029/2012PA002313, 2012.

Vecchi, G. A. and Wittenberg, A. T.: El Niño and our future climate: Where do we stand?, Wiley Interdiscip. Rev. Clim. Chang., 1, 260–270, doi:10.1002/wcc.33, 2010.

Verdon, D. C. and Franks, S. W.: Long-term behaviour of ENSO: Interactions with the PDO over the past 400 years inferred from paleoclimate records, Geophys. Res. Lett., 33, 1–5, doi:10.1029/2005GL025052, 2006.

Wang, H. J., Zhang, R. H., Cole, J. E., and Chavez, F.: El Niño and the related phenomenon Southern Oscillation (ENSO): the largest signal in interannual climate variation., Proc. Natl. Acad. Sci. U. S. A., 96, 11 071–11 072, doi:10.1073/pnas.96.20.11071, 1999.

Wang, J., Emile-Geay, J., Guillot, D., Smerdon, J. E., and Rajaratnam, B.: Evaluating climate field reconstruction techniques using improved emulations of real-world conditions, Clim. Past, 10, 1–19, doi:10.5194/cp-10-1-2014, 2014.

Wang, J., Emile-Geay, J., Guillot, D., McKay, N. P., and Rajaratnam, B.: Fragility of reconstructed temperature patterns over the Common Era: Implications for model evaluation, Geophys. Res. Lett., 42, 7162–7170, doi:10.1002/2015GL065265, 2015.

Wanner, H., Beer, J., Bütikofer, J., Crowley, T. J., Cubasch, U., Flückiger, J., Goosse, H., Grosjean, M., Joos, F., Kaplan, J. O., Küttel, M., Müller, S. A., Prentice, I. C., Solomina, O., Stocker, T. F., Tarasov, P., Wagner, M., and Widmann, M.: Mid- to Late Holocene climate change: an overview, Quat. Sci. Rev., 27, 1791–1828, doi:10.1016/j.quascirev.2008.06.013, 2008.

Wilson, R., Cook, E. R., D'Arrigo, R. D., Riedwyl, N., Evans, M. N., Tudhope, A. W., and Allan, R.: Reconstructing ENSO: the influence of method, proxy data, climate forcing and teleconnections, J. Quat. Sci., 25, 62–78, doi:10.1002/jqs.1297, 2010.

Wolter, K. and Timlin, M. S.: El Niño/Southern Oscillation behaviour since 1871 as diagnosed in an extended multivariate ENSO index (MEI.ext), Int. J. Climatol., 31, 1074–1087, doi:10.1002/joc.2336, 2011.

Wörheide, G.: The reef cave dwelling ultraconservative coralline demosponge Astrosclera willeyana Lister 1900 from the Indo-Pacific, Facies, 38, 1–88, doi:10.1007/BF02537358, 1998.

Wu, H. C., Linsley, B. K., Dassié, E. P., Schiraldi, B., and Demenocal, P. B.: Oceanographic variability in the south pacific convergence zone region over the last 210 years from multi-site coral Sr/Ca records, Geochemistry, Geophys. Geosystems, 14, 1435–1453, doi:10.1029/2012GC004293, 2013.

Wurtzel, J. B., Black, D. E., Thunell, R. C., Peterson, L. C., Tappa, E. J., and Rahman, S.: Mechanisms of southern Caribbean SST variability over the last two millennia, Geophys. Res. Lett., 40, 5954–5958, doi:10.1002/2013GL058458, 2013.

Yan, H., Sun, L., Oppo, D. W., Wang, Y., Liu, Z., Xie, Z., Liu, X., and Cheng, W.: South China Sea hydrological changes and Pacific Walker Circulation variations over the last millennium., Nat. Commun., 2, 293, doi:10.1038/ncomms1297, 2011a.

Yan, H., Sun, L., Wang, Y., Huang, W., Qiu, S., and Yang, C.: A record of the Southern Oscillation Index for the past 2,000 years from precipitation proxies, Nat. Geosci., 4, 611–614, doi:10.1038/ngeo1231, 2011b.

Yang, B., Qin, C., Wang, J., He, M., Melvin, T. M., Osborn, T. J., and Briffa, K. R.: A 3,500-year tree-ring record of annual precipitation on the northeastern Tibetan Plateau., Proc. Natl. Acad. Sci. U. S. A., 111, 2903–2908, doi:10.1073/pnas.1319238111, 2014.

Yeh, S.-W., Kug, J.-S., Dewitte, B., Kwon, M.-H., Kirtman, B. P., and Jin, F.-F.: El Niño in a changing climate, Nature, 461, 511–514, doi:10.1038/nature08316, 2009.

Yi, L., Yu, H., Ge, J., Lai, Z., Xu, X., Qin, L., and Peng, S.: Reconstructions of annual summer precipitation and temperature in north-central China since 1470 AD based on drought/flood index and tree-ring records, Clim. Change, 110, 469–498, doi:10.1007/s10584-011-0052-6, 2012.

Yuan Zhang, Wallace, J. M., and Battisti, D. S.: ENSO-like interdecadal variability: 1900-93, J. Clim., 10, 1004–1020, doi:10.1175/1520-0442(1997)010<1004:ELIV>2.0.CO;2, 1997.

Zhao, M., Read, G., and Schimmelmann, A.: An alkenone ($U_{37}^{K'}$) quasi-annual sea surface temperature record (A.D. 1440 to 1940) using varved sediments from the Santa Barbara Basin, Org. Geochem., 31, 903–917, 2000.

Zinke, J., Dullo, W. C., Heiss, G. A., and Eisenhauer, A.: ENSO and Indian Ocean subtropical dipole variability is recorded in a coral record off southwest Madagascar for the period 1659 to 1995, Earth Planet. Sci. Lett., 228, 177–194, doi:10.1016/j.epsl.2004.09.028, 2004.

Zinke, J., Pfeiffer, M., Timm, O., Dullo, W. C., Kroon, D., and Thomassin, B. A.: Mayotte coral reveals hydrological changes in the western indian ocean between 1881 and 1994, Geophys. Res. Lett., 35, 1–5, doi:10.1029/2008GL035634, 2008.

Zinke, J., Loveday, B. R., Reason, C. J. C., Dullo, W.-C., and Kroon, D.: Madagascar corals track sea surface temperature variability in the Agulhas Current core region over the past 334 years., Sci. Rep., 4, 4393, doi:10.1038/srep04393, 2014.

Zinke, J., Hoell, a., Lough, J. M., Feng, M., Kuret, a. J., Clarke, H., Ricca, V., Rankenburg, K., and McCulloch, M. T.: Coral record of southeast Indian Ocean marine heatwaves with intensified Western Pacific temperature gradient., Nat. Commun., 6, 8562, doi:10.1038/ncomms9562, 2015.

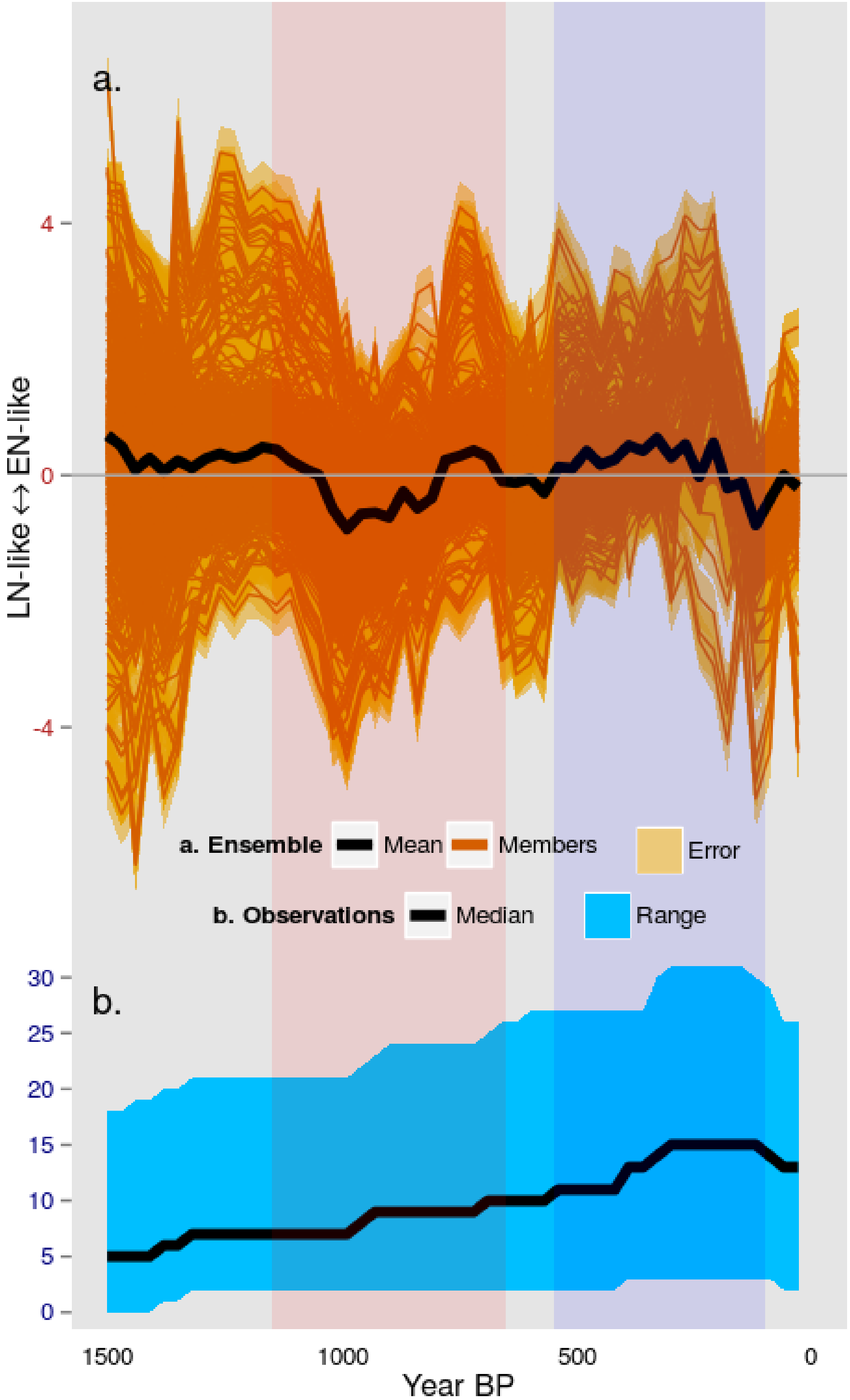

Figure 2. ~~**Precipitation and temperature ENSO ensembles.**~~ **Precipitation ENSO ensembles.** a) 30 year averaged precipitation ~~ENSO~~ reconstruction of ENSO-like climate change (black line). Individual network solutions are shown as orange lines, with the uncertainty envelope in orange shading. b) Number of proxies included in the ensemble over time, with the median in black and the range in blue. The pink and purple shaded periods are the MCA and LIA respectively. ~~c) and d) are the temperature versions of a) and b) respectively.~~

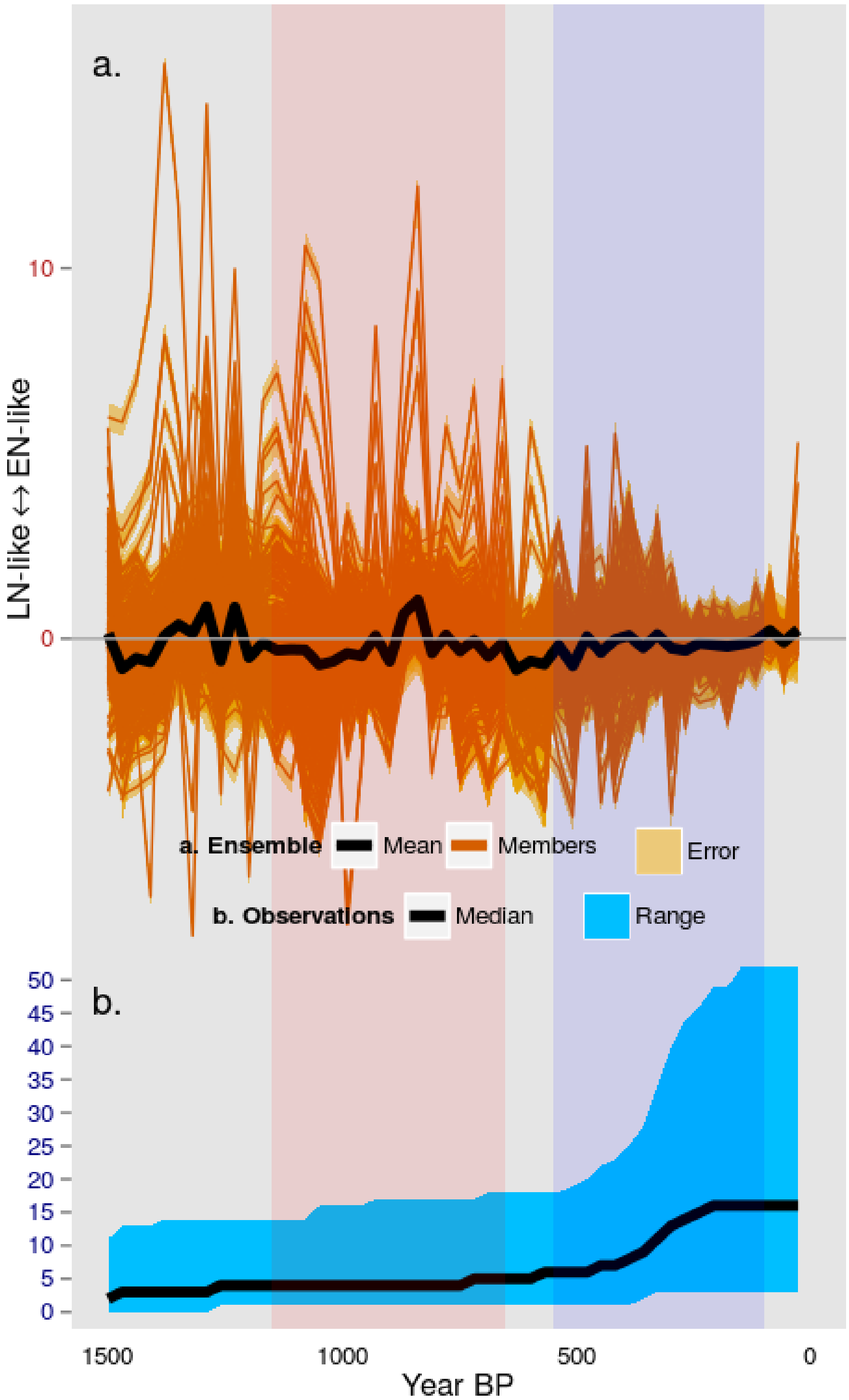

Figure 3. **Temperature ENSO ensembles.** As Fig. 2, but for temperature.

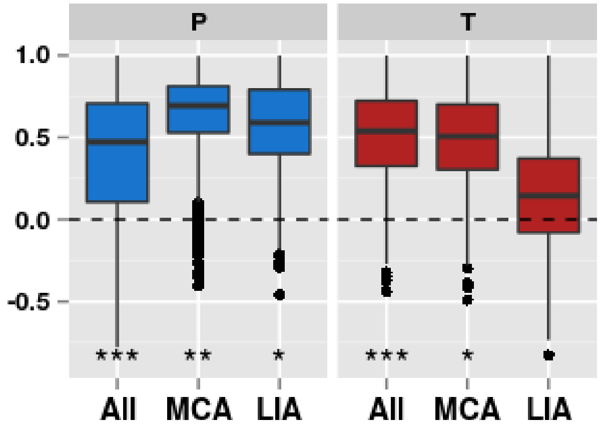

Figure 4. Within-ensemble correlations. Correlations between 1000 pairs randomly chosen from the precipitation (blue) and temperature (red) ensembles. Box plots encapsulate the space between the first and third quartile with the median shown as a black line; whiskers indicate the 95% confidence interval of the median; points are values outside this confidence interval (outliers). Statistical significance of the median value is indicated at the bottom: *** $p < 0.001$, ** $p < 0.01$, * $p < 0.05$,
SUPERSCRIPT $p < 0.1$, $p > 0.1$.

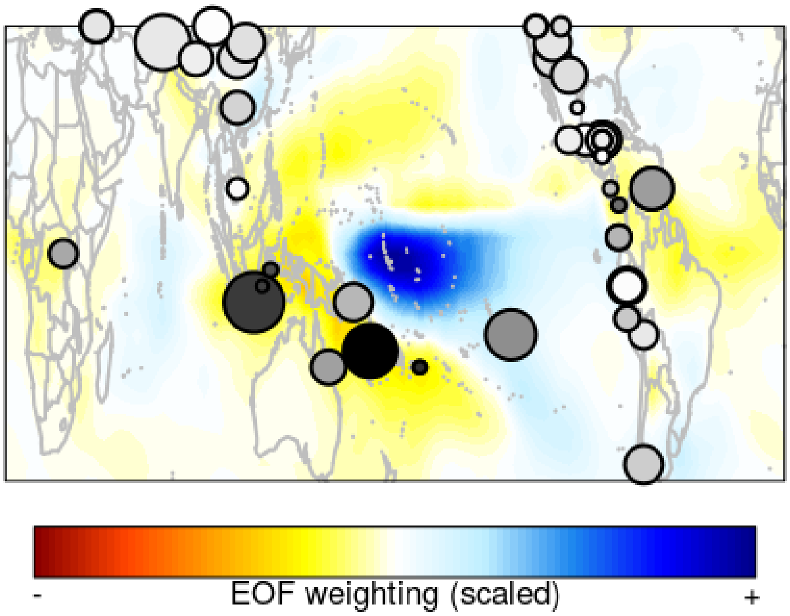

Figure 5. Precipitation EOF with proxy locations. ~~The~~ Background colours are scaled EOF values. Bubbles are individual proxies; size ~~of the bubble~~ is indicative of how often the proxy is included in the network ensemble~~. The colour is related to the proxy weights~~, shading indicates relative weighting such that darker colours are more strongly positive or negative~~; The relative signs can be gleaned from the EOF pattern~~.

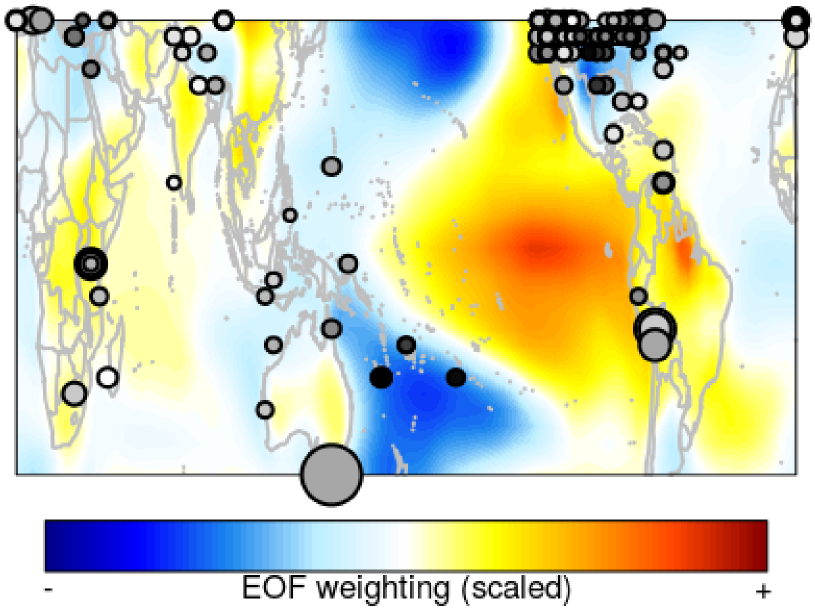

Figure 6. Temperature EOF with proxy locations. As Fig. 5, but for temperature.

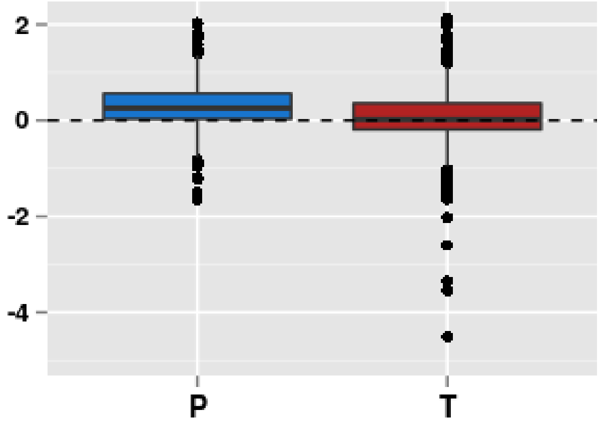

Figure 7. Difference between the means of the MCA and LIA. Difference calculated by subtracting μ_{MCA} from μ_{LIA} for each ensemble member. A positive value indicates LIA is more El Niño-like than MCA. Precipitation is on the left in blue, temperature is on the right in red. See Fig. 4 for explanation of the box plots and significance.

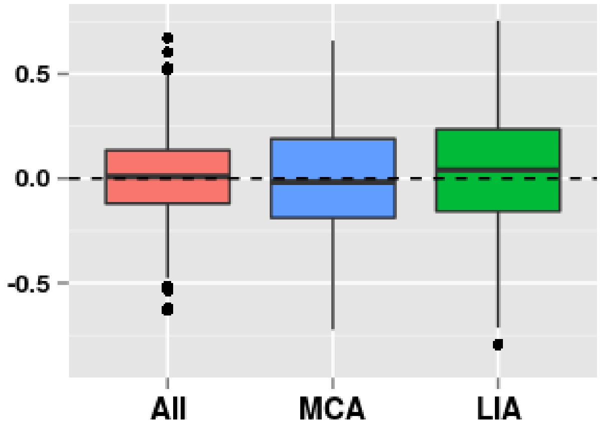

Figure 8. Precipitation – temperature correlations. Correlations between the temperature and precipitation ensemble members based on 1000 randomly chosen pairs, for the period 100-1500 yrBP ('All') and the MCA and LIA individually. See Fig. 4 for explanation of the box plots and significance.

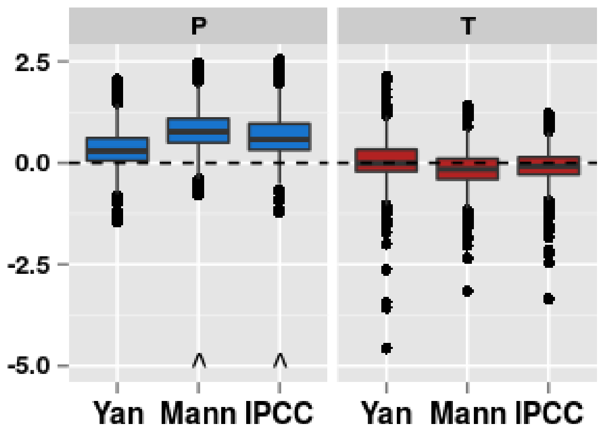

Figure 9. ~~**LOO results**. LOO results: proxy – ENSO reconstruction correlations in the real world plotted against the reanalysis-derived pseudo world~~**Sensitivity to MCA and LIA definitions**. ~~Proxy records are separated by colour~~As Fig 7, ~~with a point~~ done for ~~each network in which~~ the ~~proxy appears~~three MCA and LIA definitions listed in Sect 4. ~~Dots with black outlines are mean values; size denotes the length of~~ 'Yan' refers to the ~~proxy record~~ definition used in Yan et al. (2011b) , 'Mann' in Mann et al. (2009) , and ~~shading is as~~ 'IPCC' in Masson-Delmotte et al. (2013) . See Fig. ~~??~~4 for explanation of the box plots and significance.

Reference	Lon	Lat	Proxy	SNR	EOF
Anchukaitis and Evans (2010)	~~tree ring~~ 275	~~50~~ 10	~~-53~~ treering	~~274.7~~ N/A	~~10.2~~ N/A
Anderson (2011)	68	29	lake	~~10290~~ 0.40	0.32
Apastaégui et al. (2014)	~~83~~ 76	~~No; Dating error~~ 13	speleothem	0.40	-0.03
Asmerom et al. (2007)	255	32	speleothem	~~12087~~ N/A	~~-15~~ N/A
~~Bale et al. (2011)~~ Baker et al. (2009)	~~tree ring~~ 78	~~865~~ 10	~~-55~~ lake	~~241.8~~ 0.40	~~37.5~~ -0.22
Bird et al. (2011)	76	11	lake	~~11142~~ 0.40	~~-57~~ 0.52
Bonnefille and Chalié (2000)	~~peat~~ 356	30	pollen	~~40500~~ N/A	~~0~~ N/A
Buckley et al. (2010)	~~tree ring~~ 29	~~920~~ 19	~~-58~~ treering	~~108.3~~ 0.37	~~11.6~~ 0.04
~~Christie et al. (2011)~~ Chen et al. (2009)	~~tree ring~~ 26	~~604~~ 29	~~-52~~ lake	~~290~~ 0.40	~~-37.5~~ -0.02
~~Cleaveland et al. (2003)~~ Christie et al. (2011)	~~tree ring~~ 78	~~564~~ 2	~~-43~~ treering	~~105.8~~ 0.35	~~25.4~~ 0.48
~~Cole et al. (1993)~~ Cleaveland et al. (2003)	~~coral~~ 29	~~56~~ 24	~~-40~~ treering	~~172~~ 0.40	~~1~~ 0.42
Conroy et al. (2008) ~~c-n~~ C/N	271	-1	lake	~~9191~~ N/A	~~-54~~ N/A
Conroy et al. (2008) clay	271	-1	lake	~~9191~~ N/A	~~-54~~ N/A
Conroy et al. (2008) sand	271	-1	lake	~~9191~~ N/A	~~-54~~ N/A
Conroy et al. (2008) silt	271	-1	lake	~~9191~~ N/A	~~-54~~ N/A
~~Conroy et al. (2009)~~ Curtis et al. (1996) gastropod	73	22	lake	~~1219~~ 0.40	~~-54~~ 0.16
Curtis et al. (1996) ostracod	73	22	lake	0.40	0.16
Denniston et al. (2015)	62	10	speleothem	0.40	1.08
Díaz et al. (2002)	~~tree ring~~ 69	~~303~~ 26	~~-42~~ treering	~~255.2~~ 1.10	~~31.9~~ 0.32
Faulstich et al. (2013)	~~tree ring~~ 67	~~353~~ 28	~~-58~~ treering	~~249.9~~ 0.46	~~36~~ 0.26
Griffin et al. (2013)	~~tree ring~~ 67	~~411~~ 27	~~-58~~ treering	~~249.5~~ 0.40	~~32.5~~ 0.31
Haug et al. (2001) ~~fe~~ Fe	79	19	marine ~~sediment~~	~~14277~~ 0.40	~~110~~ -0.93
Haug et al. (2001) ~~ti~~ Ti	79	19	marine ~~sediment~~	~~14277~~ 0.40	~~110~~ -0.93
Hendy et al. (2003)	40	8	coral	~~338~~ 0.86	~~-35~~ -0.90
Hodell et al. (1995) gastropod	73	22	lake	0.40	0.16
Hodell et al. (1995) ostracod	73	22	lake	0.40	0.16
Hodell et al. (1995) s	73	22	lake	0.40	0.16
Kennett et al. (2012)	73	21	speleothem	~~1989~~ 0.40	~~-54~~ 0.00
Linsley et al. (1994) $\delta^{18}O$	75	18	coral	0.10	-1.38
Maupin et al. (2014) 10fc	43	12	speleothem	~~527~~ 2.35	~~-60~~ -0.68
Maupin et al. (2014) 5fc	160	-10	speleothem	~~70~~ N/A	~~-26~~ N/A
Medina-Elizalde et al. (2010)	73	22	speleothem	0.79	0.16
Metcalfe et al. (2010)	~~10~~ 69	22	lake	0.40	-0.16
Moy et al. (2002)	75	16	lake	~~15117~~ 0.40	~~-27~~ 0.70
Nelson et al. (2011)	65	29	lake	~~6000~~ 0.40	~~101~~ 0.24

Table 1 continued from previous page

Reference	Lon	Lat	Proxy
Oppo et al. (2009) ~~d18osw~~ $\delta^{18}Osw$	32	13	marine ~~sediment~~
Partin et al. (2007)	115	4	speleothem
Partin et al. (2013)	45	9	speleothem
Pohl et al. (2003)	~~tree ring~~ 70	~~168~~ 24	~~-50~~ treering
Rasbury and Aharon (2006) asm1	51	8	speleothem
Rasbury and Aharon (2006) asm2	51	8	speleothem
Rasbury and Aharon (2006) asm3	~~speleothem 76 -51 190.2~~ 190	-19	~~1 13 No; LengthRasbury and Aharon (2~~
Reuter et al. (2009) a	283	-6	speleothem
Reuter et al. (2009) d	76	13	speleothem
Rodbell (1999) old	75	16	lake
Rodbell (1999) recent	75	16	lake
Rodysill et al. (2012)	31	12	lake
Russell et al. (2014) $\delta^{13}C$wax	33	14	lake
Russell et al. (2014) TiO	33	14	lake
Russell and Johnson (2007)	8	15	lake
Stahle et al. (2011)	~~tree ring~~ 71	~~1179~~ 22	~~-58~~ treering
Stansell et al. (2013)	74	19	lake
Steinman et al. (2012) ~~castor~~ Castor	65	29	lake
Tan et al. (2009)	29	27	speleothem
~~Treydte et al. (2006)~~ Thompson et al. (2006) c2an	~~tree ring~~ 24	~~950~~ 27	~~-48~~ ice core
~~Yan et al. (2011b) dy2~~ Tierney et al. (2010)	~~lake~~ 120	~~926~~ -4	~~-46~~ marine
~~Yan et al. (2011b) dy4~~ Tierney et al. (2015) bc1δDwax	~~lake~~ 12	~~926~~ 29	~~-46~~ marine
Tierney et al. (2015) pδDwax	12	29	marine
~~Yan et al. (2011b) dy6~~ Treydte et al. (2006)	20	28	treering
Yan et al. (2011a) dy2	113	17	lake
~~Yang et al. (2014)~~ Yan et al. (2011a) dy4	~~tree ring~~ 113	~~3450~~ 17	~~-61~~ lake
~~Yi et al. (2012) a~~ Yan et al. (2011a) dy6	~~tree ring~~ 113	~~350~~ 17	~~-50~~ lake
Yi et al. (2012) ~~b~~	~~tree ring~~ 30	~~350~~ 28	~~-50~~ treering

Table 1. Precipitation proxy details. 'SNR' gives the signal-to-noise ratio used to make the pseudoproxies. 'EOF' gives the (unscaled) 20CRV2c EOF value used to weight the proxy. 'Start' and 'End' are starting and ending years in YearBP. 'Res' is proxy resolution, rounded to the nearest integer; sub-annual proxies are listed as having a 1-year resolution. 'Dating' refers to dating error. 'Included?' indicates whether the proxy contributed to the final ENSO reconstruction; if not, the reason for exclusion is listed ('Dating error' and 'Length' are *a priori* conditions which the proxies failed to meet. 'AOI' indicates it passed pre-processing screening, but was not selected during the add-one-in process).

~~Abram et al. (2009) mentawai coral 7244~~

Reference	Lon	Lat	Proxy	SNR	EOF	
Alibert and Kinsley (2008) Sr/Ca	~~-51~~ 151	~~98.9~~ -3	~~-1.4~~ coral	~~9~~ 0.26	~~15~~ -0.73	~~No; AOIAb~~
ar018	~~-3.6~~ 266	~~18~~ 35	~~89~~ treering	~~No; Dating errorar018~~ 0.40	~~tree ring~~ -1.63	
ar024	~~tree ring~~ 266	~~225~~ 36	~~-29~~ treering	~~265.6~~ 0.40	~~36.1~~ -1.07	
ar030	~~tree ring~~ 267	~~214~~ 35	~~-29~~ treering	~~266.5~~ 0.40	~~34.5~~ -1.42	
ar042	~~tree ring~~ 268	~~428~~ 35	~~-29~~ treering	~~268.3~~ 0.40	~~34.6~~ -1.42	
ar048	~~tree ring~~ 269	~~533~~ 36	~~-29~~ treering	~~269.1~~ 0.40	~~35.9~~ -0.94	
ar050	~~tree ring~~ 269	~~931~~ 35	~~-30~~ treering	~~268.7~~ 0.40	~~35.2~~ -0.94	
ar055	~~tree ring~~ 267	~~591~~ 36	~~-42~~ treering	~~266.7~~ 0.40	~~36.1~~ -0.94	
ar056	~~tree ring~~ 267	~~280~~ 36	~~-42~~ treering	~~266.7~~ 0.40	~~36.1~~ -0.94	
ar057	~~tree ring~~ 267	~~330~~ 36	~~-43~~ treering	~~266.8~~ 0.40	~~36.1~~ -0.94	
ar058	~~tree ring~~ 266	~~271~~ 36	~~-42~~ treering	~~265.9~~ 0.40	~~36.1~~ -1.07	
ar060	~~tree ring~~ 268	~~313~~ 36	~~-43~~ treering	~~267.8~~ 0.40	~~36.3~~ -0.94	
ar061	~~tree ring~~ 267	~~258~~ 37	~~-43~~ treering	~~267.1~~ 0.40	~~36.9~~ -0.94	
ar064	~~tree ring~~ 266	~~292~~ 34	~~-41~~ treering	~~265.8~~ 0.40	~~34.3~~ -1.63	
ar072	~~tree ring~~ 266	36	treering	0.40	-1.07	
Asami (2005) $\delta^{18}O$	145	13	coral	0.71	-0.76	
aust002	~~tree ring~~ 11	~~384~~ 47	~~-21~~ treering	~~11~~ 0.40	~~46.9~~ -0.56	
az080	~~tree ring~~ 251	~~352~~ 36	~~-21~~ treering	~~250.7~~ 0.40	~~36.1~~ 0.42	
az081	~~tree ring~~ 251	~~349~~ 36	~~-21~~ treering	~~250.6~~ 0.40	~~36.1~~ 0.42	
az082	~~tree ring~~ 251	~~574~~ 36	~~-22~~ treering	~~250.6~~ 0.40	~~36.1~~ 0.42	
az084	~~tree ring~~ 250	~~480~~ 36	~~-21~~ treering	~~249.5~~ 0.40	~~36.2~~ 0.42	
az086	~~tree ring~~ 249	~~585~~ 37	~~-21~~ treering	~~249.3~~ 0.40	~~36.8~~ 0.42	
az089	~~tree ring~~ 250	~~354~~ 34	~~-22~~ treering	~~250.2~~ 0.40	~~34.3~~ 0.20	
az091	~~tree ring~~ 248	~~261~~ 36	~~-22~~ treering	~~248.4~~ 0.40	~~35.6~~ 0.42	
az098	~~tree ring~~ 248	~~302~~ 36	~~-22~~ treering	~~248.2~~ 0.40	~~35.5~~ 0.42	
az099	~~tree ring~~ 250	~~263~~ 35	~~-23~~ treering	~~250.1~~ 0.40	~~34.5~~ 0.20	
az102	~~tree ring~~ 250	~~460~~ 37	~~-22~~ treering	~~249.5~~ 0.40	~~36.7~~ 0.42	
az104	~~tree ring~~ 246	~~356~~ 37	~~-21~~ treering	~~246.3~~ 0.40	~~36.8~~ 0.51	
az106	~~tree ring~~ 248	~~502~~ 36	~~-25~~ treering	~~247.9~~ 0.40	~~35.8~~ 0.42	
az109	~~tree ring~~ 247	~~352~~ 35	~~-21~~ treering	~~247~~ 0.40	~~35~~ 0.51	
az127	~~tree ring~~ 248	~~369~~ 37	~~-26~~ treering	~~247.8~~ 0.40	~~36.7~~ 0.42	
az129	~~tree ring~~ 248	~~468~~ 37	~~-26~~ treering	~~247.9~~ 0.40	~~36.6~~ 0.42	
az135	~~tree ring~~ 246	~~381~~ 35	~~-21~~ treering	~~246.1~~ 0.40	~~35.1~~ 0.51	
az143	~~tree ring~~ 247	~~307~~ 36	~~-22~~ treering	~~246.9~~ 0.40	~~36~~ 0.51	
az144	~~tree ring~~ 248	~~469~~ 37	~~-25~~ treering	~~248~~ 0.40	~~36.8~~ 0.42	

Table 2 continued from previous page

Reference	Lon	Lat	Proxy	SNR	EOF	Start
az505	~~tree ring~~ 248	~~257~~ 36	~~-25~~ treering	~~248~~ 0.40	~~36.4~~ 0.42	257
az510	~~tree ring~~ 248	~~1402~~ 36	~~-33~~ treering	~~248.3~~ 0.40	~~35.5~~ 0.42	1402
az527	~~tree ring~~ 249	~~320~~ 34	~~-36~~ treering	~~249.2~~ 0.40	~~34.3~~ 0.20	320
az542	~~tree ring~~ 250	34	treering	0.40	0.20	320
Bagnato et al. (2005) $\delta^{18}O$	179	-17	coral	0.16	-1.56	174
Barron (2003)	~~marine sediment~~ 235	~~15804~~ 42	marine	~~158~~ N/A	~~235.1~~ N/A	~~41.7~~ 15804
~~Boiseau et al. (1999)~~ Berke et al. (2012)	37	3	lake	N/A	N/A	173
Berke et al. (2012)	37	3	lake	N/A	N/A	2529
Black et al. (2007)	295	11	marine	0.40	0.89	729
Boiseau et al. (1999) $\delta^{18}O$	210	-18	coral	~~98~~ N/A	~~-41~~ N/A	~~210.2~~ 98
ca051	~~tree ring~~ 243	~~1992~~ 34	~~-20~~ treering	~~243.2~~ 0.40	~~34.1~~ 0.90	1992
ca066	~~tree ring~~ 239	~~479~~ 40	~~-30~~ treering	~~239.4~~ 0.40	~~40.2~~ 0.40	479
ca067	~~tree ring~~ 239	~~466~~ 40	~~-30~~ treering	~~239.4~~ 0.40	~~40.2~~ 0.40	466
ca089	~~tree ring~~ 242	~~445~~ 35	~~-31~~ treering	~~241.7~~ 0.40	~~35.4~~ 0.39	445
ca092	~~tree ring~~ 241	~~516~~ 37	~~-31~~ treering	~~241.1~~ 0.40	~~36.7~~ 0.39	516
ca094	~~tree ring~~ 242	~~422~~ 36	~~-31~~ treering	~~241.6~~ 0.40	~~35.5~~ 0.39	422
ca514	~~tree ring~~ 242	~~343~~ 36	~~-31~~ treering	~~241.8~~ 0.40	~~36~~ 0.39	343
ca528	~~tree ring~~ 242	~~1052~~ 37	~~-37~~ treering	~~241.6~~ 0.40	~~36.8~~ 0.39	1052
ca529	~~tree ring~~ 241	~~1251~~ 37	~~-37~~ treering	~~241.4~~ 0.40	~~36.5~~ 0.39	1251
ca530	~~tree ring~~ 242	~~1033~~ 37	~~-37~~ treering	~~241.8~~ 0.40	~~36.5~~ 0.39	1033
ca531	~~tree ring~~ 242	~~923~~ 37	~~-37~~ treering	~~241.8~~ 0.40	~~36.8~~ 0.39	923
ca532	~~tree ring~~ 241	~~900~~ 37	~~-37~~ treering	~~241.4~~ 0.40	~~36.5~~ 0.39	900
ca536	~~tree ring~~ 243	~~296~~ 34	~~-38~~ treering	~~242.7~~ 0.40	~~34.3~~ 0.90	296
ca544	~~tree ring~~ 243	~~-38~~ 34	~~242.9~~ treering	~~34.2~~ 0.40	0.90	243
ca546	~~tree ring~~ 243	~~209~~ 34	~~-38~~ treering	~~242.9~~ 0.40	~~34.2~~ 0.90	209
ca547	~~tree ring~~ 243	~~266~~ 34	~~-38~~ treering	~~243~~ 0.40	~~34.2~~ 0.90	266
ca552	~~tree ring~~ 243	~~322~~ 34	~~-38~~ treering	~~243~~ 0.40	~~34.1~~ 0.90	322
ca555	~~tree ring~~ 237	~~773~~ 40	~~-38~~ treering	~~237.1~~ 0.40	~~40~~ 0.40	773
ca609	~~tree ring~~ 243	~~390~~ 34	~~-45~~ treering	~~243.2~~ 0.40	~~34.1~~ 0.90	390
ca612	~~tree ring~~ 241	~~480~~ 35	~~-43~~ treering	~~240.6~~ 0.40	~~34.7~~ 0.90	480
ca619	~~tree ring~~ 238	~~587~~ 40	~~-54~~ treering	~~238.2~~ 0.40	~~40.3~~ 0.40	587
ca621	~~tree ring~~ 241	~~365~~ 36	~~-53~~ treering	~~241.3~~ 0.40	~~35.5~~ 0.39	365
ca625	~~tree ring~~ 239	~~440~~ 37	~~-53~~ treering	~~239~~ 0.40	~~37.1~~ 0.63	440
ca626	~~tree ring~~ 239	~~373~~ 37	~~-53~~ treering	~~238.8~~ 0.40	~~36.5~~ 0.63	373
ca628	~~tree ring~~ 239	40	treering	0.40	0.40	500
Charles (1997) $\delta^{18}O$	55	-5	coral	0.71	0.25	103

Table 2 continued from previous page

Reference	Lon	Lat	Proxy	SNR	EOF	Start	End	R
Charles et al. (2003) Bali	116	-8	coral	0.46	-0.55	168	-40	
Charles et al. (2003) Bunaken	125	2	coral	N/A	N/A	90	-41	
co066	~~tree ring~~ 252	~~493~~ 38	~~-28~~ treering	~~251.5~~ 0.40	~~37.6~~ -0.29	493	-28	
co067	~~tree ring~~ 252	~~680~~ 38	~~-28~~ treering	~~251.5~~ 0.40	~~37.6~~ -0.29	680	-28	
co511	~~tree ring~~ 254	~~781~~ 40	~~-39~~ treering	~~254.4~~ 0.40	~~40~~ 0.02	781	-39	
co526	~~tree ring~~ 255	~~300~~ 40	~~-30~~ treering	~~254.5~~ 0.40	~~40.4~~ 0.02	300	-30	
co532	~~tree ring~~ 254	~~310~~ 40	~~-37~~ treering	~~254.4~~ 0.40	~~40.4~~ 0.02	310	-37	
co533	~~tree ring~~ 255	~~400~~ 40	~~-37~~ treering	~~254.7~~ 0.40	~~39.9~~ 0.02	400	-37	
co538	~~tree ring~~ 255	~~280~~ 41	~~-37~~ treering	~~254.9~~ 0.40	~~40.5~~ 0.02	280	-37	
co542	~~tree ring~~ 255	~~260~~ 40	~~-37~~ treering	~~254.7~~ 0.40	~~40.2~~ 0.02	260	-37	
co543	~~tree ring~~ 254	~~380~~ 40	~~-37~~ treering	~~254.2~~ 0.40	~~40.4~~ 0.02	380	-37	
co544	~~tree ring~~ 254	~~520~~ 40	~~-37~~ treering	~~254.3~~ 0.40	~~40.1~~ 0.02	520	-37	
co545	~~tree ring~~ 255	~~620~~ 40	~~-37~~ treering	~~254.5~~ 0.40	~~40.1~~ 0.02	620	-37	
co547	~~tree ring~~ 254	~~880~~ 40	~~-37~~ treering	~~254.3~~ 0.40	~~40.4~~ 0.02	880	-37	
co548	~~tree ring~~ 255	~~300~~ 39	~~-38~~ treering	~~255.1~~ 0.40	~~38.6~~ -0.79	300	-38	
co549	~~tree ring~~ 254	~~440~~ 40	~~-37~~ treering	~~254.3~~ 0.40	~~40.4~~ 0.02	440	-37	
co550	~~tree ring~~ 255	~~260~~ 40	~~-37~~ treering	~~254.8~~ 0.40	~~40.4~~ 0.02	260	-37	
co551	~~tree ring~~ 255	~~200~~ 40	~~-37~~ treering	~~254.6~~ 0.40	~~40.1~~ 0.02	200	-37	
co563	~~tree ring~~ 254	~~252~~ 40	~~-51~~ treering	~~254.4~~ 0.40	~~40.4~~ 0.02	252	-51	
co568	~~tree ring~~ 257	~~322~~ 37	~~-48~~ treering	~~256.8~~ 0.40	~~37.2~~ -1.27	322	-48	
co569	~~tree ring~~ 256	~~486~~ 37	~~-47~~ treering	~~256.4~~ 0.40	~~37.1~~ -1.27	486	-47	
co572	~~tree ring~~ 255	~~1056~~ 40	~~-48~~ treering	~~254.5~~ 0.40	~~40.3~~ 0.02	1056	-48	
co579	~~tree ring~~ 254	~~630~~ 40	~~-52~~ treering	~~253.5~~ 0.40	~~40~~ 0.02	630	-52	
co581	~~tree ring~~ 253	~~411~~ 41	~~-50~~ treering	~~253.2~~ 0.40	~~40.8~~ 0.02	411	-50	
~~Cobb et al. (2003) full~~ Cole (2000)	40	-3	coral	~~1022~~ N/A	~~-48~~ N/A	~~197.9~~ 149	~~5.9~~ -44	
Conroy et al. (2009)	271	-1	lake	N/A	N/A	1219	-54	
Cook et al. (2000)	~~tree ring~~ 146	~~3550~~ -42	~~-41~~ treering	~~145.5~~ 0.53	~~-41.8~~ -0.71	3550	-41	
Cronin et al. (2003)	~~sediment~~ 284	38	marine	N/A	N/A	2134	-45	~~283~~
Cronin et al. (2005)	284	38	marine	N/A	N/A	2127	-45	
Damassa et al. (2006) ~~c17th~~ $\delta^{18}O$	40	-8	coral	0.66	0.54	328	~~228~~ -48	~~39~~
DeLong et al. (2012)	167	-23	coral	0.61	-2.06	301	-50	
DeLong et al. (2014)	277	25	coral	0.93	-0.57	216	-59	
Dunbar et al. (1994)	269	0	coral	N/A	N/A	343	-31	
Felis et al. (2010) UCa	142	27	coral	N/A	N/A	77	-44	
Goni et al. (2006) Cariaco	295	11	marine	0.40	0.89	256	-46	
Goni et al. (2006) Guaymas	248	28	marine	0.40	0.79	223	-38	

Table 2 continued from previous page

Reference	Lon	Lat	Proxy	SNR	EOF
~~Damassa et al. (2006) e20th~~ Goodkin et al. (2008)	296	32	coral	~~53~~ 0.40	-0.45
Guilderson and Schrag (1999) $\delta^{18}O$	166	-30	coral	N/A	N/A
~~DeLong et al. (2012)~~ Heiss (1994)	35	29	coral	~~301~~ 0.29	~~-50~~ -1.06
~~Felis et al. (2010) srea~~ Hetzinger et al. (2010) $\delta^{18}O$	-422	16	coral	~~77~~ N/A	~~-44~~ N/A
~~Felis et al. (2010) uea~~ Hetzinger et al. (2010) Sr/Ca	-422	16	coral	~~77~~ N/A	~~-44~~ N/A
ia003	~~tree ring~~ 268	~~235~~ 41	~~-31~~ treering	~~268~~ 0.40	~~40.7~~ -0.41
id002	~~tree ring~~ 244	~~278~~ 48	~~-26~~ treering	~~244.1~~ 0.40	~~47.5~~ 0.63
il010	~~tree ring~~ 270	~~279~~ 40	~~-30~~ treering	~~270.2~~ 0.40	~~40~~ -0.55
il011	~~tree ring~~ 272	~~276~~ 39	~~-30~~ treering	~~271.8~~ 0.40	~~39.4~~ -0.55
il013	~~tree ring~~ 271	~~295~~ 38	~~-31~~ treering	~~271~~ 0.40	~~37.5~~ -0.99
il014	~~tree ring~~ 271	~~298~~ 38	~~-31~~ treering	~~270.8~~ 0.40	~~37.6~~ -0.99
indi002	~~tree ring~~ 74	~~346~~ 35	~~-30~~ treering	~~74.3~~ 0.40	~~35.1~~ -0.23
indi006	~~tree ring~~ 76	~~296~~ 35	~~-31~~ treering	~~75.5~~ 0.40	~~34.6~~ -0.34
ital023	~~tree ring~~ 12	~~476~~ 47	~~-40~~ treering	~~12.1~~ 0.40	~~46.6~~ -0.75
Keigwin (1996)	~~marine sediment~~ 302	~~3125~~ 34	marine	~~25~~ 0.77	~~302.4~~ -0.41
Kellerhals et al. (2010)	292	-17	ice core	~~1595~~ 0.40	~~-45~~ 0.71
Khider et al. (2014) ~~sst~~ SST	126	7	marine ~~sediment~~	~~9960~~ N/A	~~199~~ N/A
Kilbourne et al. (2008) $\delta^{18}O$	293	18	coral	0.30	0.47
Krusic et al. (2015)	91	27	treering	0.40	-0.66
ks007	~~tree ring~~ 264	38	treering	0.40	-1.07
Kuhnert et al. (2000)	114	-22	coral	N/A	N/A
Kuhnert et al. (2005) $\delta^{18}O$	295	33	coral	0.11	-0.77
ky003	~~tree ring~~ 277	37	treering	0.40	-1.12
Linsley et al. (2000) Clipperton	251	10	coral	N/A	N/A
Linsley et al. (2006) Rarotonga Sr/Ca	201	-22	coral	0.15	-1.99
Linsley et al. (2006) Savusavu Sr/Ca	179	-17	coral	0.28	-1.56
Marchitto et al. (2010)	~~marine sediment~~ 247	~~13812~~ 25	marine	~~832~~ 0.40	~~247.3~~ 2.06
me019	~~tree ring~~ 292	~~253~~ 46	~~-31~~ treering	~~291.7~~ 0.40	~~45.5~~ -0.80
mi009	~~tree ring~~ 275	~~440~~ 47	~~-33~~ treering	~~275.1~~ 0.40	~~46.5~~ -0.83
mo003	~~tree ring~~ 269	~~257~~ 37	~~-31~~ treering	~~268.5~~ 0.40	~~37.1~~ -0.94
mo005	~~tree ring~~ 270	~~242~~ 38	~~-32~~ treering	~~269.5~~ 0.40	~~37.5~~ -0.94
mo018	~~tree ring~~ 266	~~226~~ 37	~~-29~~ treering	~~266.2~~ 0.40	~~36.6~~ -1.07
mo033	~~tree ring~~ 267	~~254~~ 37	~~-42~~ treering	~~267.2~~ 0.40	~~36.7~~ -0.94
mo036	~~tree ring~~ 266	~~261~~ 37	~~-29~~ treering	~~266.2~~ 0.40	~~36.6~~ -1.07
mo037	~~tree ring~~ 270	~~765~~ 37	~~-42~~ treering	~~269.5~~ 0.40	~~36.6~~ -0.94
mo038	~~tree ring~~ 268	~~397~~ 37	~~-42~~ treering	~~267.5~~ 0.40	~~37.2~~ -0.94

Table 2 continued from previous page

Reference	Lon	Lat	Proxy	SNR	EOF	Start	End	Res	Dating	Included?
mo039	~~tree ring~~ 268	~~286~~ 38	~~-42~~ treering	~~268.1~~ 0.40	~~37.5~~ -0.94	286	-42	1	1	Yes
mo040	~~tree ring~~ 269	~~257~~ 37	~~-43~~ treering	~~268.8~~ 0.40	~~37.1~~ -0.94	257	-43	1	1	Yes
mo043	~~tree ring~~ 269	~~812~~ 37	~~-40~~ treering	~~268.5~~ 0.40	~~37.1~~ -0.94	812	-40	1	1	Yes
morc002	~~tree ring~~ 355	35	treering	0.40	0.34	318	-34	~~355.2~~ 1	~~35~~ 1	Yes
Moustafa (2000)	34	28	coral	N/A	N/A	52	-43	1	1	~~Yes~~No; Leng
nc002	~~tree ring~~ 277	~~392~~ 36	~~-33~~ treering	~~276.6~~ 0.40	~~35.6~~ -1.12	392	-33	1	1	Yes
nc003	~~tree ring~~ 278	~~390~~ 36	~~-33~~ treering	~~278.2~~ 0.40	~~36.1~~ -1.09	390	-33	1	1	Yes
nc006	~~tree ring~~ 277	~~273~~ 35	~~-33~~ treering	~~276.8~~ 0.40	~~35.1~~ -1.12	273	-33	1	1	Yes
nc007	~~tree ring~~ 278	~~333~~ 36	~~-27~~ treering	~~278.1~~ 0.40	~~35.9~~ -1.09	333	-27	1	1	Yes
nc009	~~tree ring~~ 283	~~426~~ 37	~~-34~~ treering	~~283.4~~ 0.40	~~36.5~~ -1.11	426	-34	1	1	Yes
nj001	~~tree ring~~ 285	~~330~~ 41	~~-32~~ treering	~~285.4~~ 0.40	~~40.5~~ -0.76	330	-32	1	1	Yes
nj002	~~tree ring~~ 285	~~276~~ 41	~~-32~~ treering	~~285.4~~ 0.40	~~40.5~~ -0.76	276	-32	1	1	Yes
nm021	~~tree ring~~ 252	~~395~~ 37	~~-21~~ treering	~~252.2~~ 0.40	~~37~~ -0.29	395	-21	1	1	Yes
nm023	~~tree ring~~ 252	~~375~~ 37	~~-21~~ treering	~~252.2~~ 0.40	~~37~~ -0.29	375	-21	1	1	Yes
nm024	~~tree ring~~ 253	~~307~~ 37	~~-21~~ treering	~~252.7~~ 0.40	~~36.7~~ -0.29	307	-21	1	1	Yes
nm025	~~tree ring~~ 252	~~569~~ 36	~~-22~~ treering	~~251.9~~ 0.40	~~35.6~~ -0.29	569	-22	1	1	Yes
nm026	~~tree ring~~ 254	~~588~~ 36	~~-22~~ treering	~~253.5~~ 0.40	~~36.4~~ -0.29	588	-22	1	1	Yes
nm031	~~tree ring~~ 252	~~472~~ 35	~~-22~~ treering	~~251.5~~ 0.40	~~35.4~~ -0.29	472	-22	1	1	Yes
nm033	~~tree ring~~ 252	~~414~~ 35	~~-22~~ treering	~~251.7~~ 0.40	~~35~~ -0.29	414	-22	1	1	Yes
nm034	~~tree ring~~ 252	~~288~~ 35	~~-22~~ treering	~~252.2~~ 0.40	~~34.9~~ -0.52	288	-22	1	1	Yes
nm038	~~tree ring~~ 254	~~394~~ 36	~~-22~~ treering	~~254.3~~ 0.40	~~35.5~~ -0.29	394	-22	1	1	Yes
nm040	~~tree ring~~ 254	~~371~~ 36	~~-22~~ treering	~~254.4~~ 0.40	~~35.5~~ -0.29	371	-22	1	1	Yes
nm047	~~tree ring~~ 257	~~310~~ 37	~~-24~~ treering	~~257~~ 0.40	~~36.8~~ -1.27	310	-24	1	1	Yes
nm051	~~tree ring~~ 253	~~263~~ 36	~~-26~~ treering	~~252.8~~ 0.40	~~35.6~~ -0.29	263	-26	1	1	Yes
nm053	~~tree ring~~ 252	~~321~~ 36	~~-26~~ treering	~~252.4~~ 0.40	~~35.9~~ -0.29	321	-26	1	1	Yes
nm055	~~tree ring~~ 253	~~356~~ 37	~~-21~~ treering	~~252.7~~ 0.40	~~36.7~~ -0.29	356	-21	1	1	Yes
nm118	~~tree ring~~ 254	~~386~~ 35	~~-32~~ treering	~~254.4~~ 0.40	~~35.1~~ -0.29	386	-32	1	1	Yes
nm500	~~tree ring~~ 254	~~242~~ 36	~~-22~~ treering	~~254.3~~ 0.40	~~36.1~~ -0.29	242	-22	1	1	Yes
nm501	~~tree ring~~ 254	~~223~~ 36	~~-22~~ treering	~~253.7~~ 0.40	~~35.8~~ -0.29	223	-22	1	1	Yes
nm529	~~tree ring~~ 251	~~298~~ 36	~~-27~~ treering	~~251.2~~ 0.40	~~36~~ 0.42	298	-27	1	1	Yes
nm548	~~tree ring~~ 255	~~358~~ 37	~~-31~~ treering	~~254.5~~ 0.40	~~36.7~~ -0.29	358	-31	1	1	Yes
nm549	~~tree ring~~ 255	~~311~~ 37	~~-37~~ treering	~~254.5~~ 0.40	~~36.7~~ -0.29	311	-37	1	1	Yes
nm550	~~tree ring~~ 253	~~418~~ 36	~~-36~~ treering	~~253.3~~ 0.40	~~35.9~~ -0.29	418	-36	1	1	Yes
nm551	~~tree ring~~ 255	~~250~~ 36	~~-31~~ treering	~~254.6~~ 0.40	~~36.3~~ -0.29	250	-31	1	1	Yes
nm552	~~tree ring~~ 255	~~369~~ 36	~~-31~~ treering	~~254.6~~ 0.40	~~36.3~~ -0.29	369	-31	1	1	Yes
nm554	~~tree ring~~ 255	~~260~~ 36	~~-36~~ treering	~~254.5~~ 0.40	~~36.1~~ -0.29	260	-36	1	1	Yes

Table 2 continued on next pag

Table 2 continued from previous page

Reference	Lon	Lat	Proxy	SNR	EOF	Start	End	Res
nm555	~~tree ring~~ 253	~~346~~ 36	~~-36~~ treering	~~253.4~~ 0.40	~~35.8~~ -0.29	346	-36	1
nm556	~~tree ring~~ 253	~~378~~ 36	~~-36~~ treering	~~253.4~~ 0.40	~~35.8~~ -0.29	378	-36	1
nm557	~~tree ring~~ 254	~~395~~ 36	~~-36~~ treering	~~254.4~~ 0.40	~~36.2~~ -0.29	395	-36	1
nm558	~~tree ring~~ 253	~~297~~ 36	~~-37~~ treering	~~253.4~~ 0.40	~~35.8~~ -0.29	297	-37	1
nm559	~~tree ring~~ 255	~~559~~ 37	~~-37~~ treering	~~254.6~~ 0.40	~~36.7~~ -0.29	559	-37	1
nm560	~~tree ring~~ 255	~~1113~~ 37	~~-39~~ treering	~~254.5~~ 0.40	~~36.7~~ -0.29	1113	-39	1
nm575	~~tree ring~~ 256	~~238~~ 37	~~-48~~ treering	~~256~~ 0.40	~~36.8~~ -1.27	238	-48	1
nm576	~~tree ring~~ 256	~~324~~ 37	~~-48~~ treering	~~256.1~~ 0.40	~~36.8~~ -1.27	324	-48	1
nm577	~~tree ring~~ 256	36	treering	0.40	-1.27	355	-48	~~255.7~~ 1
Nurhati et al. (2009)	198	6	coral	N/A	N/A	64	-48	1
nv048	~~tree ring~~ 245	~~447~~ 40	~~-28~~ treering	~~244.5~~ 0.40	~~40.2~~ 0.63	447	-28	1
nv506	~~tree ring~~ 245	~~345~~ 37	~~-27~~ treering	~~244.8~~ 0.40	~~36.7~~ 0.51	345	-27	1
nv507	~~tree ring~~ 245	~~485~~ 39	~~-26~~ treering	~~245.1~~ 0.40	~~39.4~~ 0.63	485	-26	1
nv509	~~tree ring~~ 245	~~399~~ 39	~~-26~~ treering	~~245.3~~ 0.40	~~39.4~~ 0.63	399	-26	1
nv510	~~tree ring~~ 244	~~1150~~ 36	~~-34~~ treering	~~244.3~~ 0.40	~~36.3~~ 0.51	1150	-34	1
nv512	~~tree ring~~ 245	~~1630~~ 40	~~-35~~ treering	~~244.5~~ 0.40	~~40.2~~ 0.63	1630	-35	1
nv513	~~tree ring~~ 246	~~1125~~ 39	~~-33~~ treering	~~245.7~~ 0.40	~~38.9~~ 0.63	1125	-33	1
nv514	~~tree ring~~ 245	~~1648~~ 41	~~-35~~ treering	~~245.2~~ 0.40	~~40.6~~ 0.63	1648	-35	1
nv516	~~tree ring~~ 246	~~1950~~ 39	~~-34~~ treering	~~245.8~~ 0.40	~~38.9~~ 0.63	1950	-34	1
nv517	~~tree ring~~ 244	~~1630~~ 36	~~-34~~ treering	~~244.3~~ 0.40	~~36.3~~ 0.51	1630	-34	1
oh003	~~tree ring~~ 276	~~288~~ 40	~~-35~~ treering	~~275.6~~ 0.40	~~39.9~~ -0.83	288	-35	1
oh006	~~tree ring~~ 279	~~325~~ 40	~~-48~~ treering	~~279~~ 0.40	~~40~~ -0.90	325	-48	1
ok001	~~tree ring~~ 265	~~275~~ 37	~~-29~~ treering	~~265.3~~ 0.40	~~36.7~~ -1.07	275	-29	1
ok004	~~tree ring~~ 264	~~213~~ 37	~~-29~~ treering	~~263.6~~ 0.40	~~36.7~~ -1.07	213	-29	1
ok007	~~tree ring~~ 264	~~339~~ 36	~~-45~~ treering	~~263.8~~ 0.40	~~36.2~~ -1.07	339	-45	1
ok013	~~tree ring~~ 262	~~270~~ 36	~~-29~~ treering	~~261.6~~ 0.40	~~35.6~~ -1.37	270	-29	1
ok016	~~tree ring~~ 264	~~205~~ 35	~~-29~~ treering	~~264.4~~ 0.40	~~35.1~~ -1.07	205	-29	1
ok019	~~tree ring~~ 265	~~326~~ 34	~~-29~~ treering	~~265.4~~ 0.40	~~34.3~~ -1.63	326	-29	1
ok025	~~tree ring~~ 262	~~259~~ 34	~~-45~~ treering	~~262.3~~ 0.40	~~34.1~~ -1.99	259	-45	1
ok028	~~tree ring~~ 261	~~264~~ 35	~~-29~~ treering	~~261.4~~ 0.40	~~34.7~~ -1.99	264	-29	1
ok031	~~tree ring~~ 265	~~-32~~ 34	~~265.4~~ treering	~~34.3~~ 0.40	-1.63	265	-32	1
Oppo et al. (2009) ~~sst~~ SST	119	-5	marine ~~sediment~~	~~1925~~ 0.40	~~-5~~ -0.38	~~118.5~~ 1925	~~-4.5~~ -5	11
or040	~~tree ring~~ 242	~~275~~ 46	~~-41~~ treering	~~242~~ 0.40	~~45.8~~ 0.25	275	-41	1
pa001	~~tree ring~~ 282	~~341~~ 41	~~-31~~ treering	~~282.3~~ 0.40	~~40.7~~ -0.75	341	-31	1
pa005	~~tree ring~~ 280	~~327~~ 40	~~-31~~ treering	~~280.3~~ 0.40	~~39.8~~ -0.90	327	-31	1
pa007	~~tree ring~~ 282	~~415~~ 40	~~-31~~ treering	~~282.4~~ 0.40	~~40.2~~ -0.75	415	-31	1

Table 2 continued from previous page

Reference	Lon	Lat	Proxy	SNR	I
pa009	~~tree ring~~ 284	~~319~~ 40	~~-31~~ treering	~~283.6~~ 0.40	~~39.~~
pa012	~~tree ring~~ 282	~~338~~ 40	~~-31~~ treering	~~281.5~~ 0.40	~~39.~~
Powers et al. (2011)	~~lake sediment~~ 34	~~667~~ -10	lake	~~-46~~ N/A	~~34~~
Quinn et al. (1998)	167	-23	coral	0.33	
Quinn et al. (2006) $\delta^{18}O$	152	4	coral	N/A	
Richey et al. (2009) ~~fisk~~ Fisk	268	28	marine ~~sediment~~	~~702~~ 0.40	~~-5~~
Richey et al. (2009) ~~garrison~~ Garrison	266	27	marine ~~sediment~~	~~529~~ 0.40	~~-5~~
Saenger et al. (2009) ext	281	26	coral	0.73	
Saenger et al. (2011) ggc	~~marine sediment~~ 284	~~1500~~ 33	marine	~~100~~ 0.40	~~283.~~
Saenger et al. (2011) mc	~~marine sediment~~ 284	~~1700~~ 33	marine	~~100~~ 0.40	~~283.~~
spai009	~~tree ring~~ 358	~~262~~ 40	~~-38~~ treering	~~357.9~~ 0.40	~~40~~
spai011	~~tree ring~~ 358	~~465~~ 40	~~-38~~ treering	~~357.9~~ 0.40	~~40~~
spai013	~~tree ring~~ 0	~~265~~ 40	~~-42~~ treering	~~0.1~~ 0.40	~~4~~
spai016	~~tree ring~~ 355	~~283~~ 41	~~-38~~ treering	~~355.2~~ 0.40	~~40~~
spai018	~~tree ring~~ 355	~~263~~ 40	~~-39~~ treering	~~355.1~~ 0.40	~~40~~
spai019	~~tree ring~~ 356	~~427~~ 41	~~-38~~ treering	~~356~~ 0.40	~~40~~
spai029	~~tree ring~~ 358	~~239~~ 40	~~-33~~ treering	~~358.1~~ 0.40	~~40~~
spai036	~~tree ring~~ 356	~~201~~ 41	~~-33~~ treering	~~356~~ 0.40	~~40~~
spai037	~~tree ring~~ 356	~~289~~ 41	~~-35~~ treering	~~356.2~~ 0.40	~~40~~
spai038	~~tree ring~~ 356	~~351~~ 41	~~-34~~ treering	~~356.1~~ 0.40	~~40~~
spai041	~~tree ring~~ 1	~~269~~ 40	~~-35~~ treering	~~0.7~~ 0.40	~~40.~~
spai045	~~tree ring~~ 358	~~312~~ 40	~~-35~~ treering	~~358.1~~ 0.40	~~40~~
spai046	~~tree ring~~ 358	~~306~~ 40	~~-35~~ treering	~~358.1~~ 0.40	~~40~~
Stott et al. (2002) ~~gruber~~ *G.Ruber*	126	6	marine ~~sediment~~	0.40	
Sundqvist et al. (2013)	29	-24	speleothem	0.46	
Thompson et al. (1995)	282	-9	ice core	0.40	
Thompson and et Al. (1997)	82	35	ice core	0.40	
Thompson et al. (2002) furt	37	-3	ice core	0.40	
Thompson et al. (2002) knif2	37	-3	ice core	0.40	
Thompson et al. (2002) knif3	37	-3	ice core	0.40	
Thompson et al. (2002) ksif1	37	-3	ice core	0.40	
Thompson et al. (2002) ksif2	37	-3	ice core	0.40	
Thompson et al. (2003) Dasuopu	86	28	ice core	0.40	
Thompson et al. (2003) Dunde	96	38	ice core	0.40	
Thompson et al. (2006) c1 $\delta^{18}O$	89	34	ice core	N/A	
~~Stott et al. (2002) gsacculifer~~ Thompson et al. (2006) c2 $\delta^{18}O$	~~marine sediment~~ 89	~~67592~~ 34	ice core	0.40	

Table 2 continued from previous page

Reference	Lon	Lat	Proxy	SNR
Thompson et al. (2006) Dunde an	~~100~~ 96	~~86~~ 38	~~No; Dating error~~ice core	0.40
~~Sundqvist et al. (2013)~~ Thompson et al. (2006) Dunde $\delta^{18}O$	~~speleothem~~ 96	~~315~~ 38	~~-43~~ ice core	~~29.2~~ 0.40
Thompson et al. (2013) nd	289	-14	ice core	~~945~~ 0.40
Thompson et al. (2013) sd	289	-14	ice core	~~1724~~ 0.66
~~Tiwari et al. (2015)~~ Tierney et al. (2015) bc1 SST	44	45	marine ~~sediment~~	~~4772~~ 0.40
Tierney et al. (2015) p SST	44	45	marine	0.40
Tiwari et al. (2015)	74	13	marine	0.40
tn008	~~tree ring~~ 276	36	treering	0.40
Tudhope et al. (2001) Laing	145	-4	coral	N/A
~~turk001~~ Tudhope et al. (2001) Madang	~~tree ring~~ 146	~~658~~ -5	~~-51~~ coral	~~31.1~~ N/A
turk001	31	40	treering	0.40
turk005	~~tree ring~~ 30	~~580~~ 37	~~-38~~ treering	~~29.9~~ 0.40
turk006	~~tree ring~~ 30	~~590~~ 37	~~-38~~ treering	~~29.9~~ 0.40
ut013	~~tree ring~~ 250	~~517~~ 41	~~-21~~ treering	~~250~~ 0.40
ut018	~~tree ring~~ 251	~~461~~ 39	~~-22~~ treering	~~250.8~~ 0.40
ut020	~~tree ring~~ 250	~~505~~ 38	~~-21~~ treering	~~250.1~~ 0.40
ut021	~~tree ring~~ 249	~~385~~ 37	~~-21~~ treering	~~249.2~~ 0.40
ut023	~~tree ring~~ 250	~~603~~ 38	~~-22~~ treering	~~250~~ 0.40
ut024	~~tree ring~~ 250	~~674~~ 38	~~-20~~ treering	~~250.3~~ 0.40
ut501	~~tree ring~~ 250	~~315~~ 41	~~-21~~ treering	~~250.1~~ 0.40
va008	~~tree ring~~ 281	~~290~~ 38	~~-28~~ treering	~~280.7~~ 0.40
va009	~~tree ring~~ 281	~~363~~ 38	~~-32~~ treering	~~280.6~~ 0.40
va010	~~tree ring~~ 281	~~419~~ 38	~~-32~~ treering	~~280.5~~ 0.40
va012	~~tree ring~~ 278	~~305~~ 37	~~-32~~ treering	~~278.3~~ 0.40
van Hengstum et al. (2015) whc4	~~marine sediment~~ 295	~~2792~~ 32	marine	~~-56~~ 0.40
Vasquez-Bedoya et al. (2012) ext	273	21	coral	1.04
wa048	~~tree ring~~ 238	~~664~~ 47	~~-29~~ treering	~~238.4~~ 0.40
wa056	~~tree ring~~ 239	~~691~~ 47	~~-29~~ treering	~~238.5~~ 0.40
wa057	~~tree ring~~ 239	~~520~~ 48	~~-30~~ treering	~~239~~ 0.40
wa058	~~tree ring~~ 237	~~533~~ 48	~~-30~~ treering	~~236.7~~ 0.40
wa063	~~tree ring~~ 239	~~364~~ 47	~~-30~~ treering	~~238.5~~ 0.40
wa065	~~tree ring~~ 239	~~408~~ 48	~~-32~~ treering	~~239.2~~ 0.40
wa085	~~tree ring~~ 239	47	treering	0.40
Wörheide (1998)	146	-15	coral	0.40
Wu et al. (2013) Sr/Ca	186	-20	coral	N/A
Wurtzel et al. (2013)	295	11	marine	0.40

Table 2 continued from previous page										
Reference	Lon	Lat	Proxy	SNR	EOF	Start	End	Res	Dating	Included?
wv002	~~tree ring~~ 281	39	treering	0.40	-0.90	440	-29	~~280.6~~ 1	~~38.9~~ 1	Yes
Zhao et al. (2000)	240	34	marine	0.40	1.05	653	9	1	5	Yes
Zinke et al. (2014) AC	44	-23	coral	0.40	0.00	290	-44	1	1	Yes
Zinke et al. (2014) HAI	114	-29	coral	0.88	-0.46	155	-60	1	1	Yes
Zinke et al. (2015) Ning	114	-22	coral	N/A	N/A	71	-58	1	1	No; Length
Zinke et al. (2015) Rowley	119	-17	coral	0.63	-0.63	152	-59	1	1	Yes

Table 2. Precipitation proxy details. ‘SNR’ gives the signal-to-noise ratio used to make the pseudoproxies. ‘EOF’ gives the (unscaled) 20CRV2c EOF value used to weight the proxy. ‘Start’ and ‘End’ are starting and ending years in YearBP. ‘Res’ is proxy resolution, rounded to the nearest integer; sub-annual proxies are listed as having a 1-year resolution. ‘Dating’ refers to dating error. ‘Included?’ indicates whether the proxy contributed to the final ENSO reconstruction; if not, the reason for exclusion is listed (‘Dating error’ and ‘Length’ are *a priori* conditions which the proxies failed to meet. ‘AOI’ indicates it passed pre-processing screening, but was not selected during the add-one-in process).